

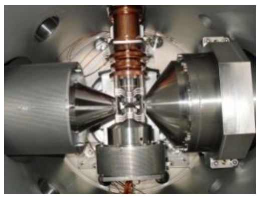
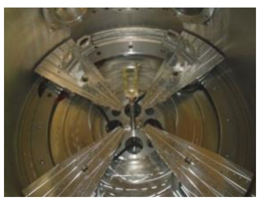
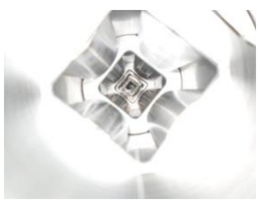


Large area diamond detectors as heavy ion beam profilers

M. PARLOG & J. PERRONNEL
Laboratoire de Physique Corpusculaire de Caen

Journée d'étude sur les détecteurs diamants
The 9th of June 2015

I Introduction:

- *Goal and framework: beam profilers – SPIRAL2, SPARC, EURISOL*
  … & focal plane of the associated spectrometers

II The synthetic diamond: (*properties, fabrication, principle of detection)*

- *Single-crystal (sc-CVD) and polycrystalline (pc-CVD) sensors*
- *Response and charge collection = f(material quality & thickness, ion A,Z&E, HV)*

III Non-segmented detectors:

- *Construction at LPC and tests at GSI (classical electronics) and GANIL (sampling)*
- *Stability of the signal in time; pulse shape analysis (PSA)*

IV Double-sided multi-strip detectors:

- *construction at LPC and tests at GANIL (PSA); analysis in progress*

V Conclusions and prospective

I. Introduction

II Diamond properties:

Excellent radiation hardness due to:
- the highest thermal conductivity
- the high energy of 80 eV to remove an ion

No p-n junction is required:
- due to the large band gap;
- simply metallic electrodes (like an ionization chamber);

High electric fields, up to 6 V/µm:
- due to the high resitivity;
- small dark current (negligible intrinsic carrier concentration at room temperature)

Narrow pulses, due to:
- the low capacitance;
- the high carrier mobility;

CVD diamonds:
allow big detector areas, can be metalized with any desired shape, can be wire bonded, can be operated as « noise-free » particle counter

Tab. 1. Physical Properties of Diamond and Silicon

Physical properties at 300K	**Diamond**	**Silicon**
Band Gap (eV)	5,45	1,12
Electron mobility (cm^2/Vs) Kittel 1800	1800-2200 ?	1500
Hole mobility (cm^2/Vs) Kittel 1200	1600-2400 ?	600
Resistivity ρ (Ω.cm)	$>10^{11}$	$2,3.10^5$
Dielectric constant ε_r	5,7	11,9
Thermal conductivity (W/cm.K)	20	1,27
Lattice constant (Å)	3,57	5,43
Energy to remove an atom from the lattice (eV)	80	28
Energy to create a pair e-h (ev)	13	3,6

Signal formation

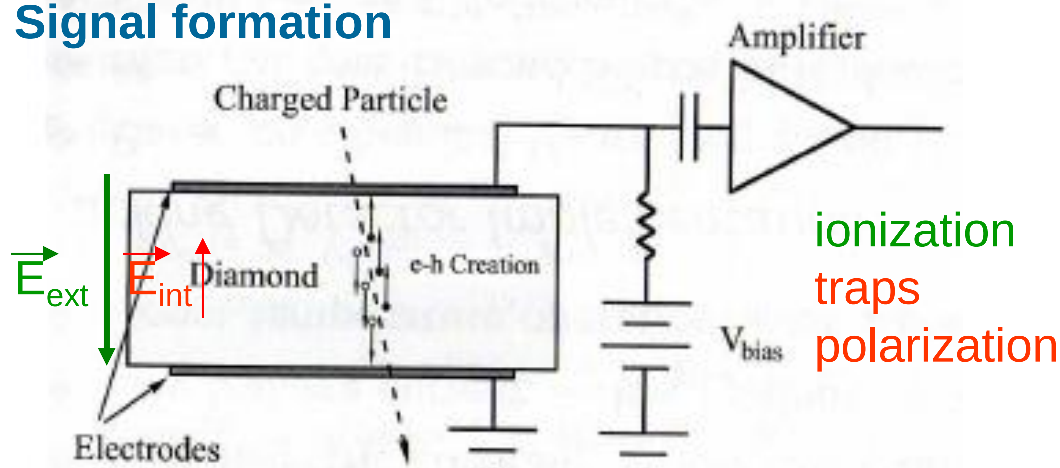

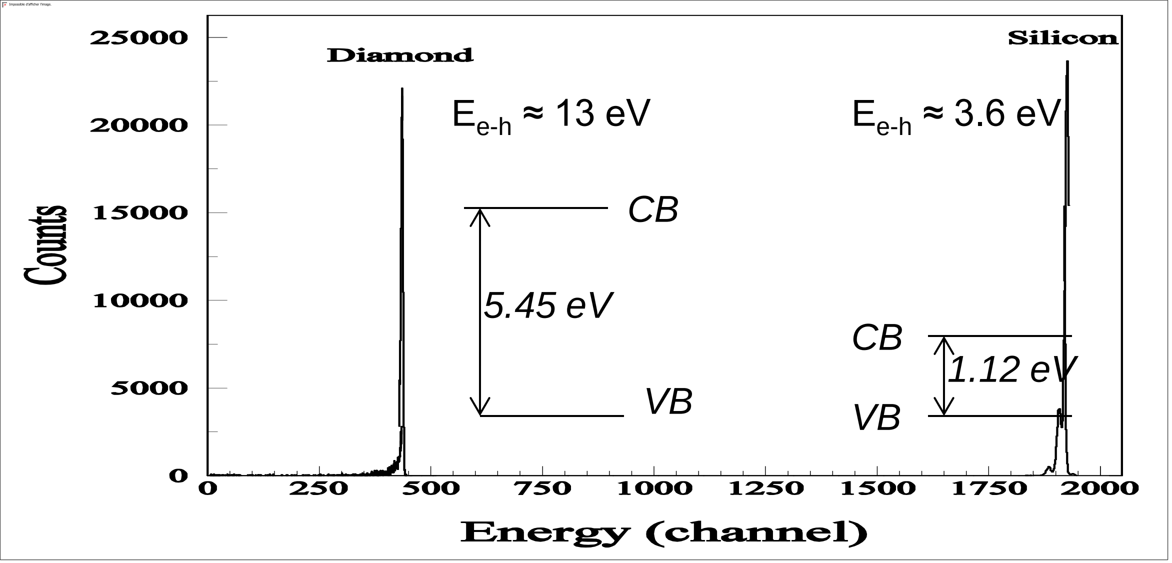

The CVD diamond detectors may behave in very different ways:

Single-crystal diamond detector (CEA Saclay) of 20 µm thickness, adaped to the range. (courtesy of J.-L. Lecouey –LPC)

The signal is 4 lower (left peak) than in a Si detector (right)

^{241}Am: α of 5.5MeV Range ~15 µm

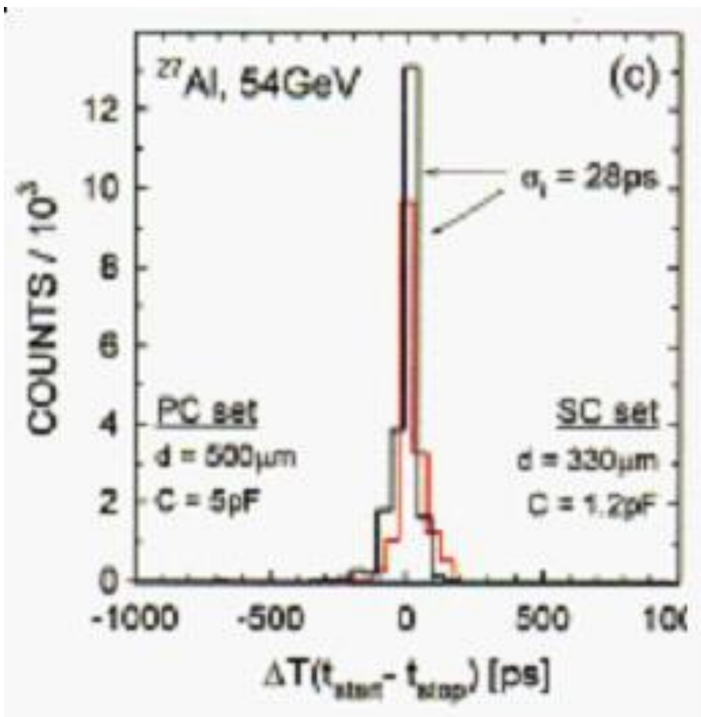

GSI:
Signals & TOF
E. Berdermann for the NoRHDia collaboration

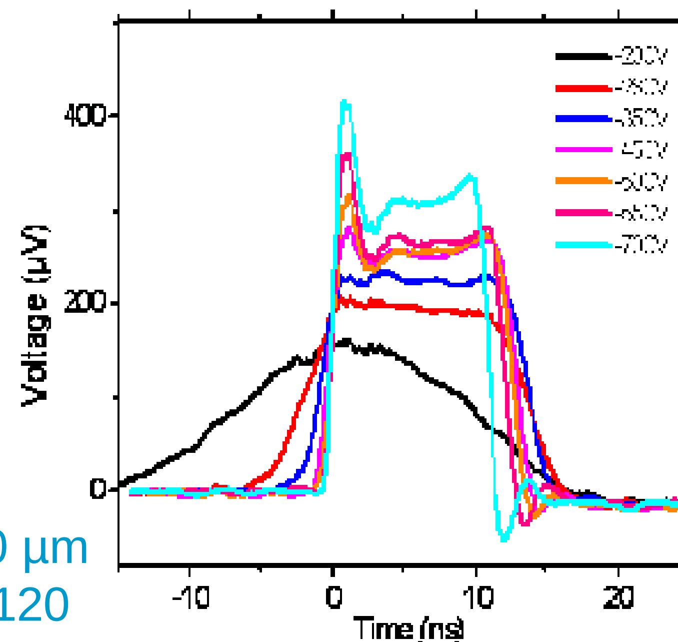

700 µm VT120 ORTEC

courtesy of Dr. H. Hamrita, LIST – CEA Saclay

II. Synthetic Diamond

II. Diamond

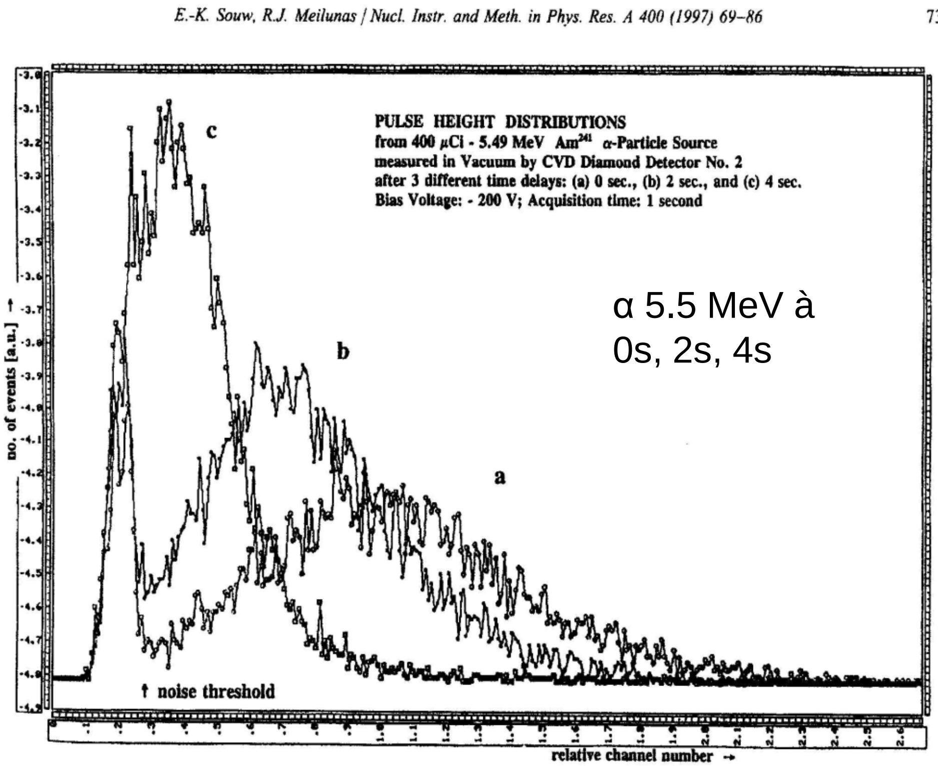

The CVD diamond detectors may behave in very different ways:

Polycrystalline-crystal diamond drawback:

the bulk polarization

Solutions:

- Previous radiation;
- Subbandgap light;
- Electronic procedure;
-Thermic procedure

- Good material!!!

the salutary solution

Requirements for a (radioactive) beam profiler working below 10^6 pps:

- The **beam profile** (X,Y) - **resolution of 1mm** over an **active area of up to $50x50mm^2$**.
- The device should operate at **beam intensities as low as ~1 pps and up to ~10^6pps**.
- The detector should exhibit **a fast rise time** for timing applications (TOF ~0,5 ns) as well as **a short response time** to enable operation at ~1000000 pps.
- The detector should have **a large dynamic range** – both very light and very heavy ions with energies ranging from **a few to ~250 MeV/nucleon** should be detectable.
- The detectors should be **robust and radiation hard** so as to reduce to a minimum their replacement or removal for repair.
- Provide for an **accurate and precise measurement** of the intensity.
- For safety reasons the detector must have **a good vacuum integrity**.
- **Insensitive to the decay of the radioactive ions** (ie., e-,e+,g , etc).

From a practical point of view (eg, use by operators during beam tuning) the detectors should be **as simple and straightforward** to operate as possible.

Alternative: the large area synthetic polycrystalline diamond (chemical vapour deposition – CVD), have properties matching very closely those needed to fulfil the above requirements (**R&D SPIRAL2 in LPC and SPARC Task 4.1 at FAIR)**

1 MeV => 77000 e- => 12.3 fC

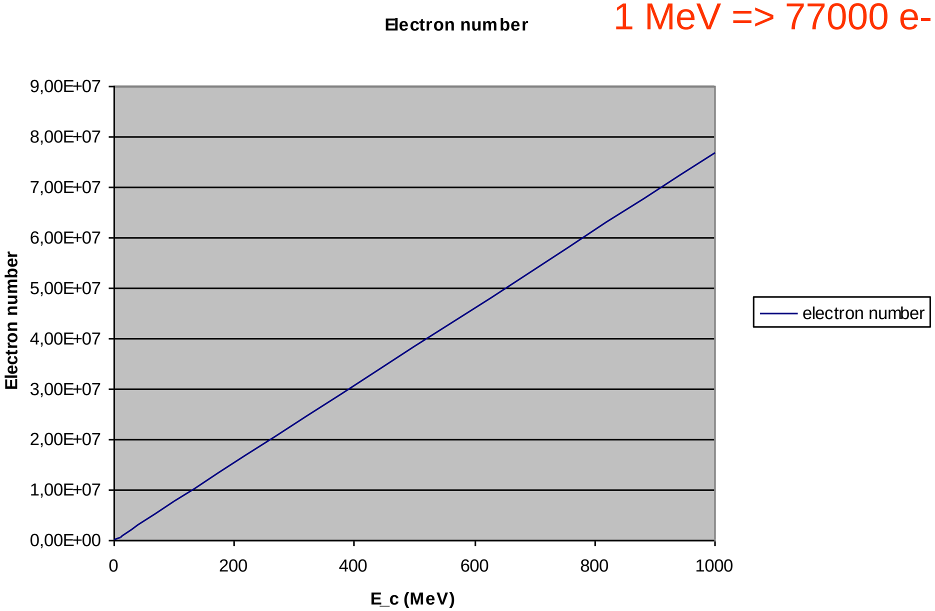

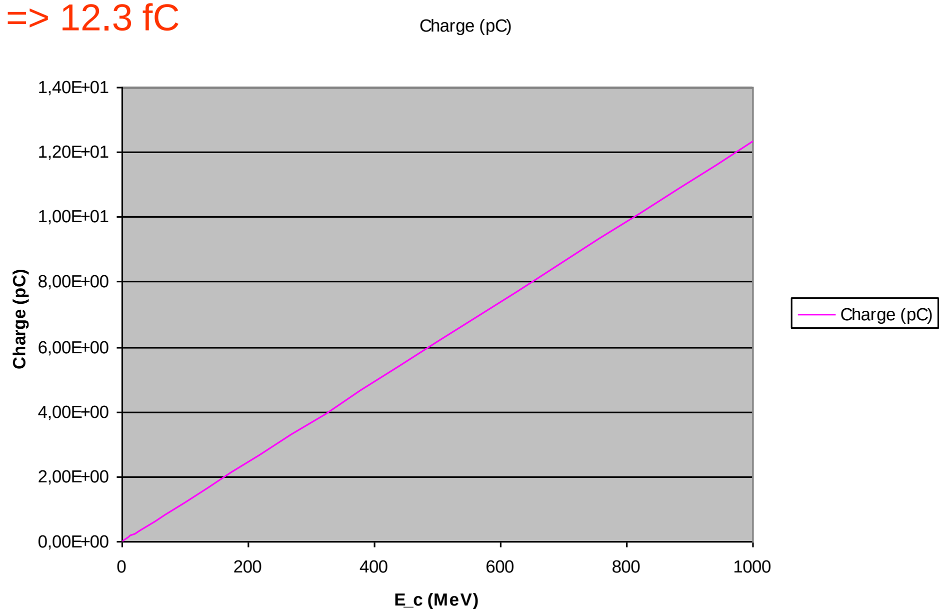

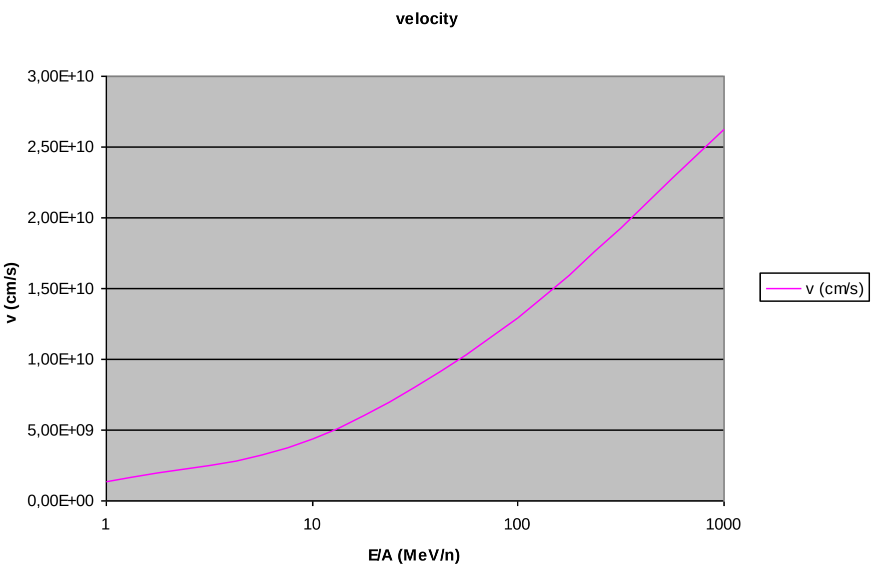

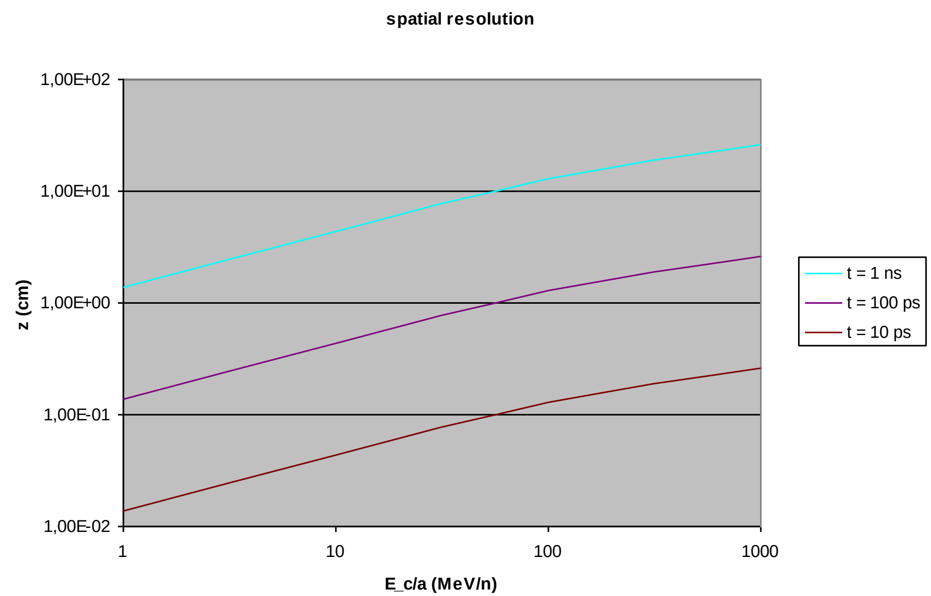

Croissance du diamant Chemical Vapor Deposited (CVD)

Synthèse à partir du méthane CH_4 et d'hydrogène H_2

Réaction des atomes d'hydrogène avec la surface, création de sites actifs

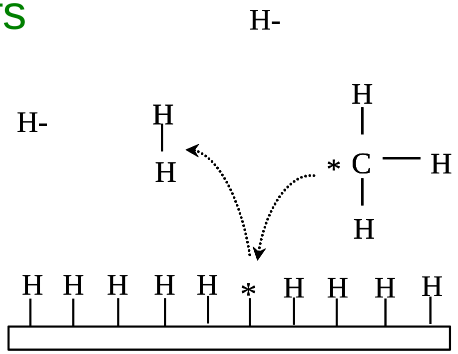

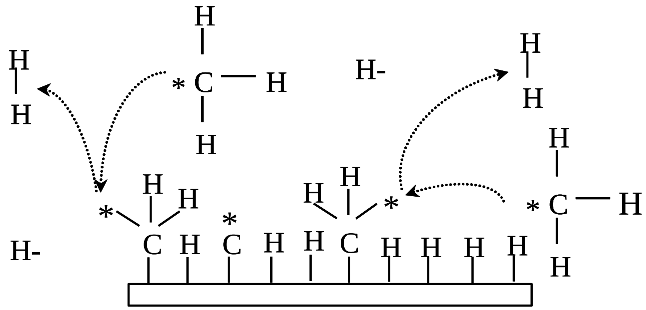

Extraction d'hydrogène

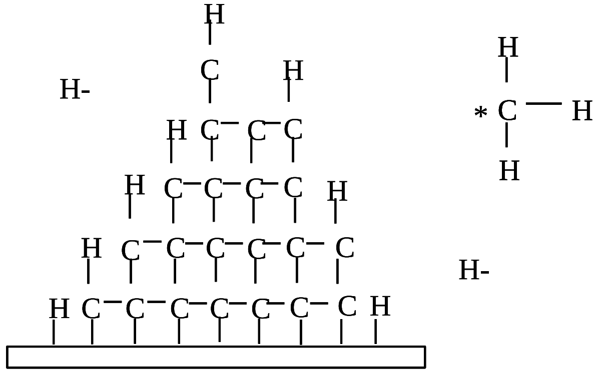

Liaison des atomes de carbone avec leurs voisins : formation du cristal de diamant

H. Hamrita - CEA

III Not-segmented detectors: pollycristalline diamond

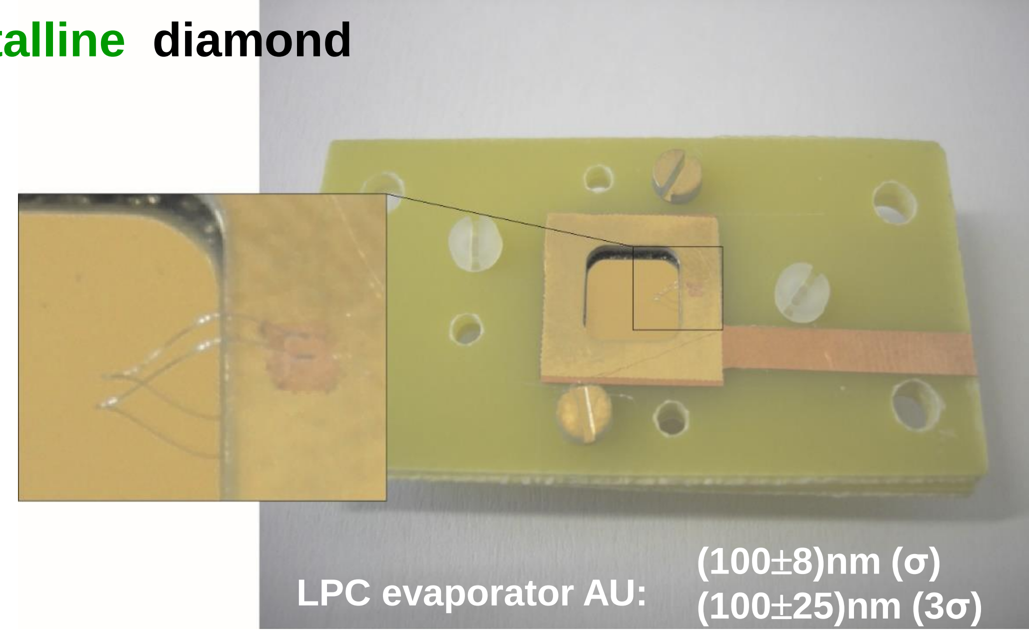

Cleaning: eau régale + ultra-sounds

($1/5\ H_2O + 3/5\ HCl + 1/5\ HNO_3$)

Electrodes: Au (ageing) or Al;

if not: CrAu, NiAu, TiPtAu

Contacts: bonding

(Al wire – soldering T + ultra-sounds)

Voltage: ± 1V/ μ or higher

Irradiation: growth face or nucleation face – to be compared

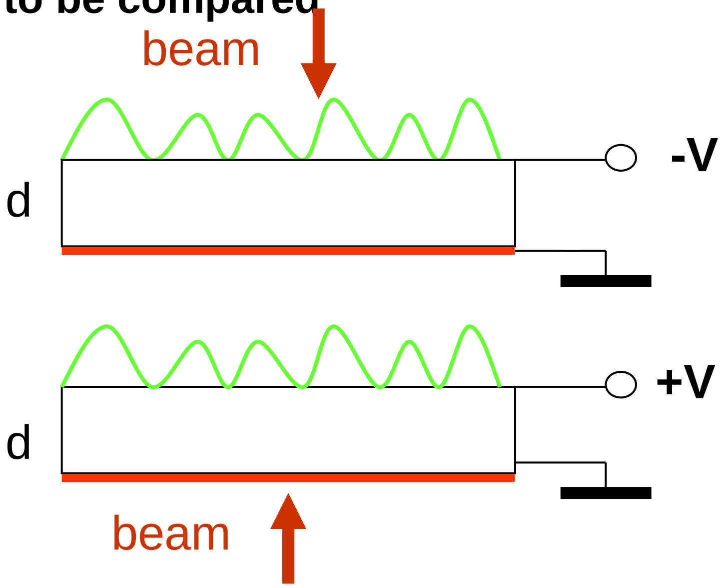

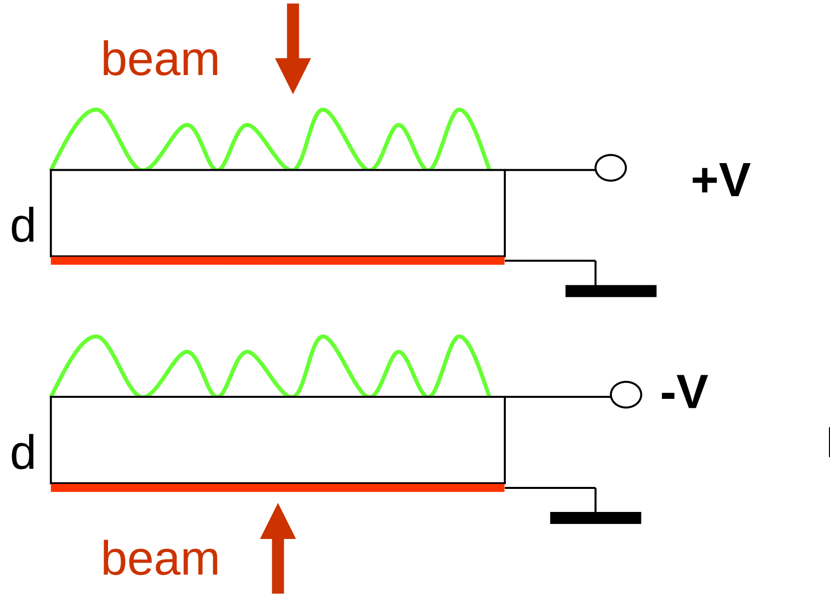

Range<<d: transit electrons

Range<<d: transit holes

III Not-segmented detectors: pollycristalline diamond

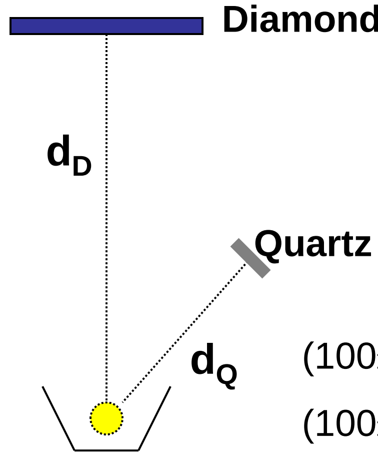

(100±8)nm (σ)

(100±25)nm (3σ)

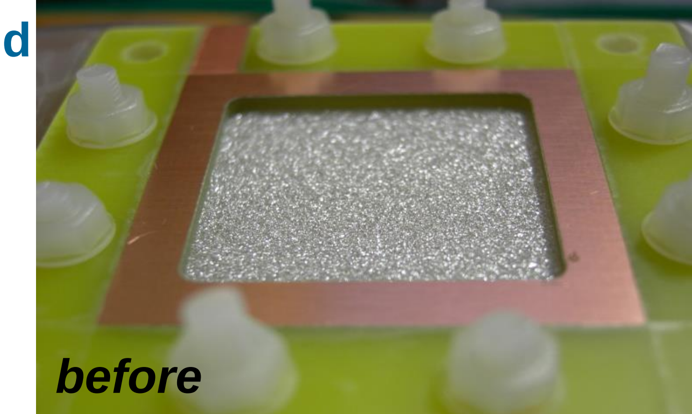

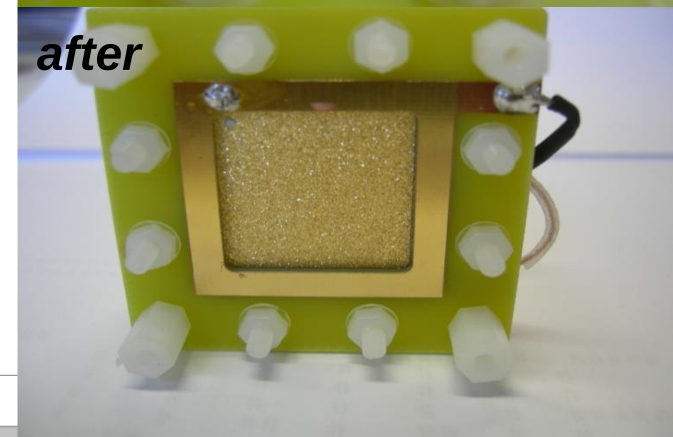

$$e_Q = e_D (d_D / d_Q)^2$$

e – thickness

d - distance

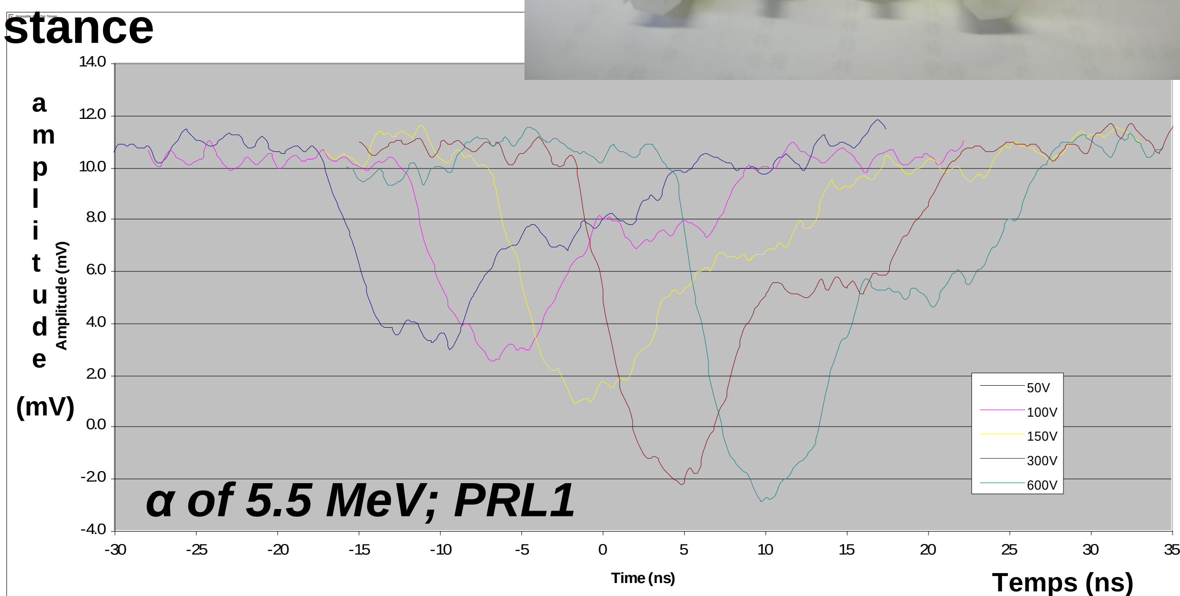

Amplitude variation of signals - different voltages HV

The LPC evaporator – J. Perronnel :

18 Juin 2015 Dispositifs & Installations

Incomplete collection of charge carriers: when the HV increases, the amplitude increases, the collection being improved

Company 1:

det1: P1N ELA (as grown) 300 µ

det2: P2 ELP 500 µ

Tests of not-segmented detectors in HI beams

SC	3,5 g/cm3
PC ELP	3,4
PC ELA	3,3
PC ELS	2,9

Electronics & Acquisition:

GSI:

- classical

GANIL:

- MATACQ – VME (400 MHz BW -> 0,9ns; 2GHz sampling)

- oscillo LeCroy 64Xi (600 MHz BW -> 0,6ns; 10Gs/s)

Alumine

det1 **Comp1 P1N ELA** 300 µm

det2 **Comp1 P2 ELP** 500 µm

det3 **Company 2** 630 µm

det4 **Company 2** 200 µm

Company 3

det5 165 µm

det6 100 µm

det7 70 µm

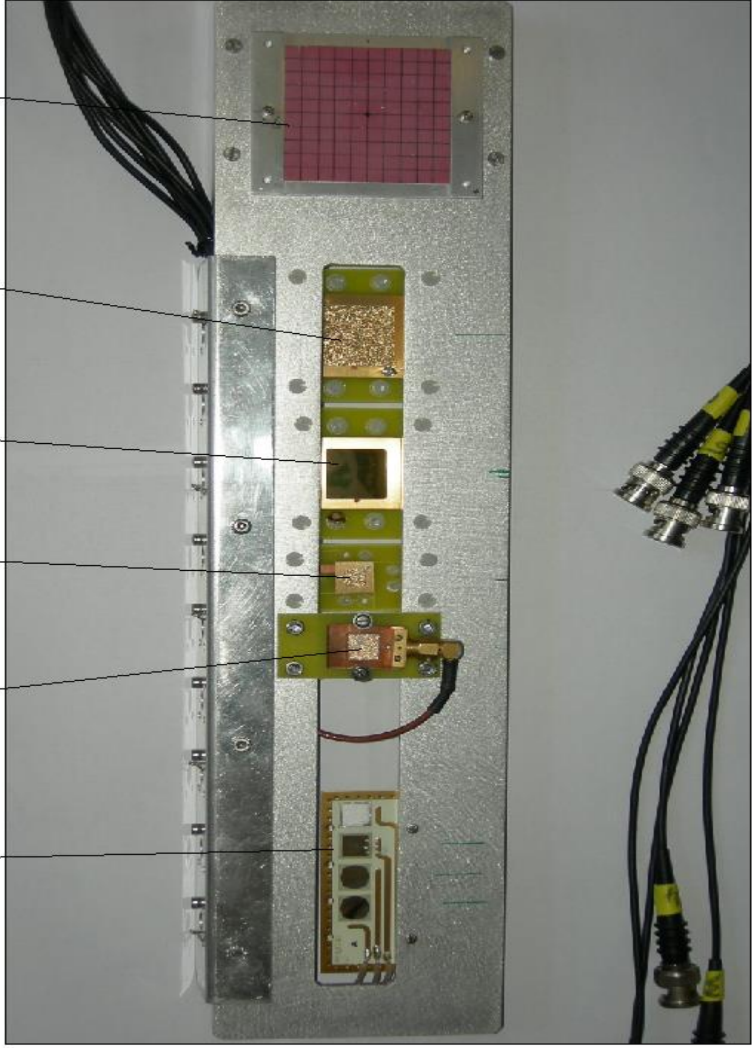

Table 2. Energy per nucleon and range of the ions which have served to test the uni-strip diamond detectors.

& a 500µ sc tested in 6AMeV 238U beam

~50 m	GSI ^{124}Xe	GANIL ^{58}Ni	GANIL ^{13}C	GANIL ^{13}C	LPC α
E/A (MeV)	50	10.9	11.1	7.3	1.2
Range (µ)	440	63	196	98	15

ε=100% (A. Bräuning Demian)

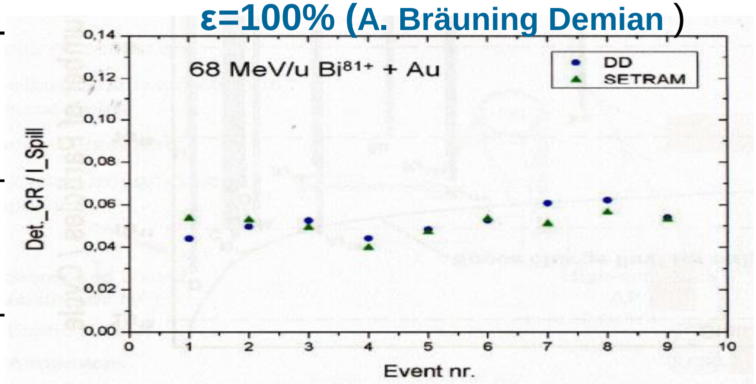

6.2 GeV ^{124}Xe (3.4 GeV in 300 μ)

GSI: ~3*10^7p/spill; ~3*10^6p/det runs of a few min, for hours

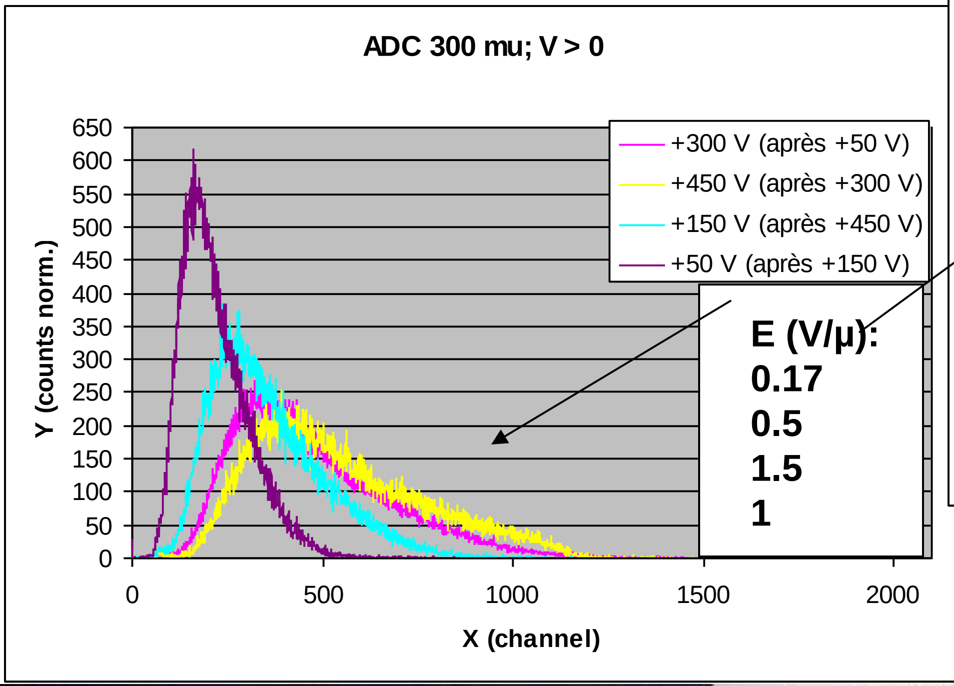

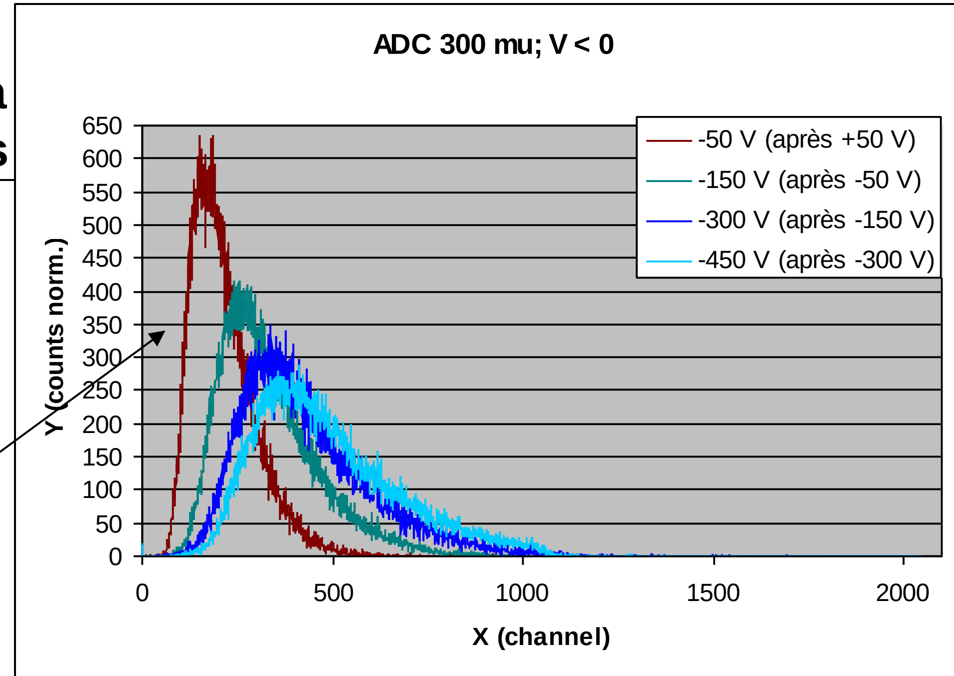

Amplitude spectra: the distribution becomes narrower when the electric field diminishes.

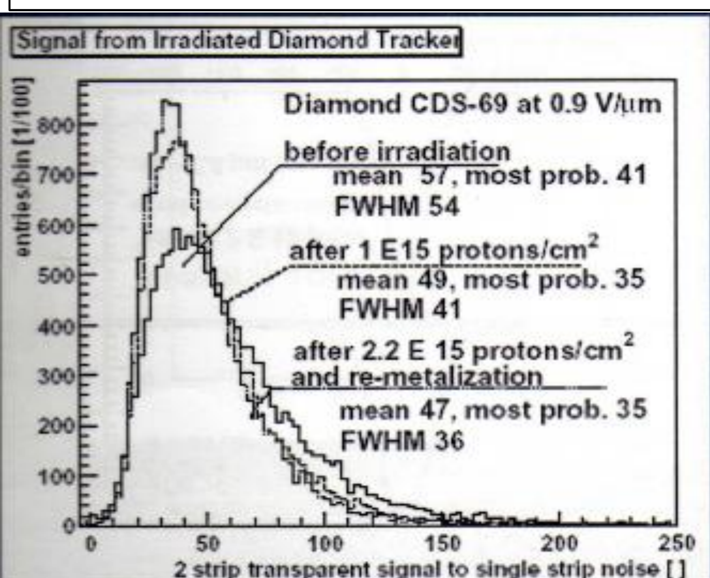

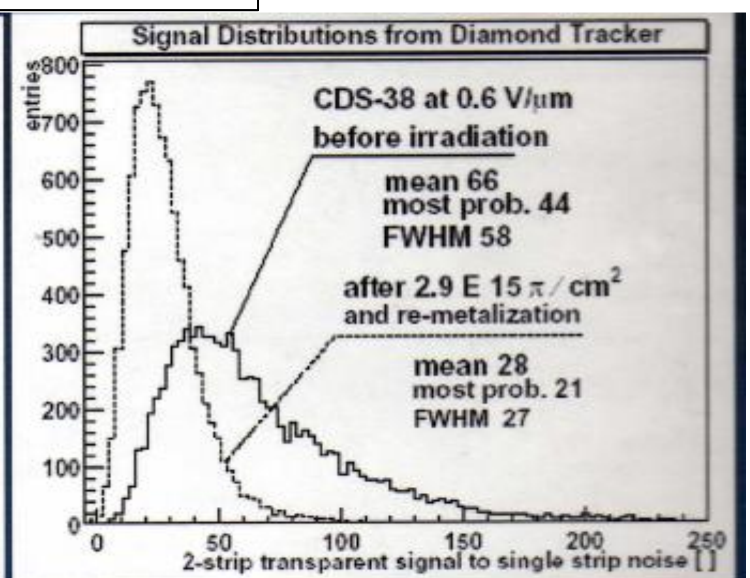

P. Delpierre, RD 42
Journées de prospective du CPPM, 2006

Conjecture: during the irradiation, the electric field may diminish due to the progressive bulk polarization.

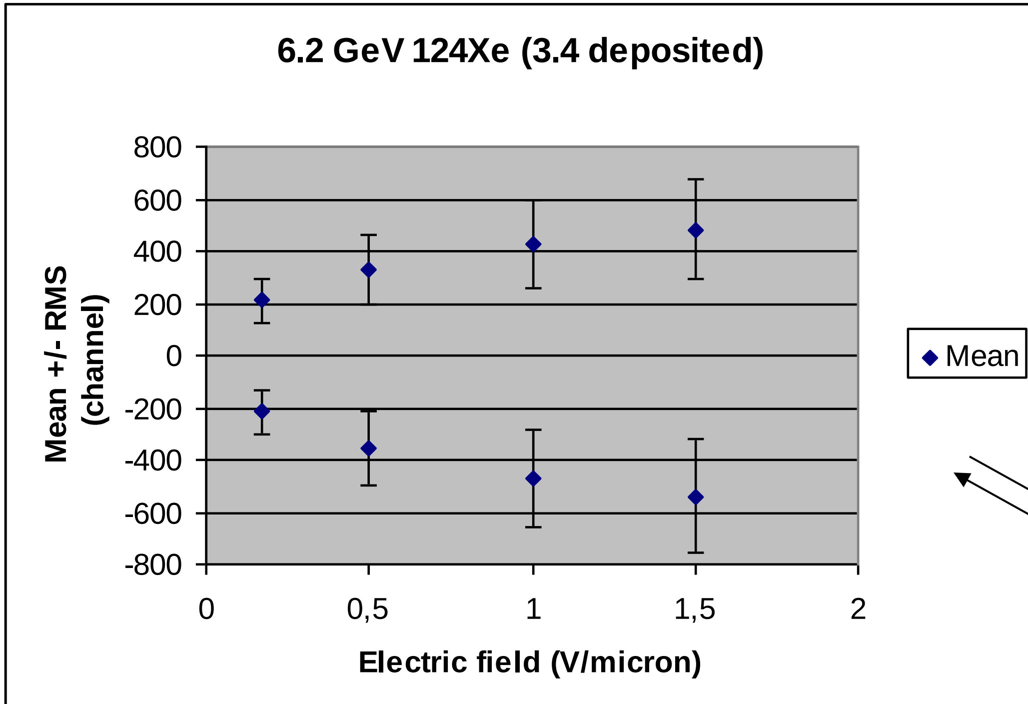

Slightly higher amplitude (~10%) for U > 0, i.e. when the holes coming from the higher carrier density have a shorter drift road.

The relative RMS (%) remains practically the same

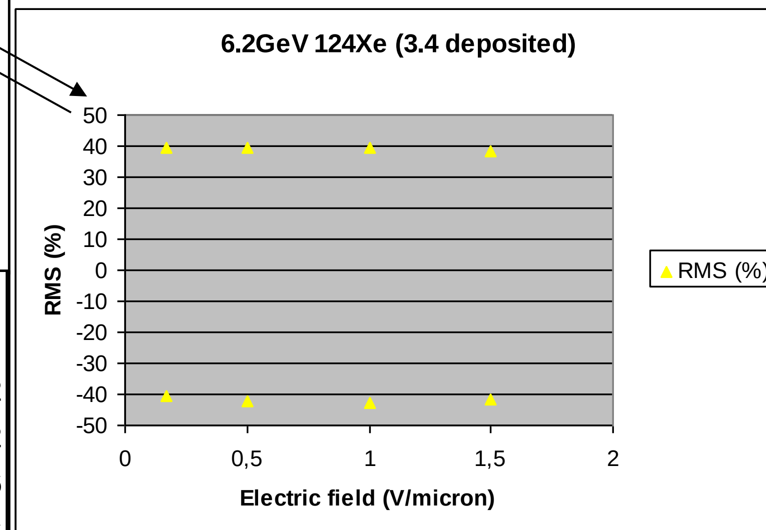

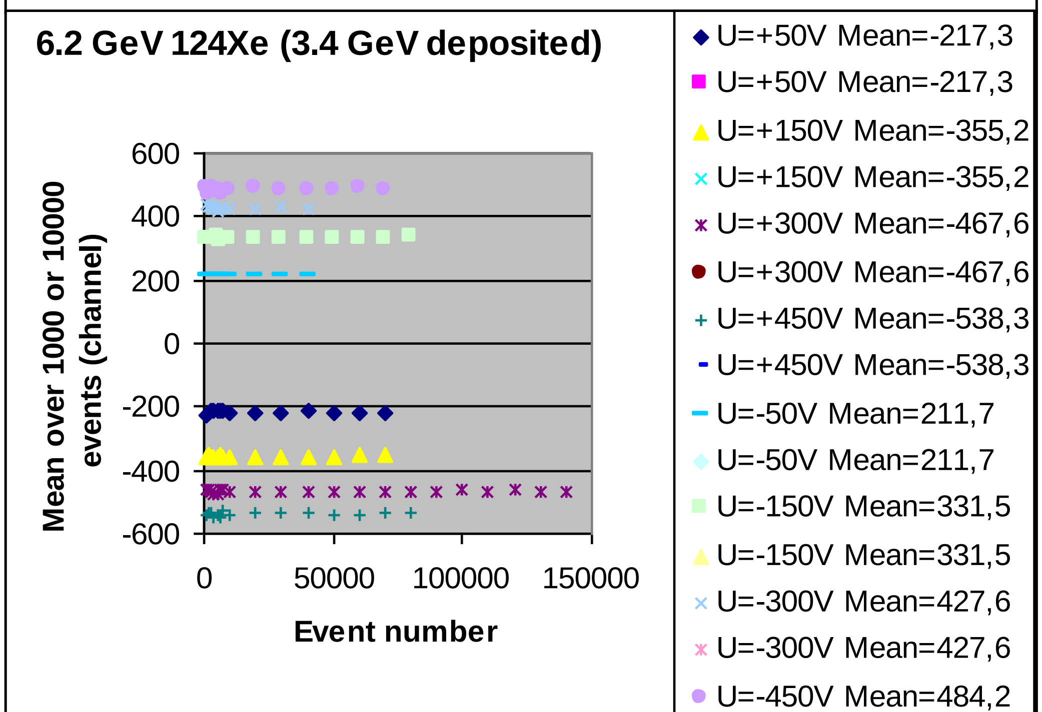

Groups of 1000 or 10000 events, chronologically taped, show the same distribution ==> no signal attenuation observed

Ramo-Shockley theorem: $i(t)=-q(t).\vec{v}(t).\vec{E}^*/1V$

$$i(t) = -q\begin{pmatrix} v \\ 0 \end{pmatrix} \bullet \begin{pmatrix} 1V/d \\ 0 \end{pmatrix}$$

$q_e=-e$; $q_h=e$

$v_e=\mu_e*E$; $v_h=\mu_h*E$

$$\mathbf{v}_e = \begin{pmatrix} \pm v_e \\ 0 \end{pmatrix}; \mathbf{v}_h = \begin{pmatrix} \pm v_h \\ 0 \end{pmatrix} \qquad E^* = \begin{pmatrix} 1V/d \\ 0 \end{pmatrix}$$

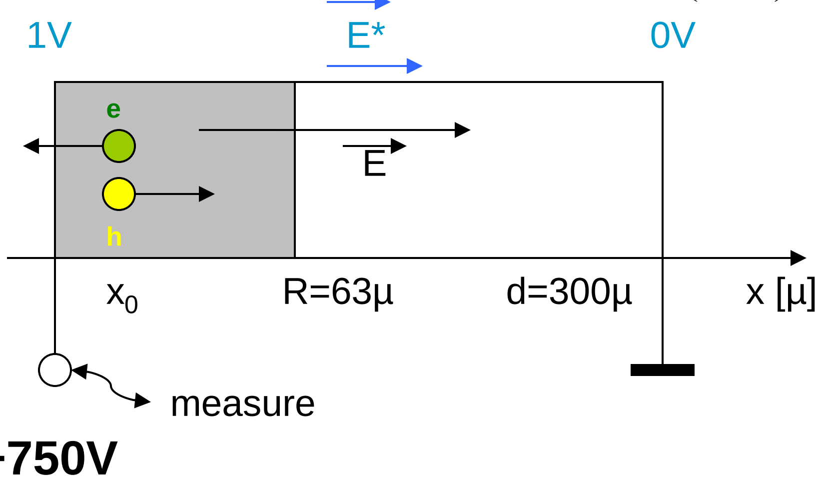

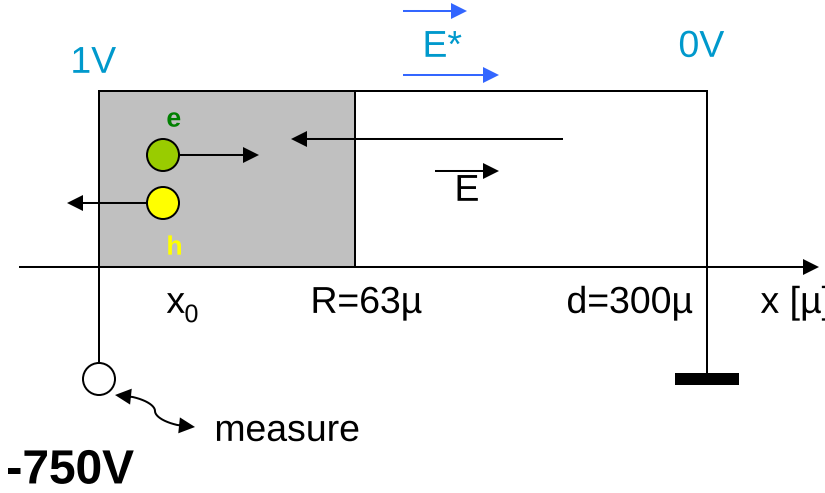

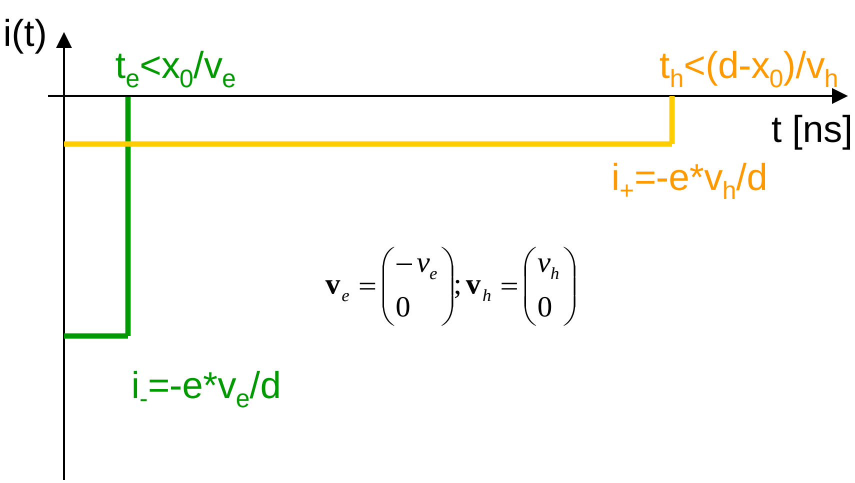

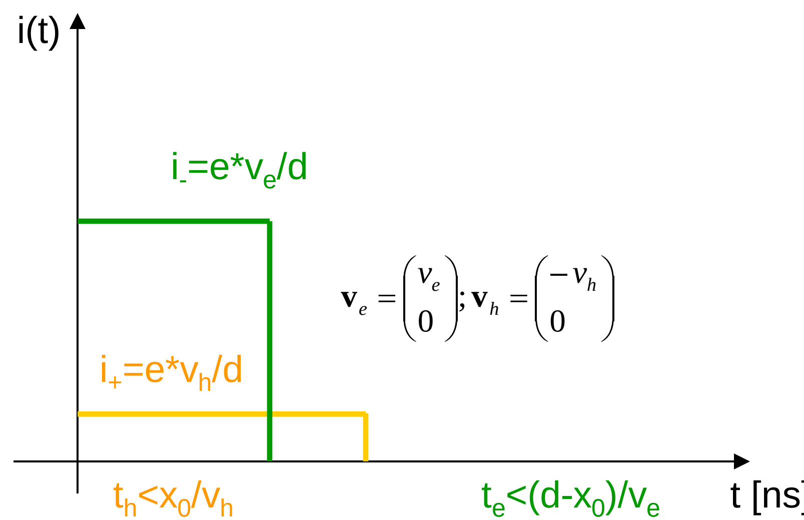

E =750V/300μ=2,5V/μ; v_h=v_e=v_sat=120μ/ns

^{58}Ni; E=634MeV; R=63μ; Q_G=7,813 pC

^{58}Ni; E=634MeV; R=63µ;

Q_G=634*10^{+6}eV/13eV*1,602*10^{-19}C=7,813 pC

Q_{e_i}=-0,807 pC;
Q_{h_i}=-6,979 pC;
Q_i=-7,787pC

Q_{e_i}=6,979 pC;
Q_{h_i}=0,807 pC;
Q_i=7,787pC

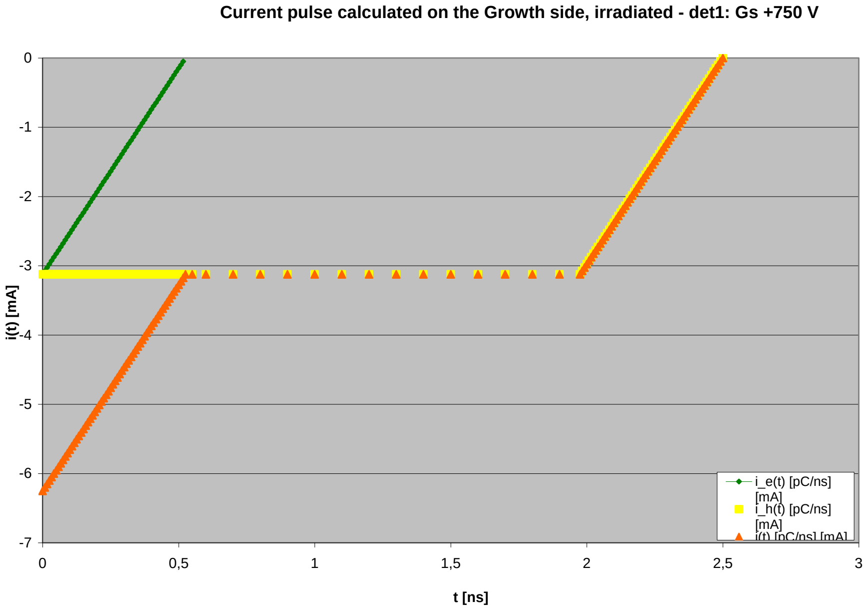

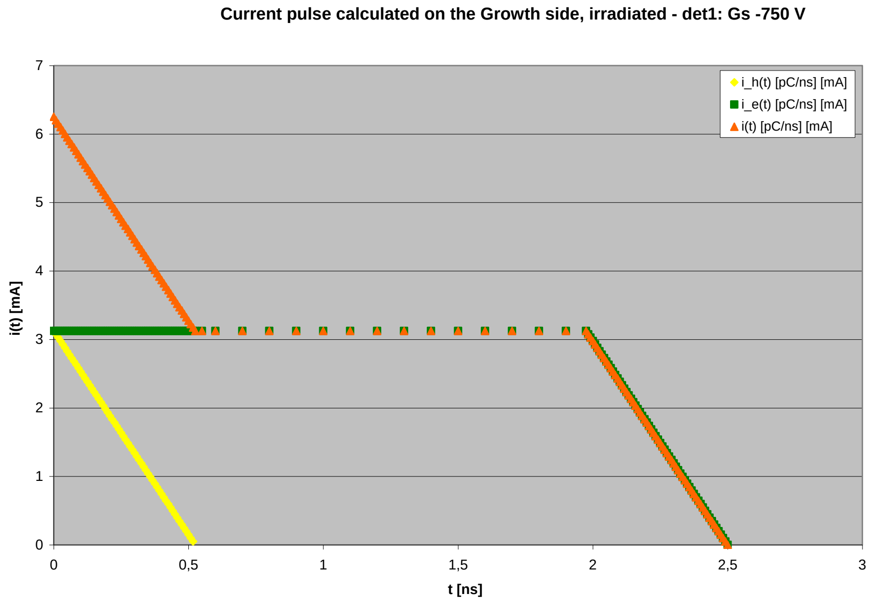

E =750V/300µ=2,5V/µ; v_h=v_e=v_sat=120µ/ns

holes: long drift way

electrons: long drift way

$-dq/dx = q/w_s$

$q(x) = q_0 \exp(-x/w_s)$

$q(t) = q_0 \exp(-t/t_s)$

Schubweg (feed path) $w_s \approx 200\ \mu$ (E. Griesmayer et al., "High-Resolution Energy and Intensity Measurements with CVD Diamond at REX-ISOLDE", CERN BE-Note-2009-028); $t_s = w_s/v\_sat = 1{,}67\,ns$

$$Q_{e\_C} = Q_G \frac{w_s}{R}\left(1 - e^{-\frac{R}{ws}}\right)$$ **= -6,072 pC;**

$$Q_{h\_C} = Q_G \frac{w_s}{R}\left(e^{-\frac{d-R}{ws}} - e^{-\frac{d}{ws}}\right)$$ **= -2,049 pC;**

$$Q_{h\_C} = Q_G \frac{w_s}{R}\left(1 - e^{-\frac{R}{ws}}\right)$$ **= +6,072 pC;**

$$Q_{e\_C} = Q_G \frac{w_s}{R}\left(e^{-\frac{d-R}{ws}} - e^{-\frac{d}{ws}}\right)$$ **=+2,049 pC;**

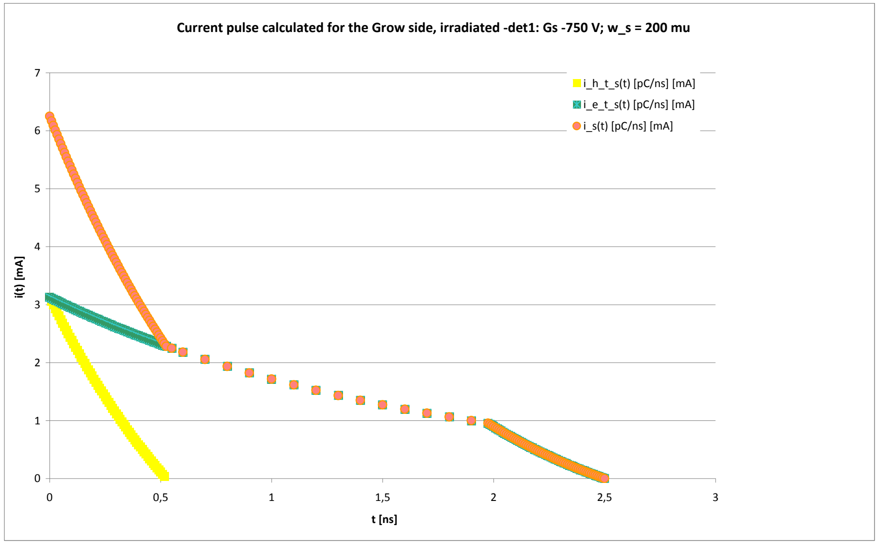

Q_{e_i}=-0,728 pC;
Q_{h_i}=-3,773 pC;
Q_i=-4,500 pC

holes: long drift way

Q_{e_i}=+3,773 pC;
Q_{h_i}=+0,728 pC;
Q_i=+4,500 pC

electrons: long drift way

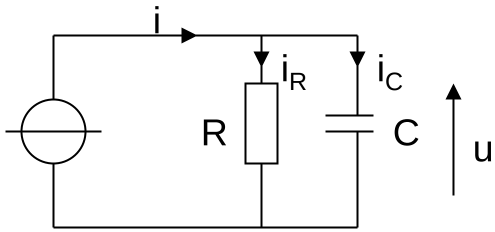

C = 89 pF;
R = 50 Ω;
τ=RC=4,45 ns

$$i(t) = \frac{u(t)}{R} + C\frac{du(t)}{dt}$$

w(1/3) = 7,8 ns
tr(10%90%) = 1,4 ns
Q_i~4,5 pC

MATACQ – VME (400 MHz BW) 0,9ns 70 m cable

$i(t)=I_{0j}+a_jt+b_jt^2$; j=1,2,3

$u(t)=D_j{*}\exp(-t/\tau)+V_{0}j+A_jt+B_jt^2$

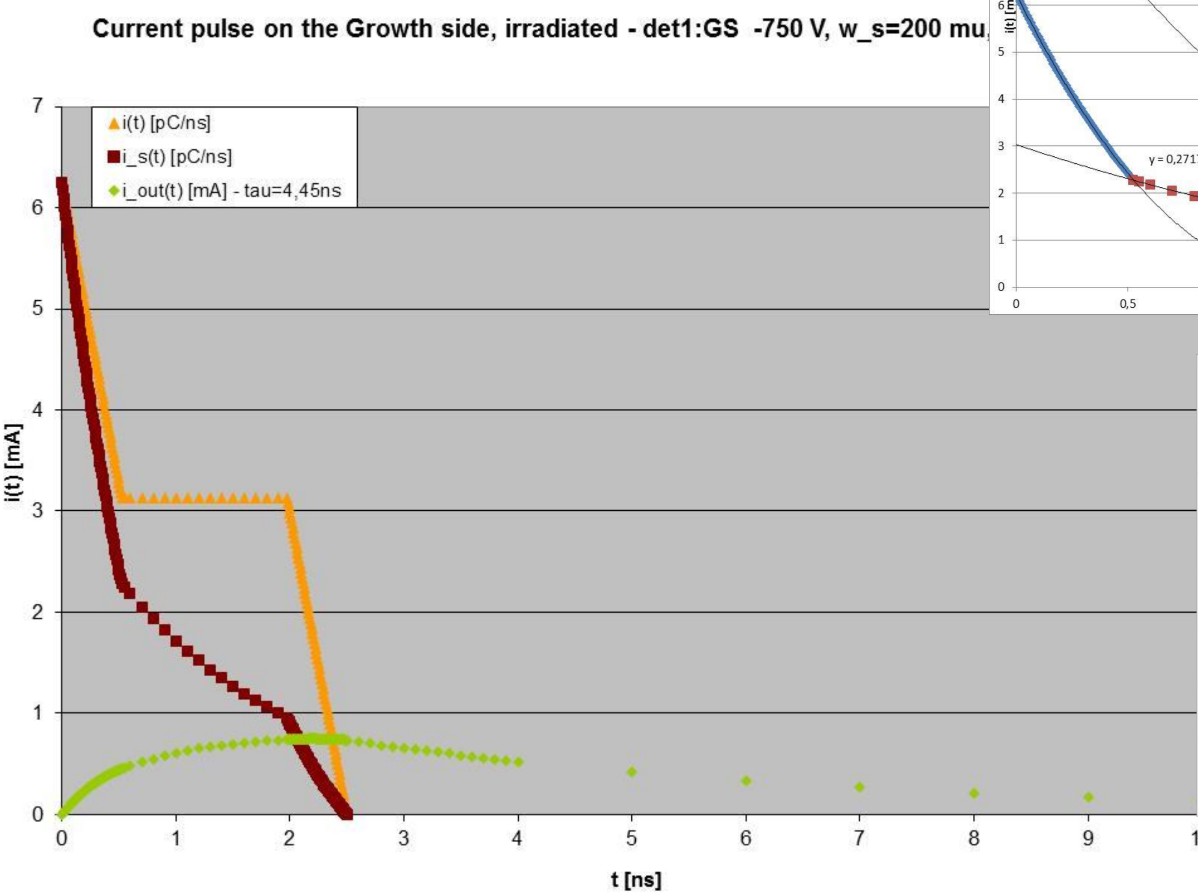

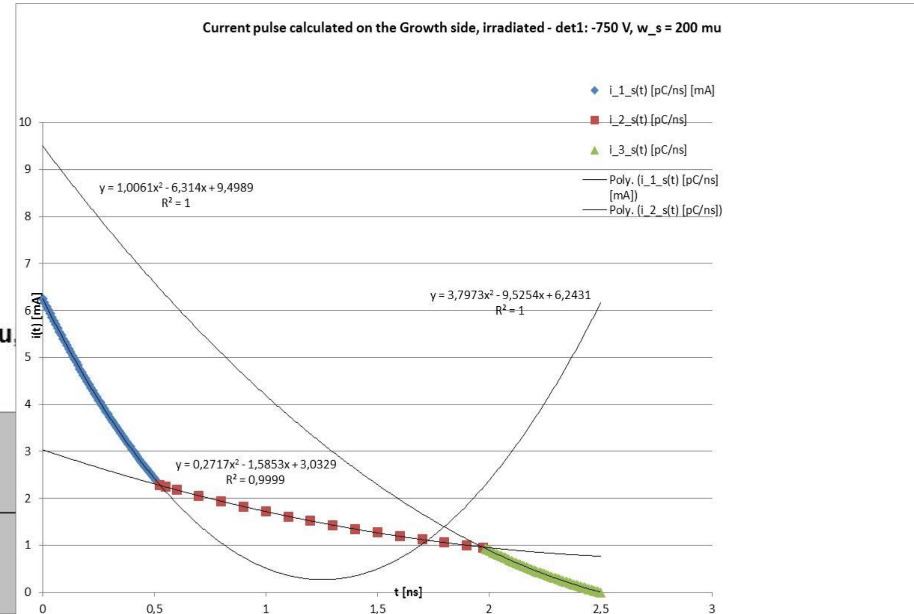

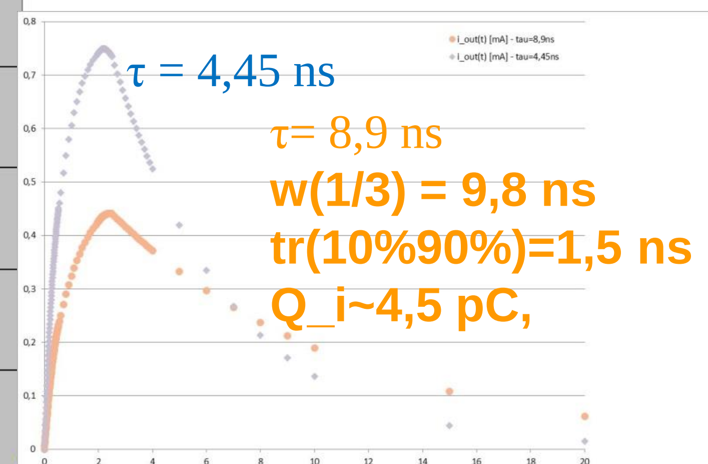

τ = 4,45 ns

τ= 8,9 ns

w(1/3) = 9,8 ns
tr(10%90%)=1,5 ns
Q_i~4,5 pC,

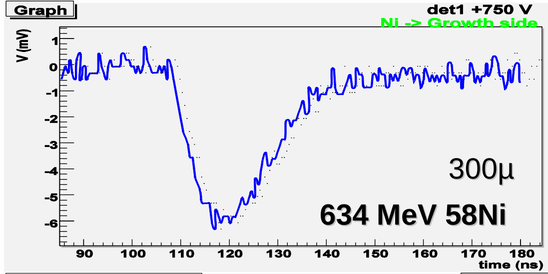

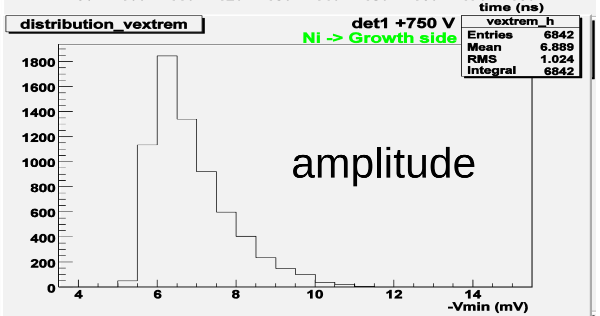

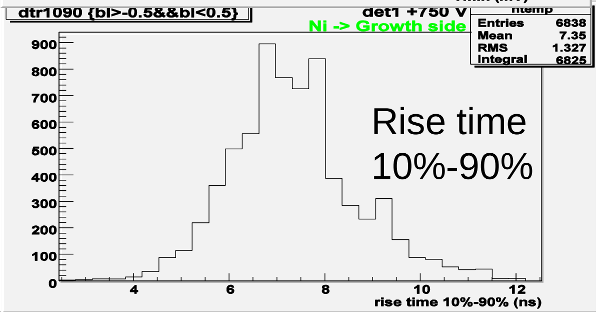

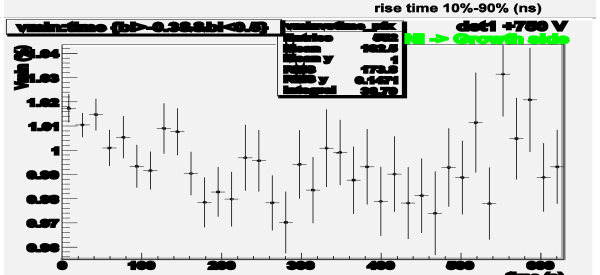

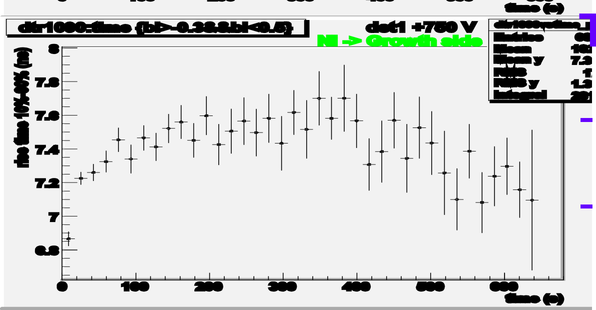

d - thickness; R – range: R<<d

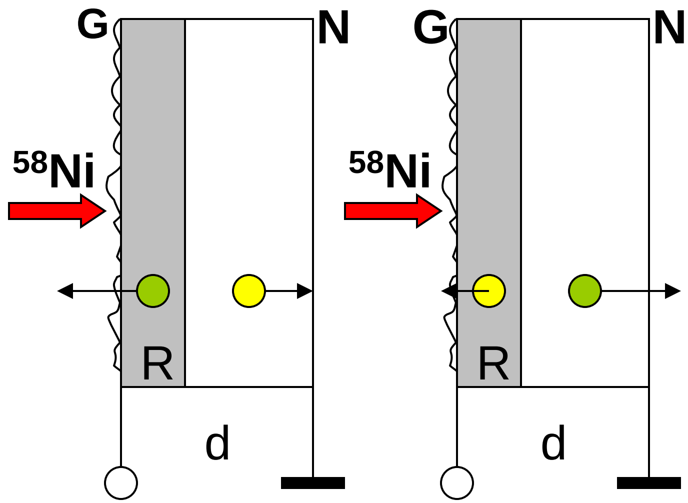

+750V

$0 \leq S_e \leq R$

$d-R \leq S_h \leq d$

-750V

$0 \leq S_h \leq R$

$d-R \leq S_e \leq d$

favourable

S_e – drift **électrons -**

S_h – drift **holes +**

Tests - not-segmented detectors:

- $S_h < S_e$ – favourable
- d adequate to R

E=2,5V/µ

GANIL – SME: ~10^4 pps

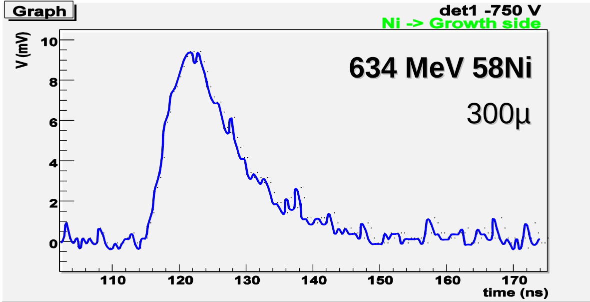

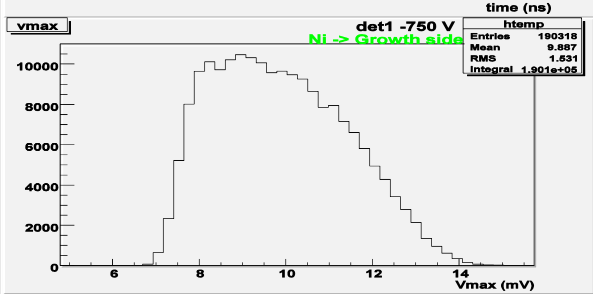

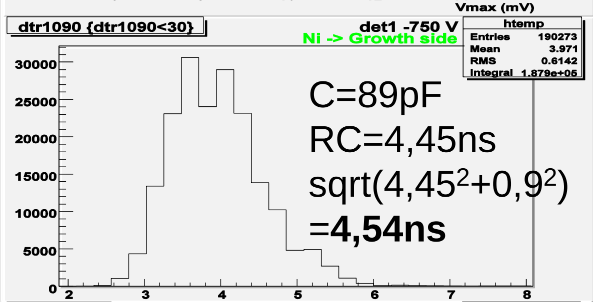

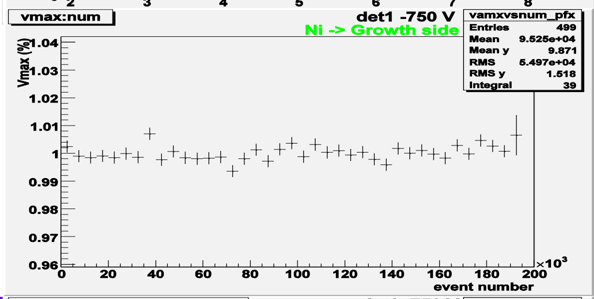

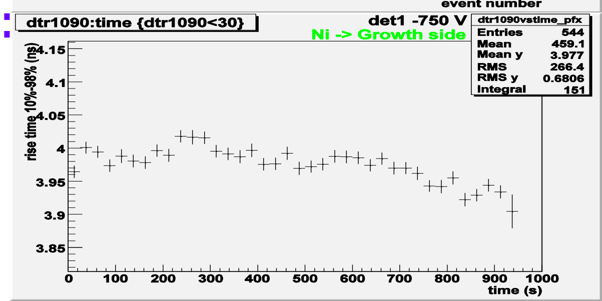

300 µ; E = 2,5 V/µ

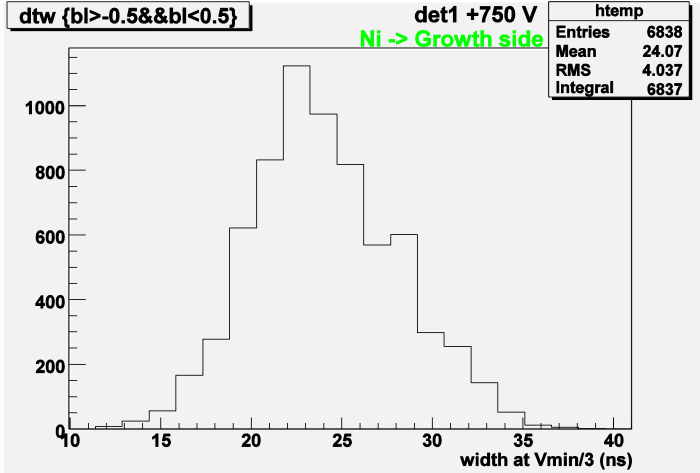

Width at 1/3Vextrem (ns)

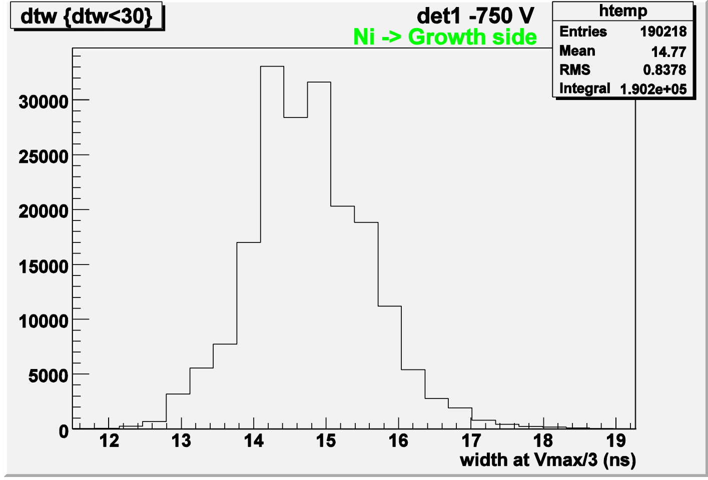

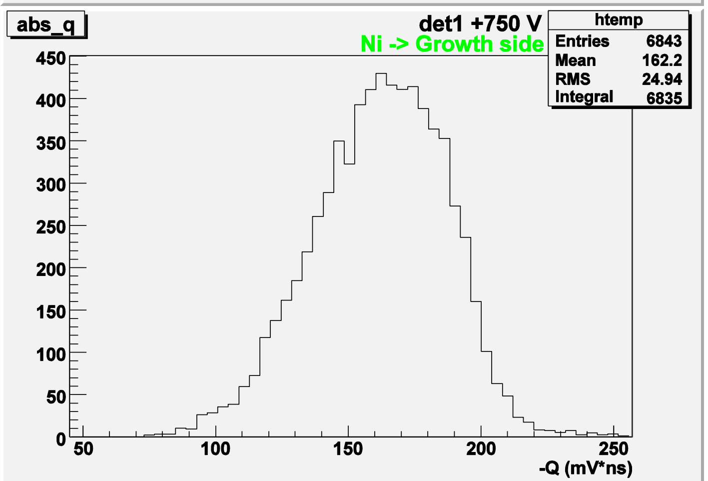

Charge (mV*ns)

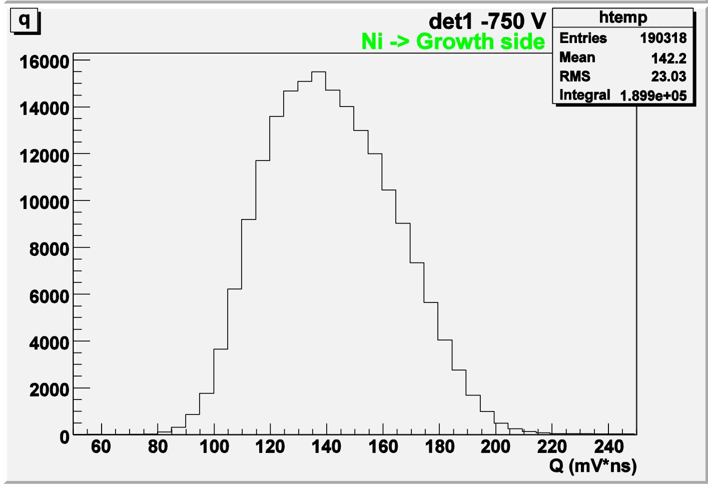

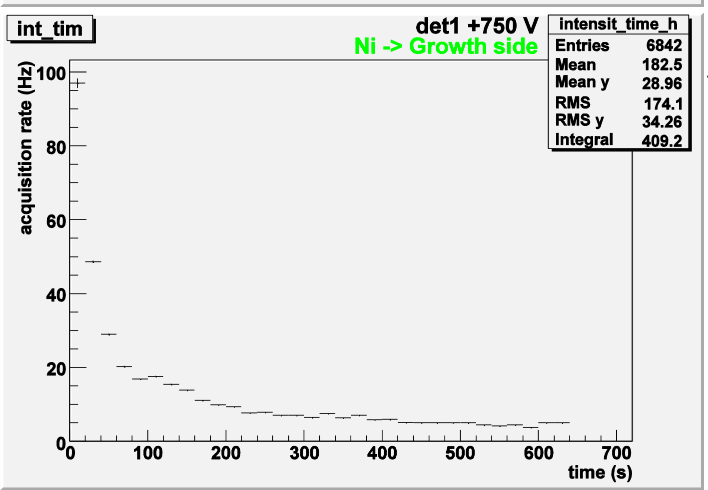

Acquisition rate (Hz)

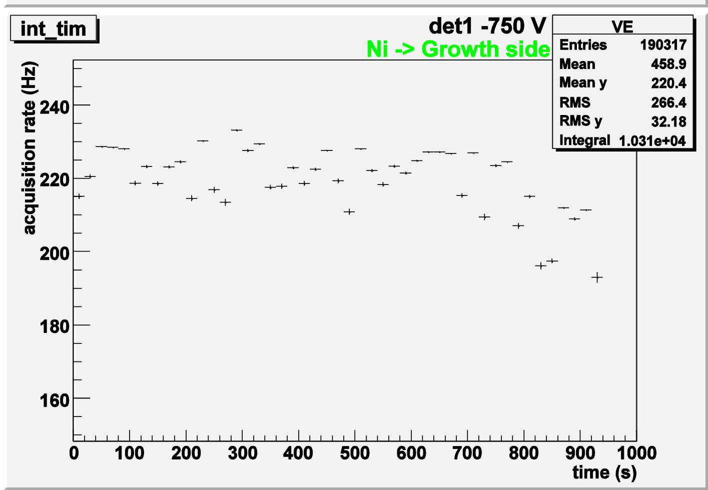

d - thickness; R – range: R<<d

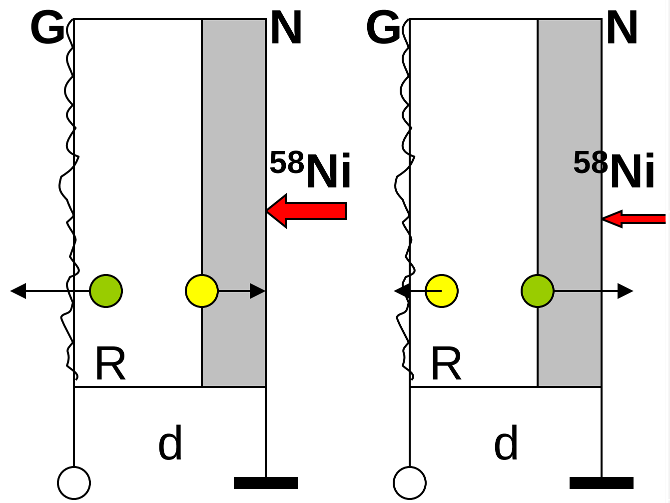

+750V

$0 \leq S_h \leq R$

$d-R \leq S_e \leq d$

favourable

-750V

$0 \leq S_e \leq R$

$d-R \leq S_h \leq d$

S_e – drift **électrons -**

S_h – drift **holes +**

Tests - not-segmented detectors:

- $S_h < S_e$ – favourable
- d adequate to R

GANIL – SME: ~10^4 pps

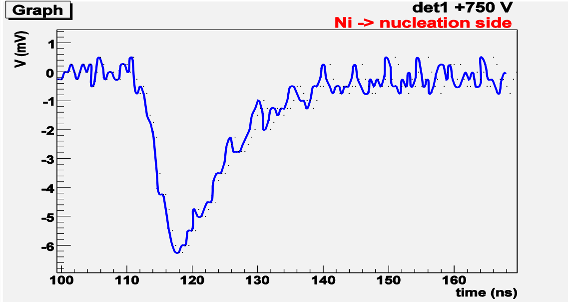

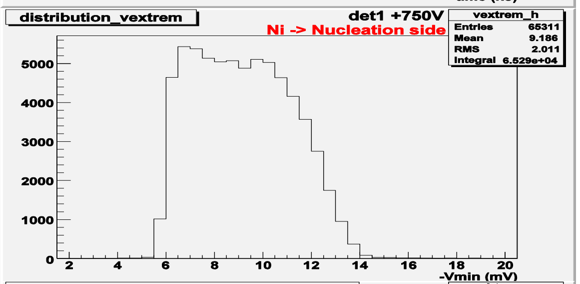

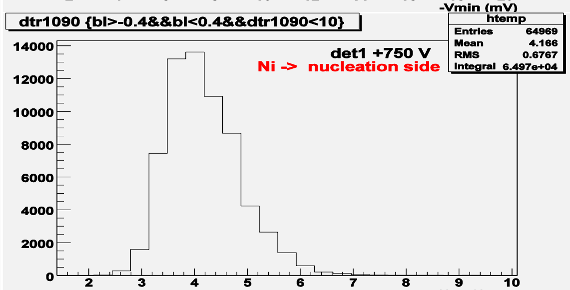

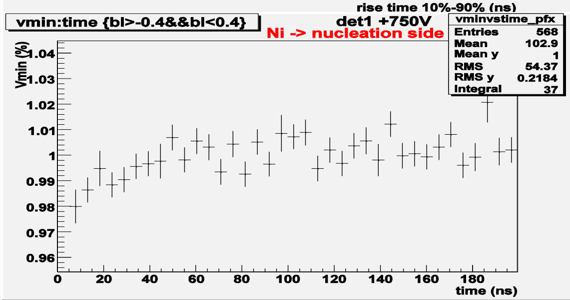

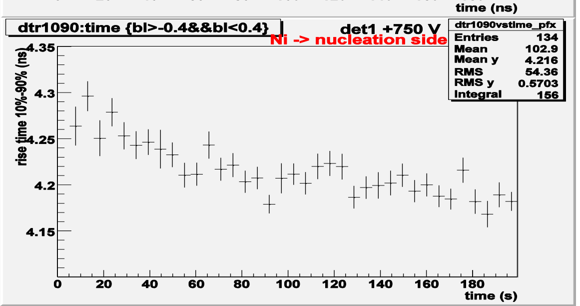

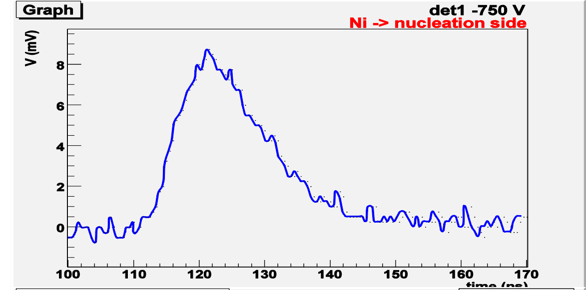

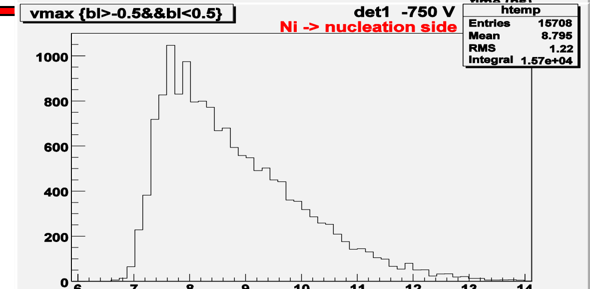

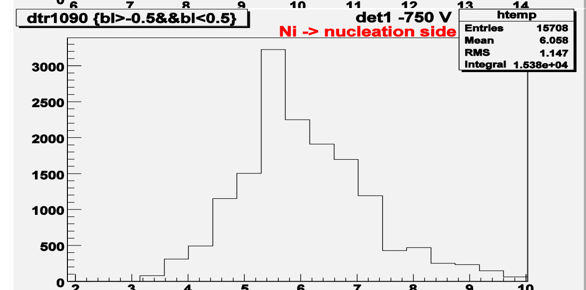

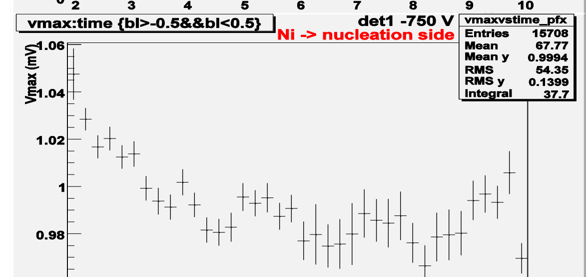

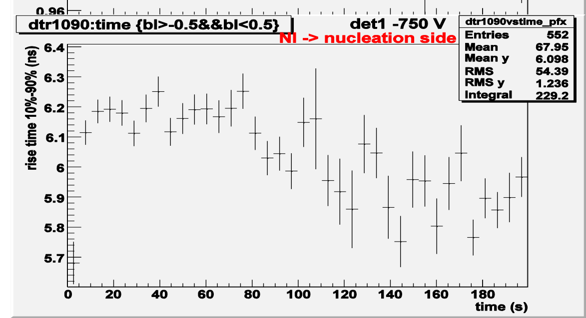

300 μ; E = 2,5 V/μ

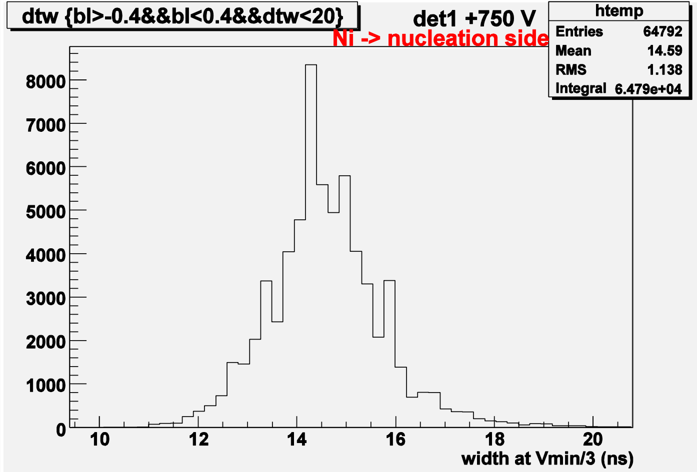

Width at 1/3Vextrem (ns)

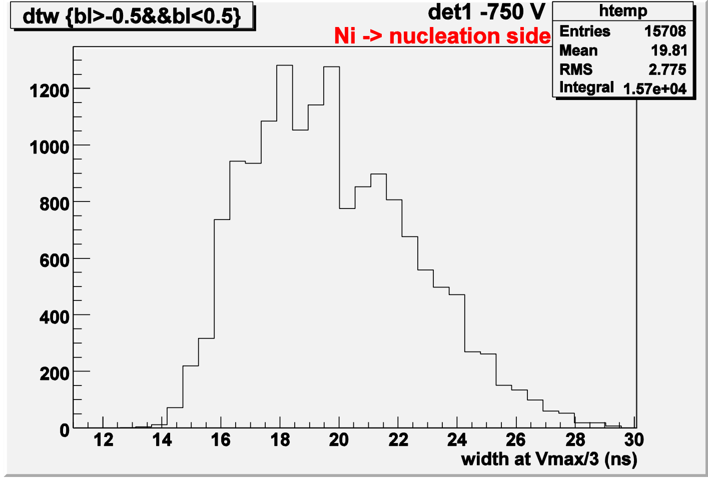

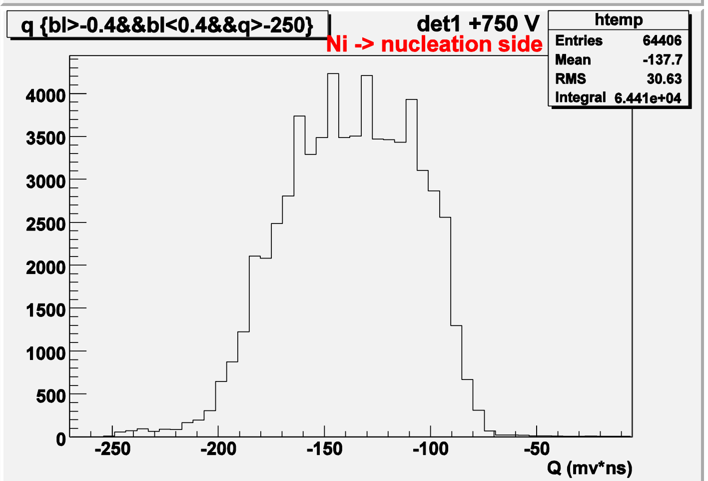

Charge (mV*ns)

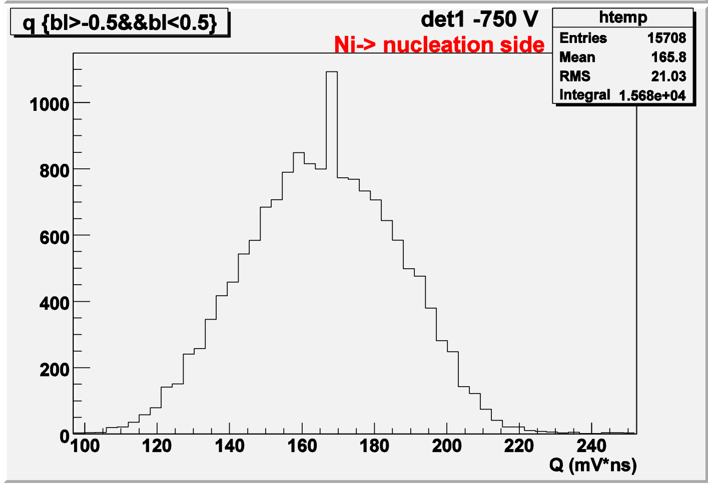

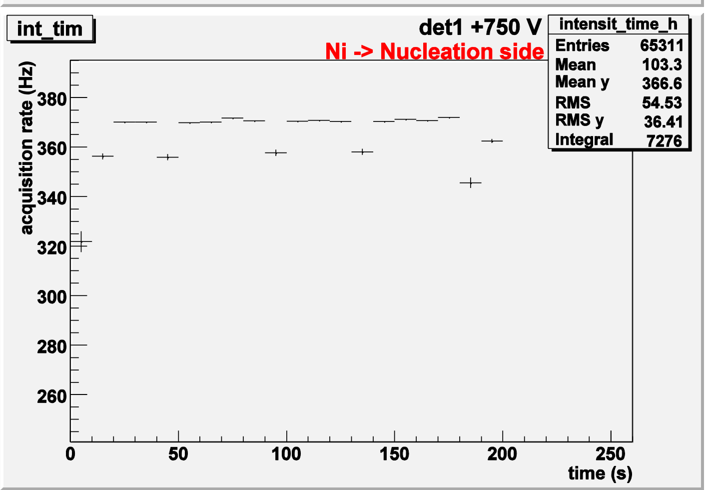

Acquisition rate (Hz)

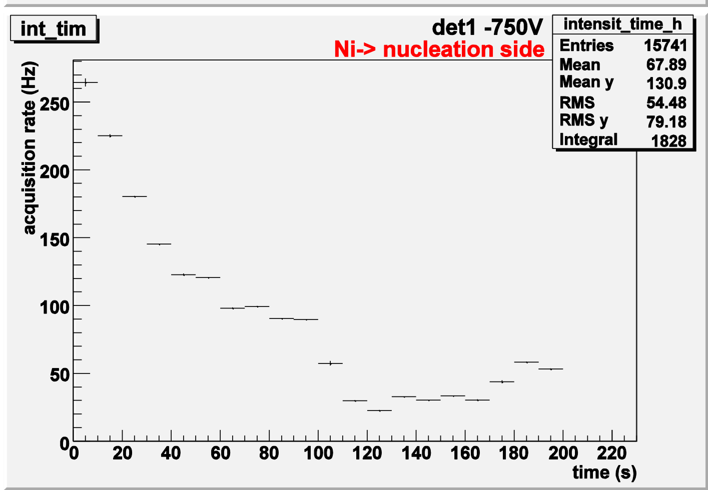

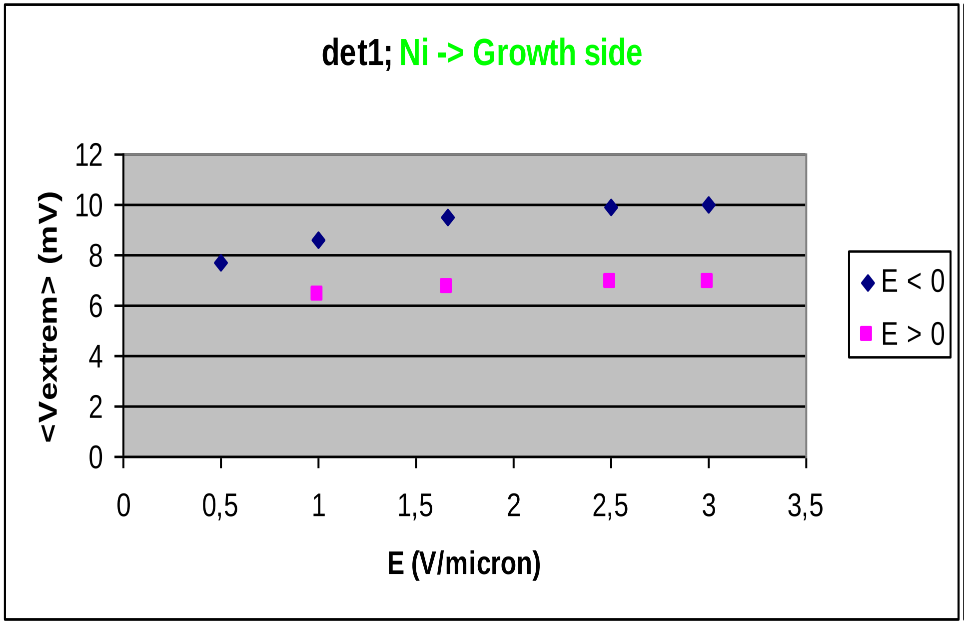

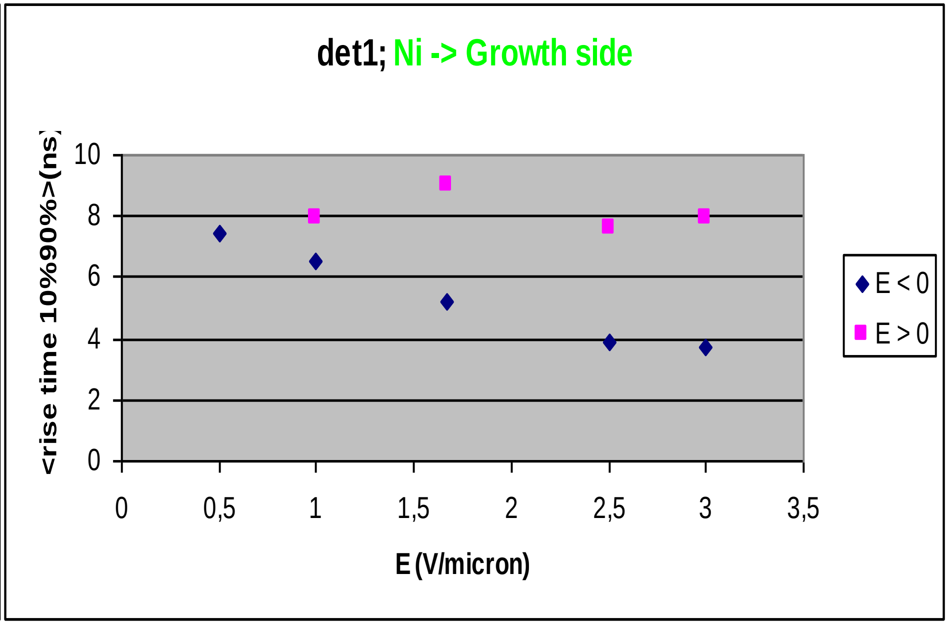

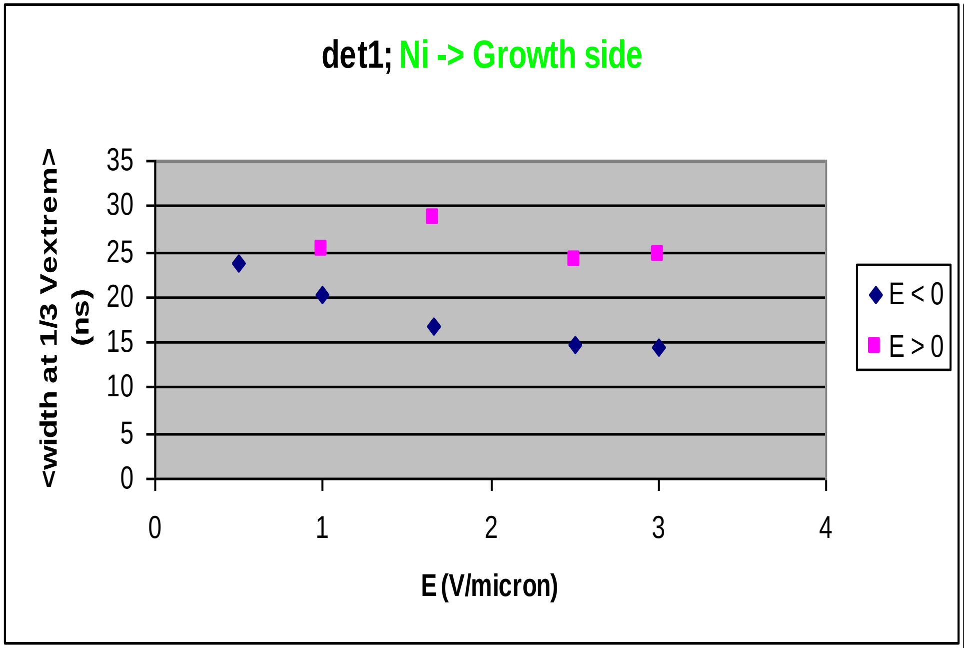

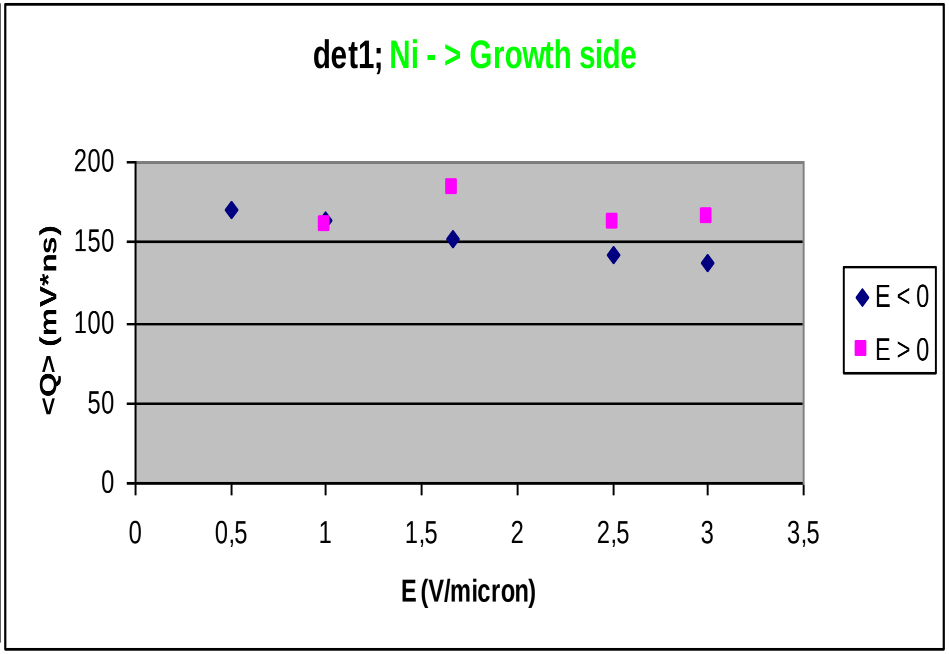

When R<d, the signal is higher and faster when the **electrons** drift on a **longer** way then the **holes**.

Similar results for det2

Table 3. Synthetic results concerning the shape of the signal induced by **634 MeV ^{58}Ni** ions, having a **range of ~ 60 µm** in a uni-strip diamond detector **P1N ELA of 300 µm** at **E = 2,5 V/µ** .

irradiated face	**G face U (V) long tranzit**	<V_{extrem}> (mV)	Rms V (mV)	<Q> (mV*ns)	Rms Q (mV*ns)	tr (ns)	rms tr (ns)	<$w_{1/3}$> (ns)	Rms w (ns)
G	+750 holes	6.9	1.0	162	25	7.4	1.3	24.1	4.0
G	-750 electrons	9.9	1.5	142	23	4.0	0.61	14.8	0.84
N	+750 electrons	9.2	2.0	138	31	4.2	0.68	14.6	1.1
N	-750 holes	8.8	1.2	166	21	6.1	1.1	19.8	2.8

Faster and higher signals are generally preferred for beam monitoring. The conclusion emerging from Table 2 is that, when **the range of the ion is much shorter then the detector thickness** and the distances of drift for the two types of carriers to the electrodes are different, **the voltage has to be chosen in such a way that the holes have the shortest drift road, regardless of the irradiated side**. This will have several beneficial effects: **higher signal amplitude, shorter signals, characterized by a faster rise time and a shorter fall too.** The quality of the signals, somehow better on the fourth line of the table as compared to that on the first line - both of them concerning the long drift distance for the holes – may show that the signal degradation is a little bit smaller when their road leads to the growth side, with bigger diamond crystallites and therefore a higher quality (for the fourth line) than when their road leads towards the nucleation side, including more graphite (first line).

V (V)	v_e (mu/ns)	v_h(mu/s)	w_s_e (mu)	w_s_h (mu)	I_m (mA)	V_m (mV)	Q_in (pC)	Q_out (MV*ns)	**t_r (ns)**	w_1/3 (ns)
-750	**120**	**120**	**200**	**200**	**0,737**	**36,85**	**4,5**	**225**	**1,34**	**7,78**
-750	**120**	**120**	**180**	**220**	**0,706**	**35,3**	**4,291**	**214,55**	**1,15**	**6,8**
750	**120**	**120**	**180**	**220**	**-0,77**	**-38,5**	**-4,684**	**-234,2**	**1,34**	**6,75**
-750	**120**	**120**	**100**	**100**	**0,481**	**24,05**	**3,01**	**150,5**		
-750	**120**	**120**	**90**	**110**	**0,45**	**22,5**	**2,826**	**141,3**	**0,567**	**6,875**
750	**120**	**120**	**90**	**110**	**-0,532**	**-26,6**	**-3,185**	**-159,25**	**0,86**	**6,85**
-750	**120**	**60**	**180**	**220**	**0,7106**	**35,53**	**4,324**	**216,2**	**1,1235**	**6,75**
750	**120**	**60**	**180**	**220**	**-0,529**	**-26,45**	**-4,655**	**-232,75**	**1,87**	**9,01**
-750	**18**	**12**	**180**	**220**	**0,321**	**16,05**	**4,313**	**215,65**	**2,75**	**16,25**
750	**18**	**12**	**180**	**220**	**-0,251**	**-12,55**	**-4,67**	**-233,5**	**2,1**	**23,36**
-750	**18**	**12**	**90**	**110**	**0,267**	**13,35**	**2,85**	**142,5**	**2,25**	**13,36**
750	**18**	**12**	**90**	**110**	**-0,225**	**-11,25**	**-3,14**	**-157**	**3,06**	**19,25**
-750	***9***	***6***	***88,25***	***116,5***	***0,1844***	***9,22***	***2,82***	***141,32***	***3,5***	***19,25***
750	***9***	***6***	***88,25***	***116,5***	***-0,1614***	***-8,07***	***-3,22***	***-161,46***	***2,88***	***25,12***
-750	***6***	***9***	***88,25***	***116,5***	***0,1536***	***7,68***	***1,54***	***138,97***	***2,33***	***22,9***
750	***6***	***9***	***88,25***	***116,5***	***-0,1838***	***-9,19***	***-3,51***	***-175,54***	***4,6***	***18,11***
-750	**4,5**	**3**	**88,5**	**117,5**	**0,12**	**6**	**2,82**	**141**	**4,66**	**26,45**
750	**4,5**	**3**	**88,5**	**117,5**	**-0,108**	**-5,4**	**-3,29**	**-164,5**	**4,22**	**34,8**

Difficulty: t_r

Kittel mobilities:
e-> 1800 cm2/(Vs) = 180 mu2/(Vns)
h->1200 cm2/(Vs) = 120 mu2/(Vns)

V_e = 9 mu/ns
V_h = 6 mu/ns

➔ **E = 0,05 V/mu instead of 2,5 V/mu**

Or, **plasma delay** – to compare different A,Z

Italics - + MATACQ contribution – via Z Transform

Or, **long cable** contribution to t_r

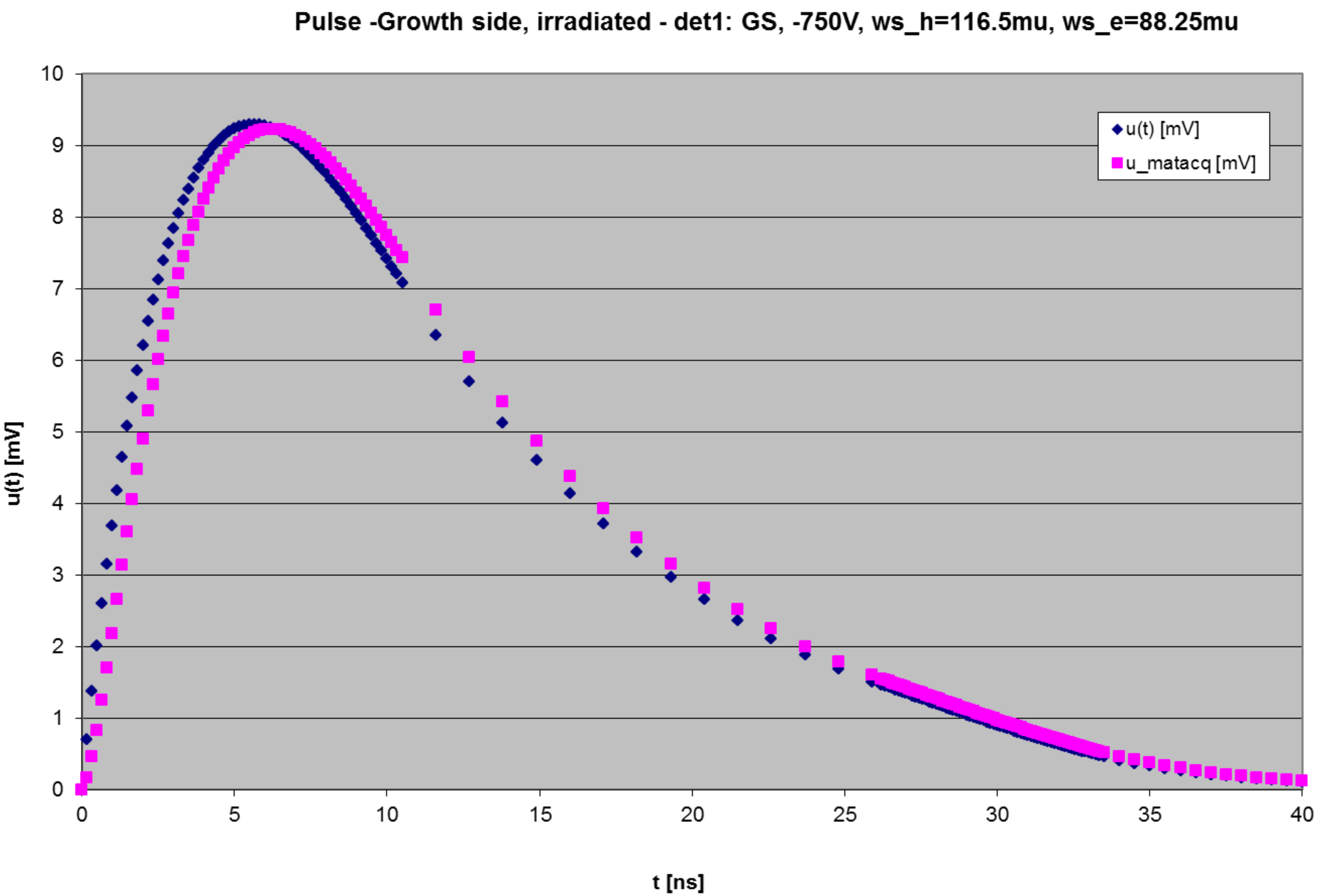
Pulse -Growth side, irradiated - det1: GS, -750V, ws_h=116.5mu, ws_e=88.25mu
u(t) [mV]
u_matacq [mV]
u(t) [mV]
t [ns]
0
1
2
3
4
5
6
7
8
9
10
0
5
10
15
20
25
30
35
40

IV Multi-strip detctors: Company 1 - ELP vs ELS

ELP (Electronic Premium Grade) – processed from a polycrystalline wafer with a starting thickness of 1 mm; the final thickness is achieved by removal from the nucleation surface; therefore, thinner the thickness of an ELP plate is, higher its quality; but under 0.2 mm, the risk of breaking in the process of lapping and polishing is much increasing;
ELS (Electronic Standard Grade) – processed from a polycrystalline wafer with a minimum removal of 100 µm. Comparing the two types of material was one of the objectives of our study.

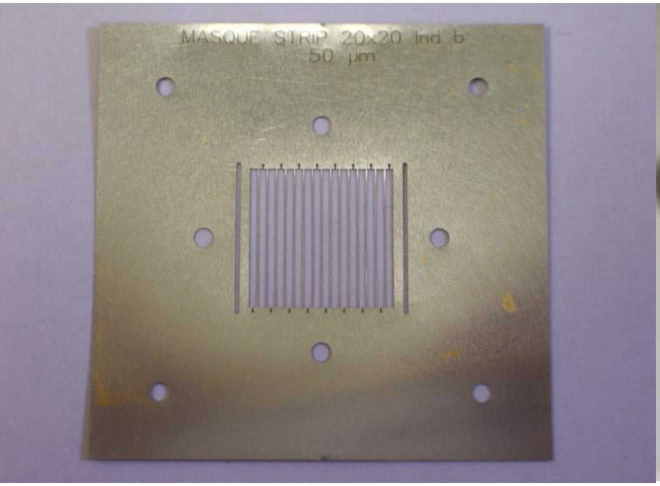

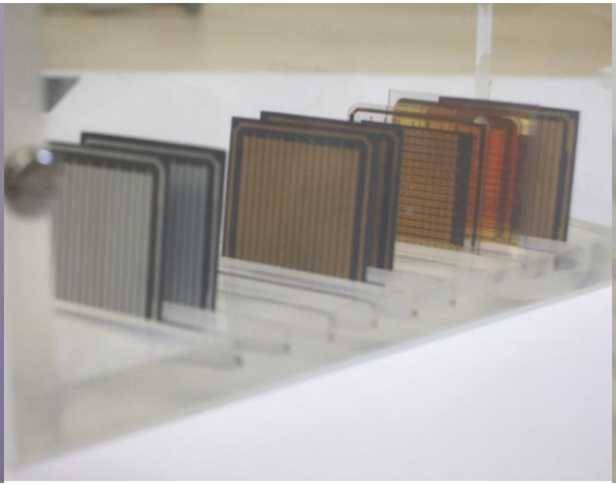

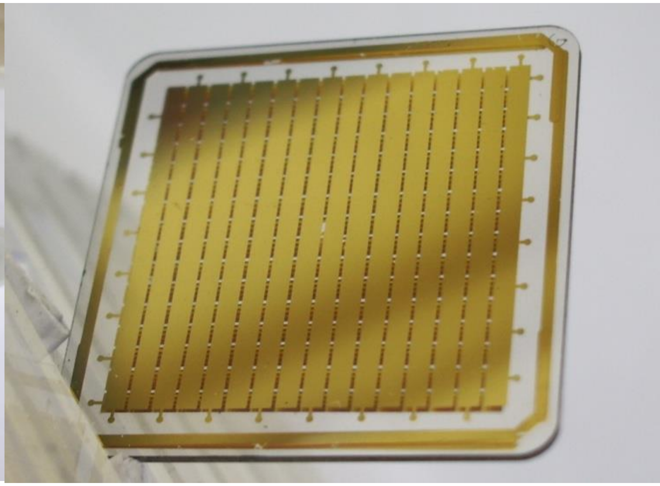

Strip pitch: 0.9mm inter-strip gap: 0.1mm
efficiency: 90%

The BERGER files for the masks & PCBs were done at LPC

Flange and connectors

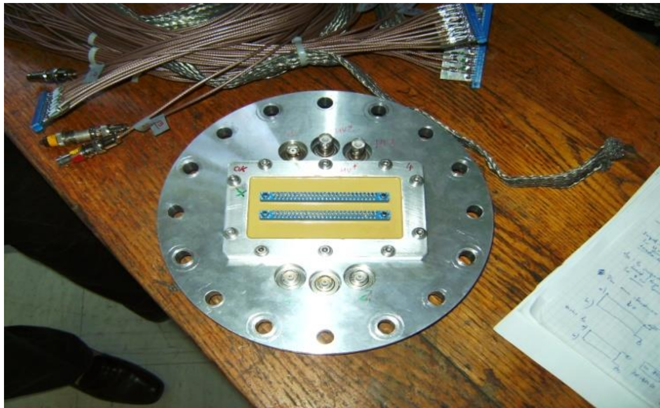

Det III:

5.5 MeV α

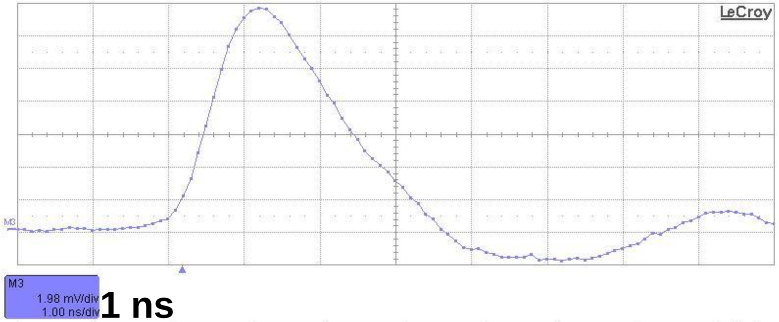

1 ns

PRL: developped at LPC

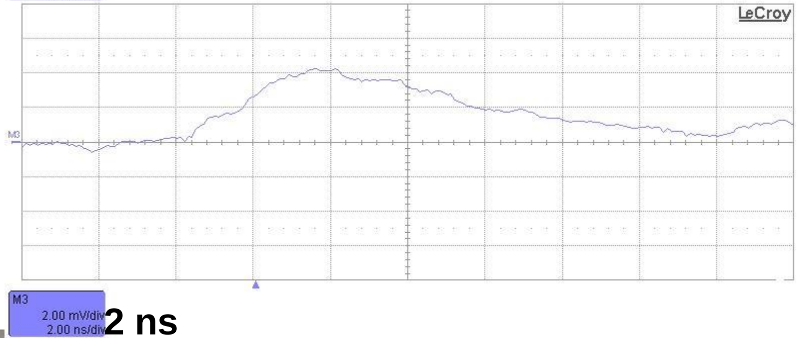

2 ns

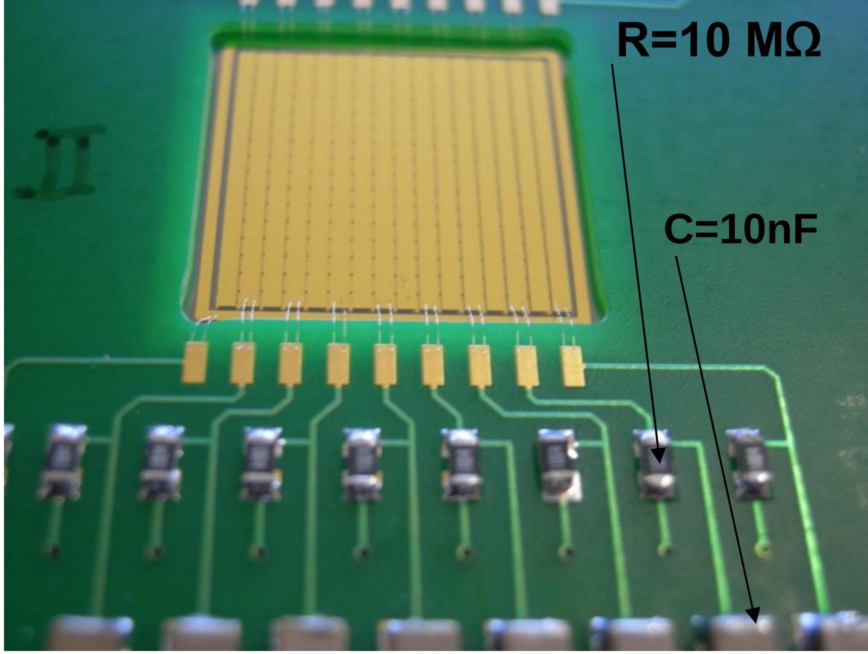

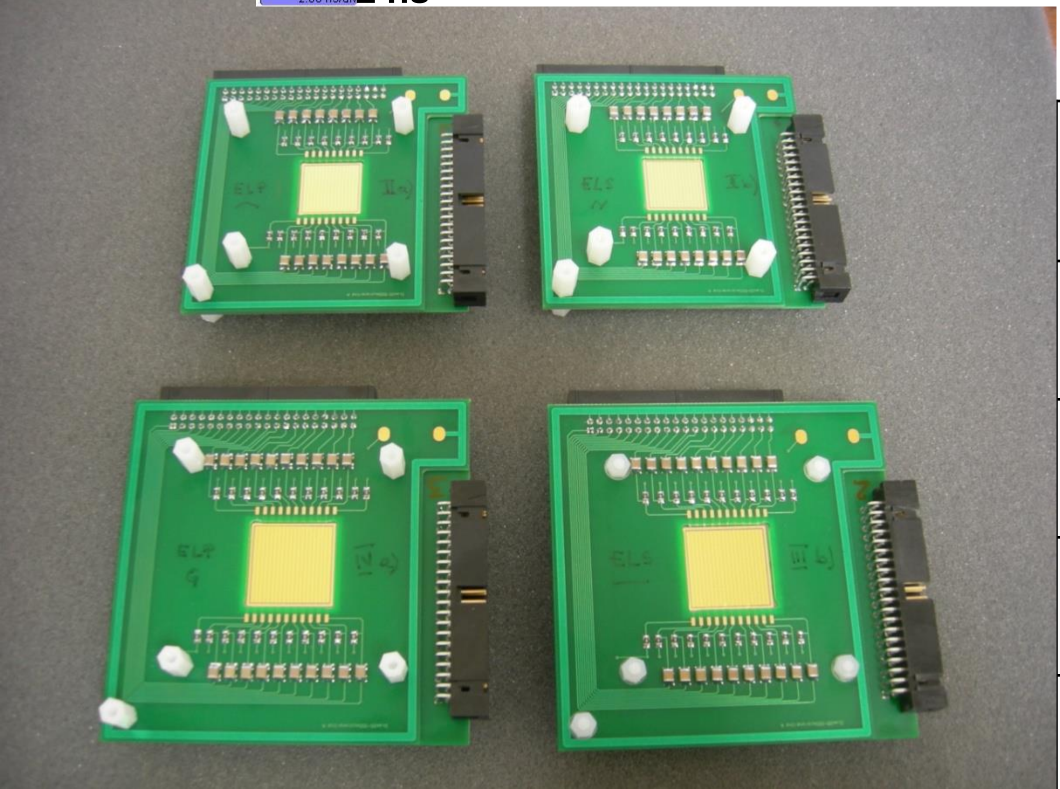

Table 3. the multi-strip detectors built at LCP; a) and b) are the 2 faces

Detecteur	P2 - Type	Densité (g/cm3)	Epaisseur (μm)	Surface active (mm2)	Nombre de pistes
I	ELS	2.9	565	16x16	a)16 G b)16 N
II	ELP	3.4	575	16x16	a) 16 b) 16
III	ELS	2.9	240	20x20	**a) 1** **b) 20**
IV	ELP	3.4	350	20x20	a) 20 b) 20

Les tests au GANIL: sur la ligne SME (sortie moyenne énergie)

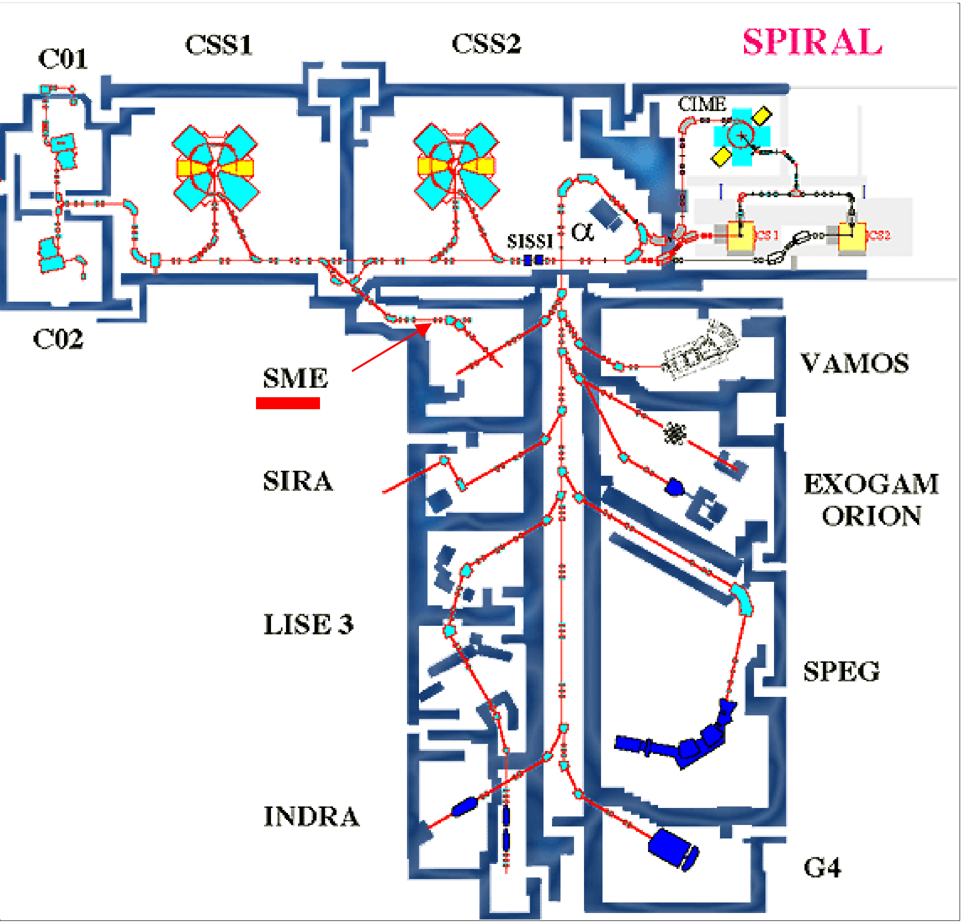

Installation des détecteurs

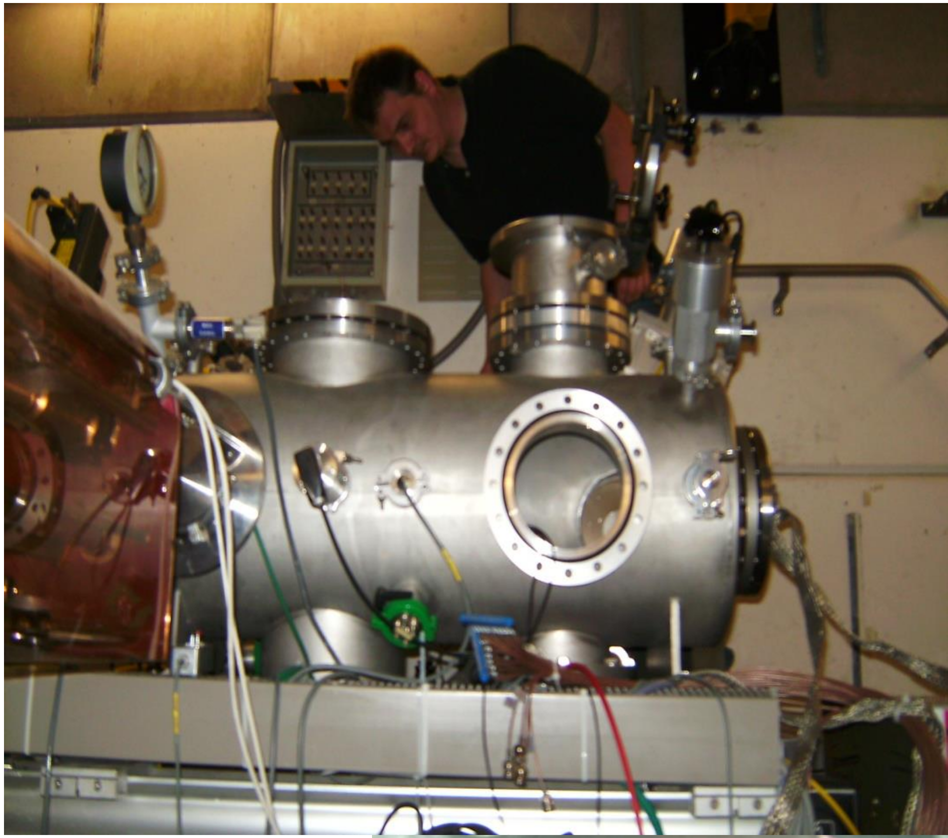

Table 4. Ions used in GANIL

Plaque + détecteur + alumine

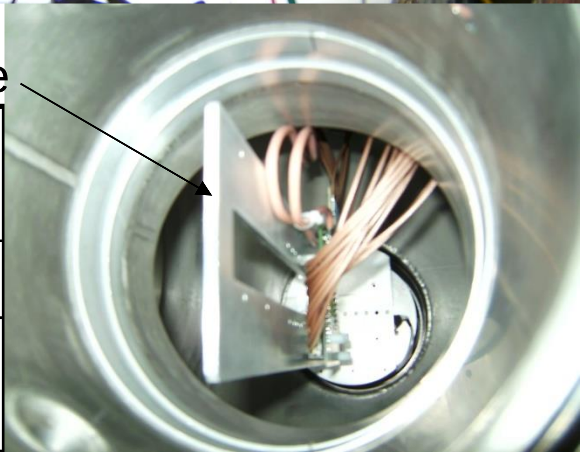

~2,5 m	GANIL ^{70}Zn	GANIL ^{36}S	GANIL ^{36}S	GANIL ^{16}O	LPC α
E/A (MeV)	8.7	7.2	3.9	13.7	1.2
Range (μ) ELS range (μ) ELP	63 55	48 42	26 22	225 198	15 13

Induction d’un signal transitoire sur les pistes adjacentes

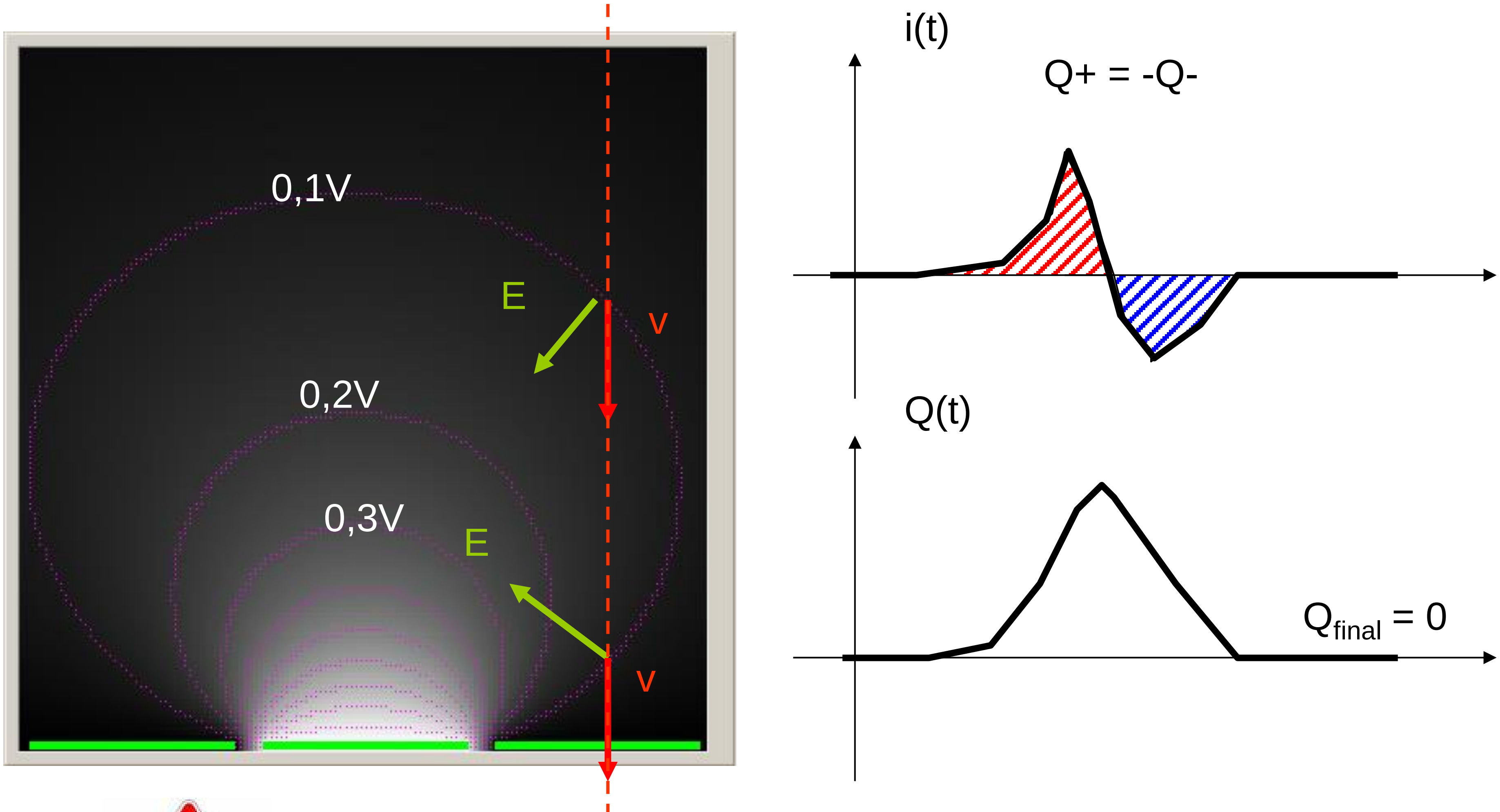

Il peut également y avoir des problèmes sur les interpistes
→ Répartition du signal sur des pistes contigües

Résultats pour les détecteurs multipiste: *images prises sur l'oscilloscope LeCroy*

HT sur la face b) irradiée (1V/µ)

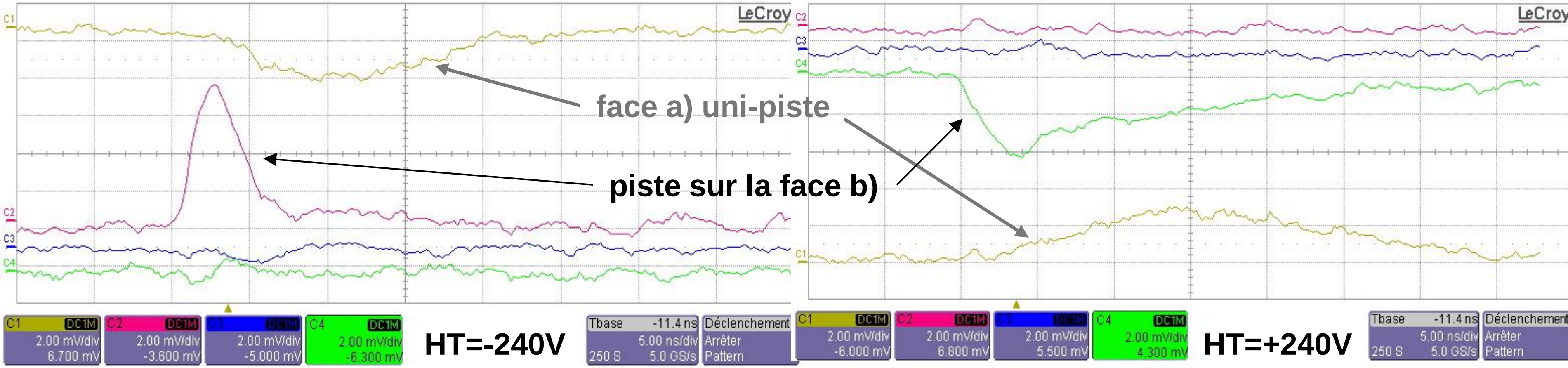

Signals induced by ^{36}S of 7.2 AMeV in the detector III of ELS type

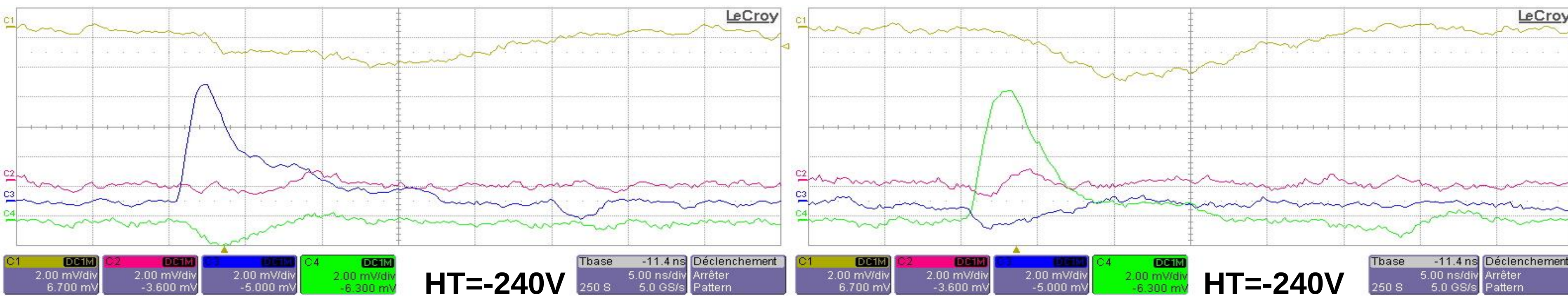

Signals induced by ^{36}S of 7.2 AMeV in the detector III of ELS type: examples of cross-talk between neighbouring strips on the irradiated face (blue and green)

Résultats pour les détecteurs multipiste: *images prises sur l'oscilloscope LeCroy*

Coincident signals on the two sides of the detector **HT sur la face a) irradiée (1V/µ)**

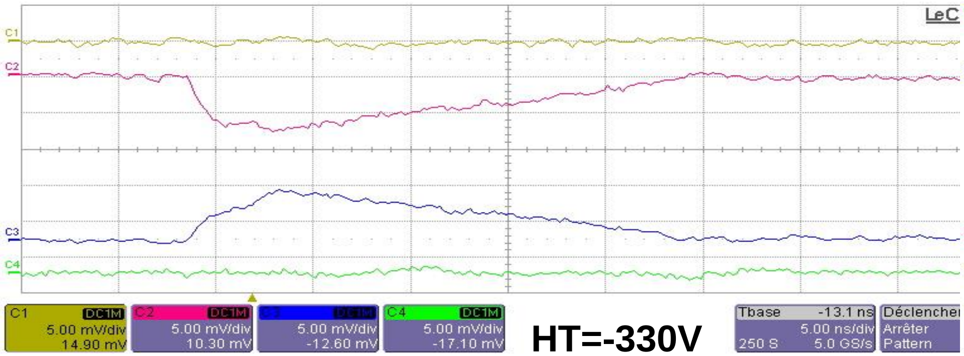

HT=-330V

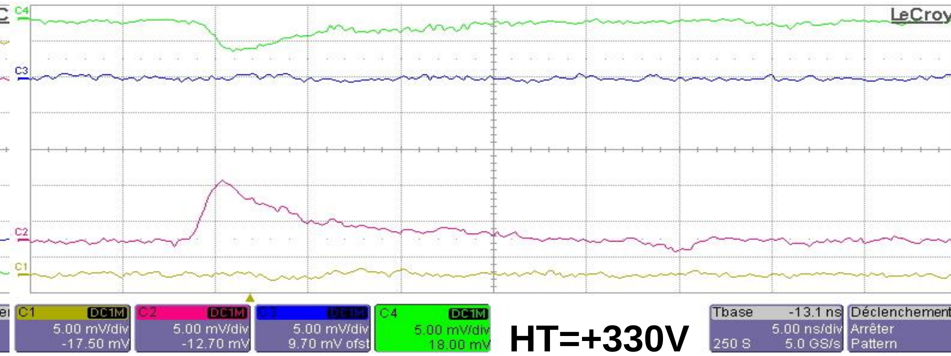

HT=+330V

Signals induced by ^{36}S of 7.2 AMeV in the detector IV of ELP type

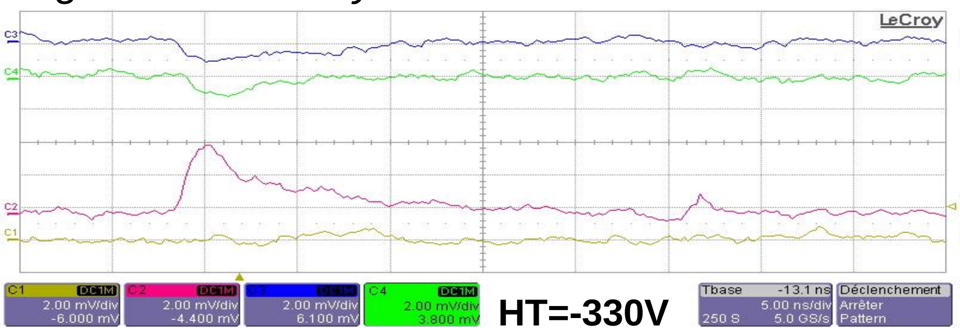

HT=-330V

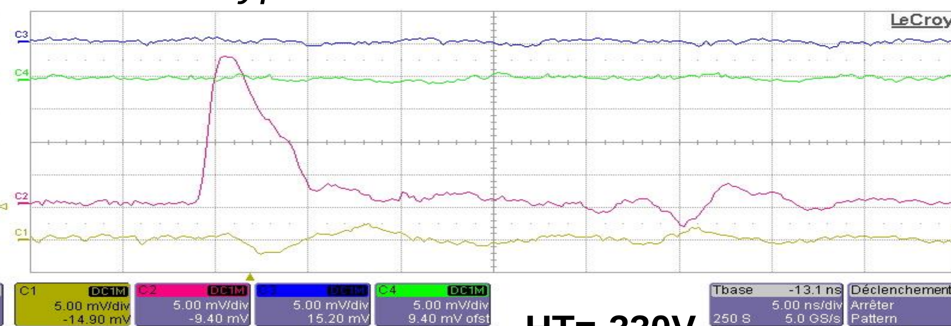

HT=-330V

The particle is probably passing between strips (left); example of cross-talk (right)

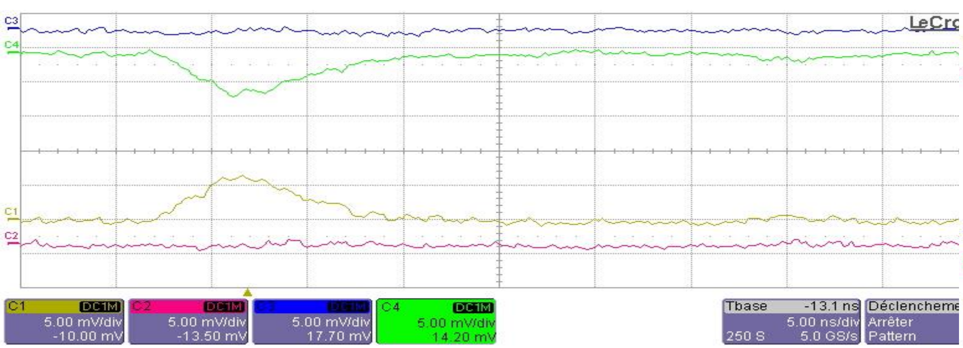

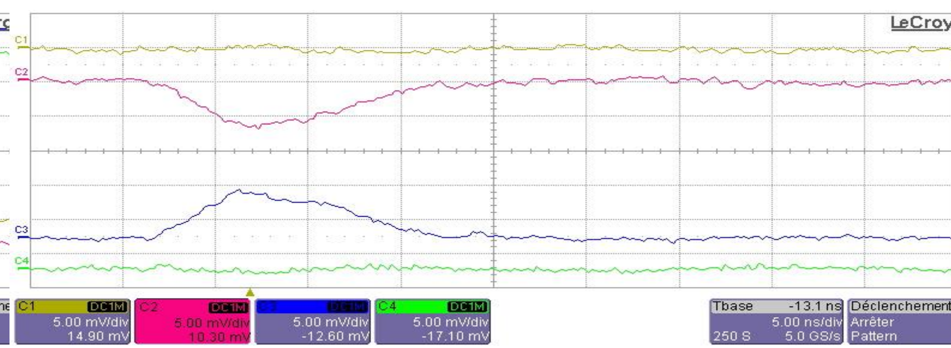

Signals induced by ^{36}S of 3.9 AMeV in the detector IV of ELP type (-330 V)

Det iv ELP, 350 μ, -200 V, E=0.6V/μ board 3, channel 0; O –> Growth side: 13.7 AMeV

S=18mm2; C=2,57 pF RC=0,13ns

Matacq -> 0,9 ns

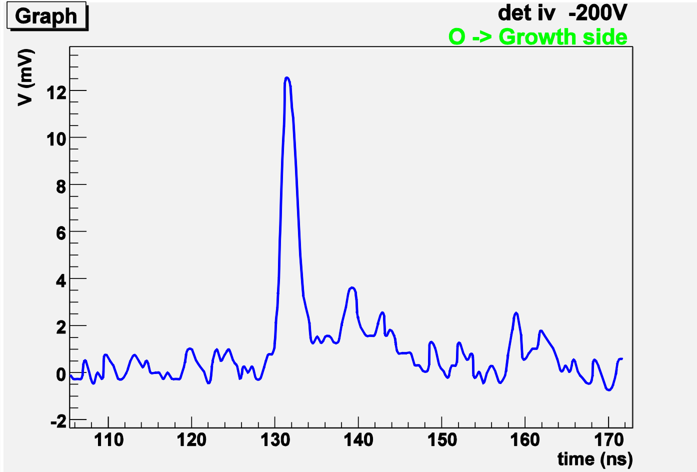

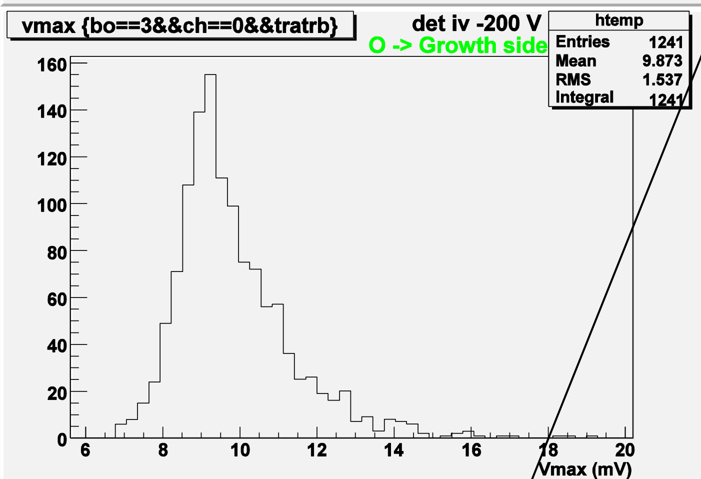

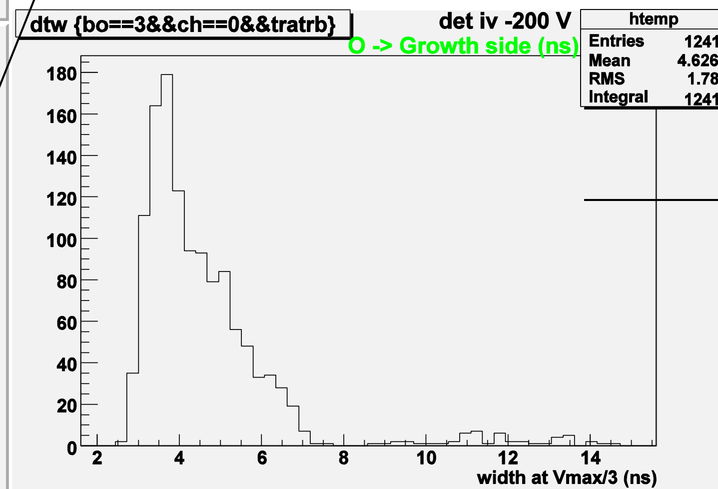

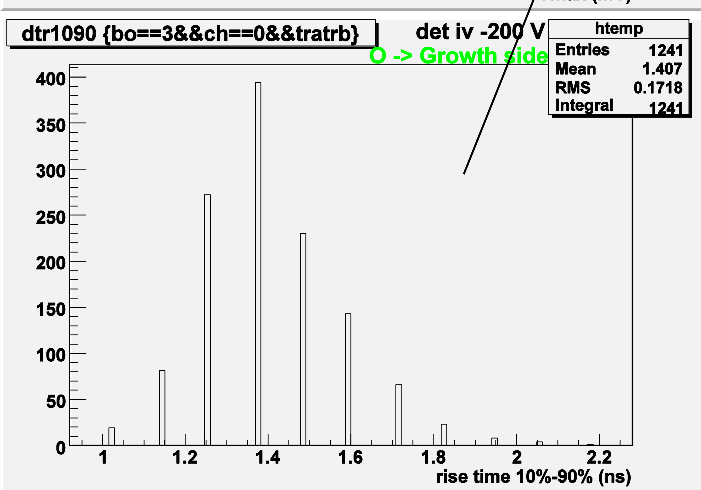

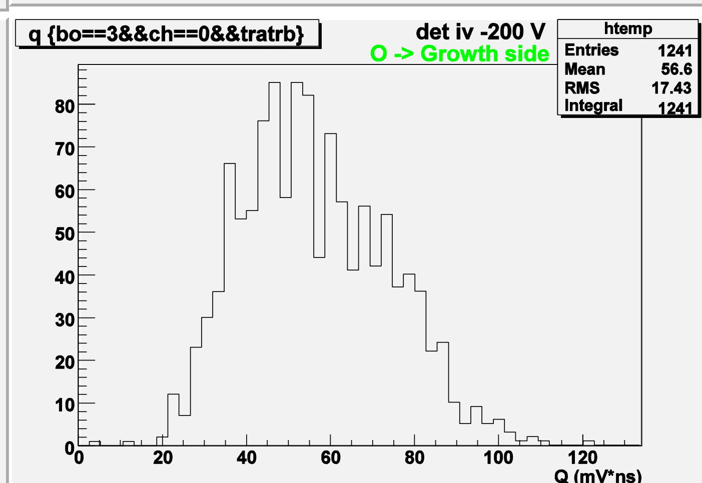

Acquisition:
MATACQ – VME (400 MHz BW; 2GHz sampling) – 12 channels
- oscillo LeCroy 64Xi (600 MHz BW; 10Gs/s) – 4 channels

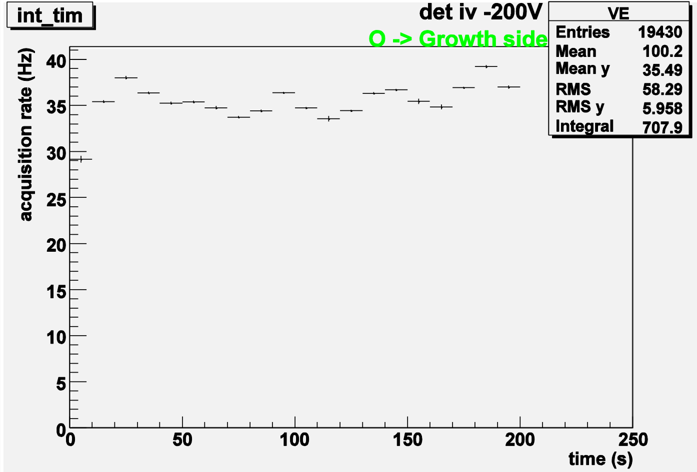

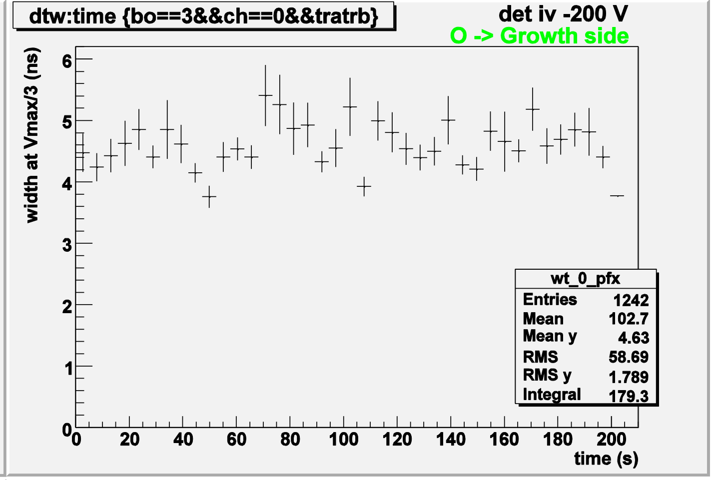

Det iv ELP, 350 μ -200 V, E=0.6V/μ board 3;

O: 13.7 AMeV

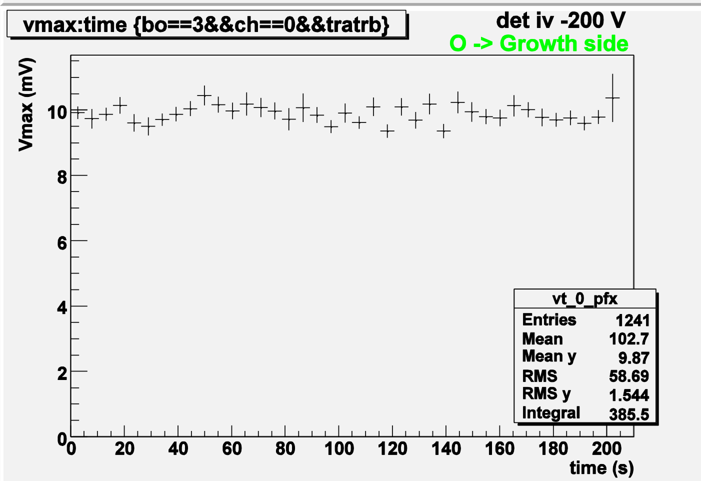

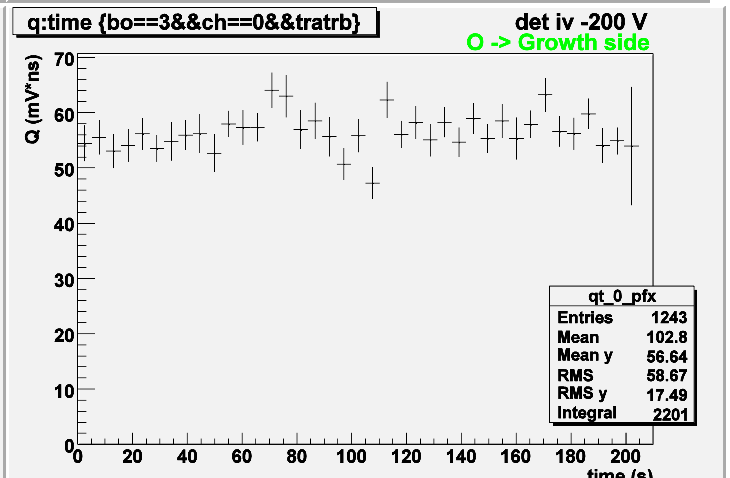

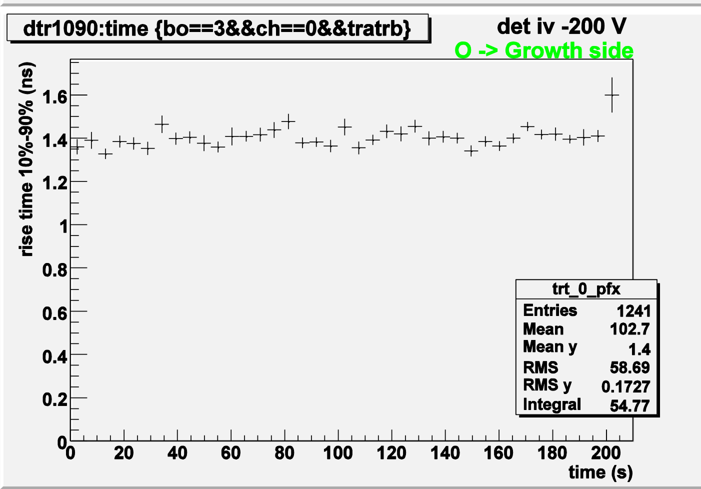

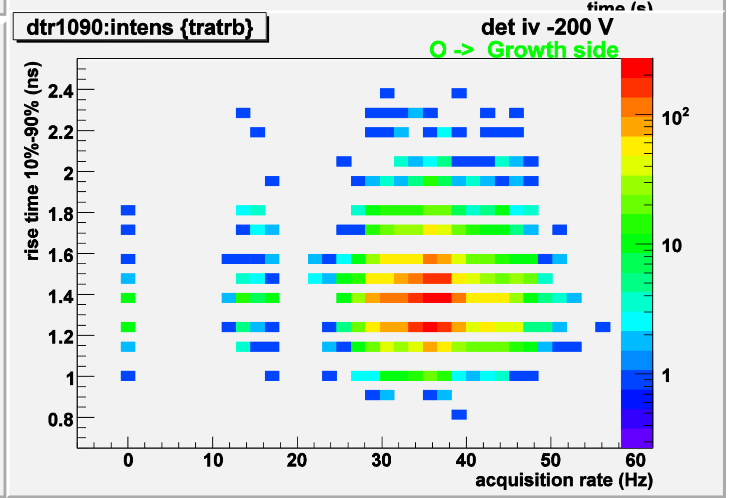

FASTER

Fast Acquisition SysTem for nuclEar Research

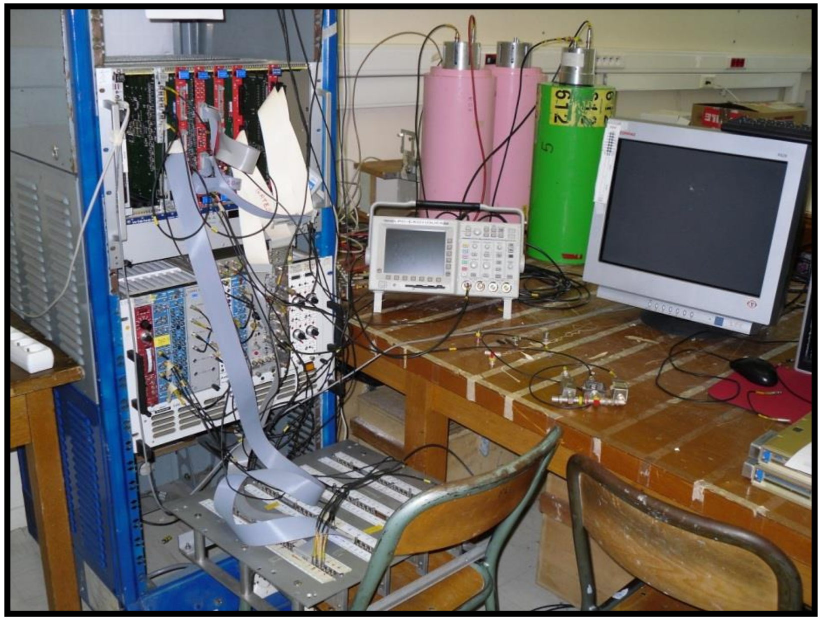

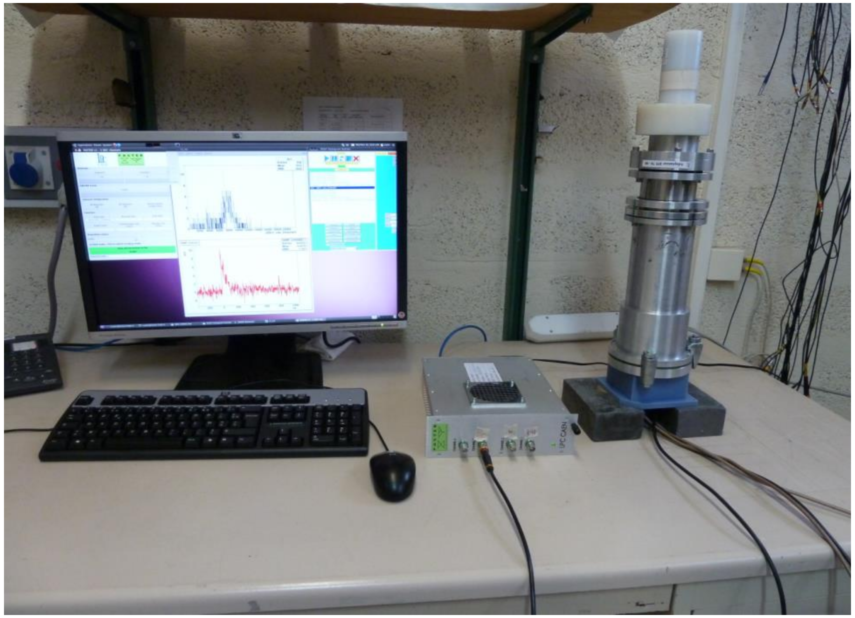

Objectifs:

- L'objectif de FASTER est de concevoir une plateforme de développement d'acquisition numérique modulaire avec les contraintes suivantes.
  - Générique, adaptable, extensible
  - 1 à quelques centaines détecteurs
  - Utiliser au maximum les nouveaux standards
  - Plusieurs niveaux de décision
  - Temps réel et distribution d'horloge simplifiée

FASTER (voir D. Etasse – la 18 Juin 2015 - journée Dispositifs & Installations)

3 Cartes mères développées
- Syroco_V2
- NIM
- AMC

3 Fonctions de mesures développées
- QDC-TDC_{HR}
- ADC-TDC
- Synchro RF

2 Cartes filles de conversion analogique↦digital:
- CARAS : rapide, adaptée aux fonctions QDC, TDC, synchro RF, ADC
- MOSAHR : grande dynamique, adaptée à la spectroscopie haute résolution (ADC)

BILAN
- Utilisé dans plusieurs configurations
- Qualité des mesures
- Performances élevées

FUTUR
- Développer des aspects dynamiques du modèle
- Augmentation des performances
- Développement de nouveaux modules
- Peut répondre aux besoins de NFS, DESIR.

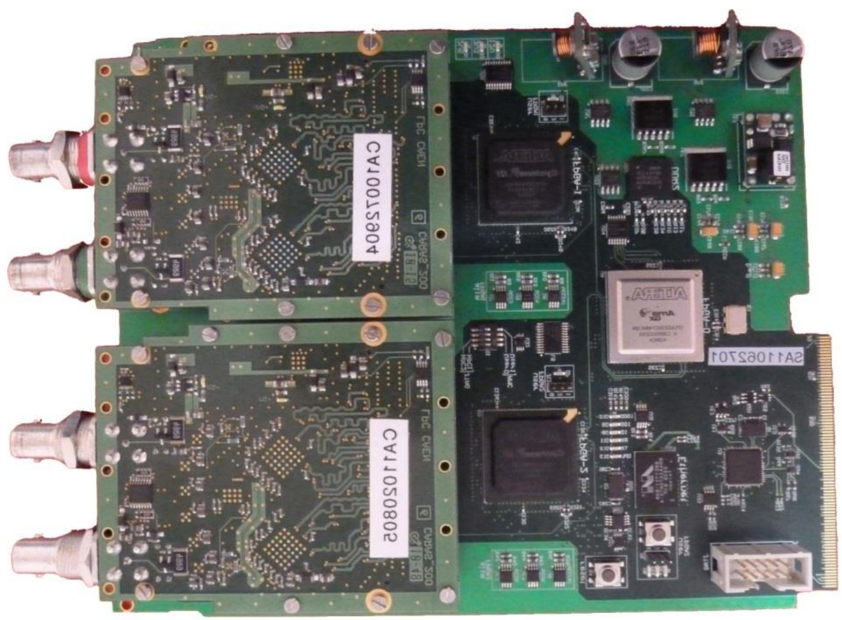

Det_8x8_pistes (ELS - 300µm: TiPtAu);

HV = -750 V on Nucleation; source α on Growth, PRL1, FASTER

Piste4_4_-750V_nuclear

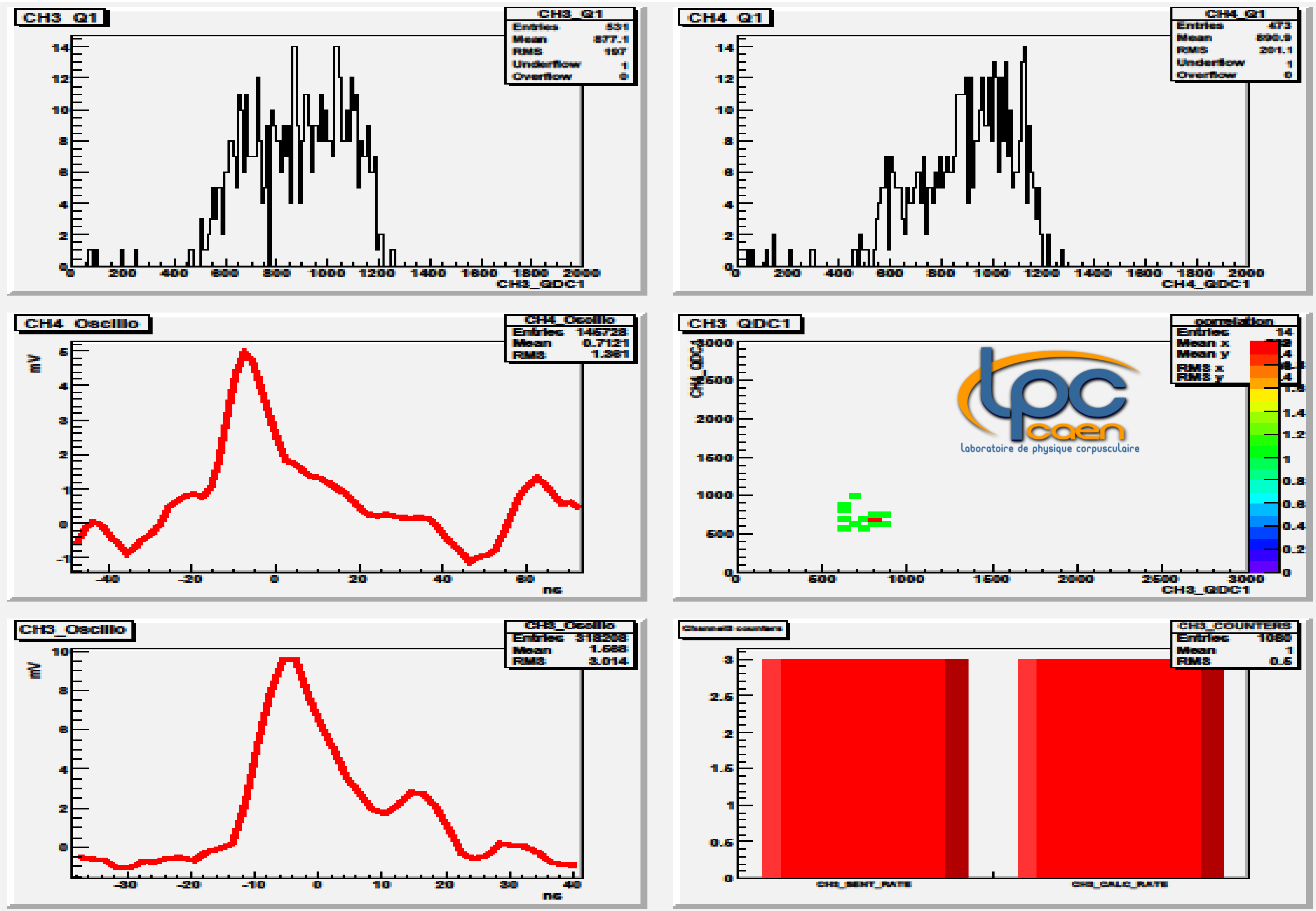

projet diamant (voir **L. Leterrier** Electronique front-END – journée thématique **17 Juin 2015 -LPNHE**)

Détecteur à pistes

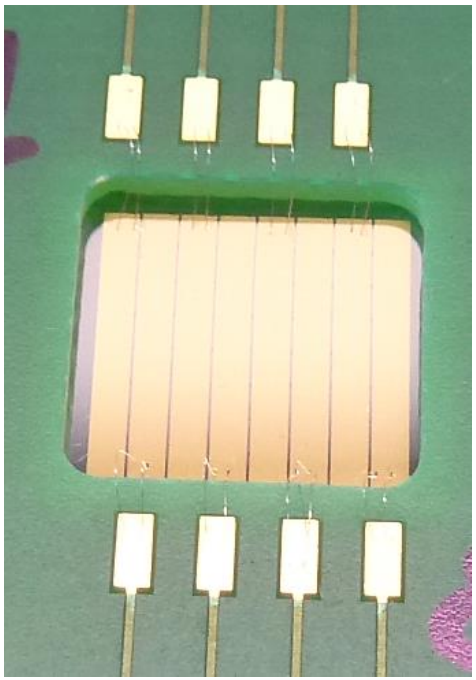

Jérôme Perronnel

Carte fille ETC (Eight Time Channels)

Jérôme Langlois / Laurent Leterrier

2. Synoptique de la carte ETC

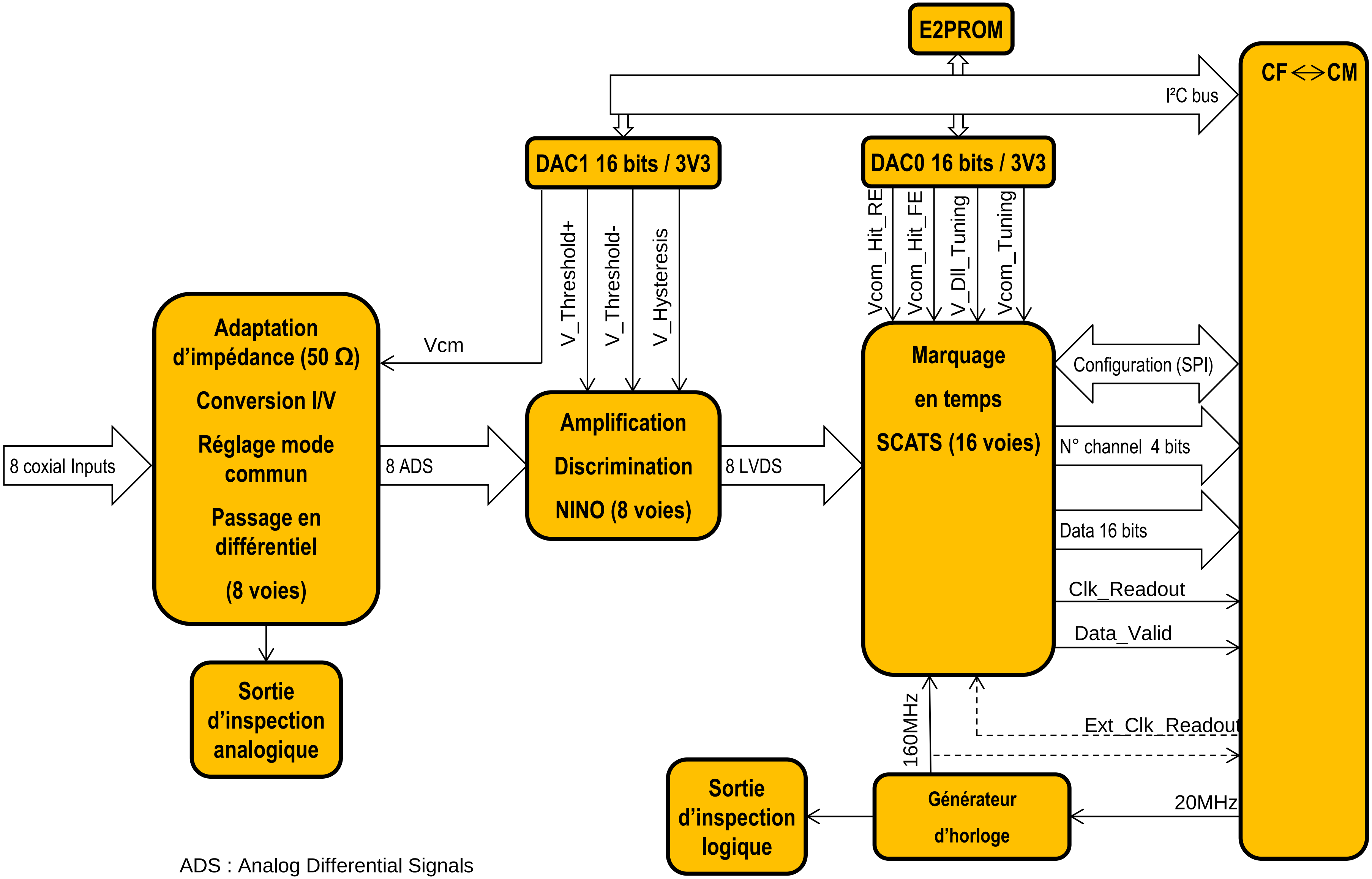

ADS : Analog Differential Signals
LDVS : Low Voltage Differential Signals
---- : Lien optionnel

L. LETERRIER – leterrier@lpccaen.in2p3.fr

Réunion Objectifs Scientifiques – 2015 - Projet diamants

2015:
1) micro-électronique:
carte fille ETC (Eight Time Channels: NINO + SCATS pour 16 pistes)
2) instrumentation:
(développement détecteurs + logiciel pilotage carte ETC + daq)
3) informatique: (acq+RHB)

2016: solution I.
1) micro-électronique:
carte ETC (DISCRI + SCATS -> refaites après correction et multipliées LAL)
2) instrumentation:
(développement détecteurs + logiciel carte ETC + daq)
3) informatique: (acq+RHB)

2016: solution II.
1) micro-électronique:
carte ETC (refaite après correction + nouveaux tests)
Discri low walk (préoccupations pour FRACAS avec le LAL)
2) instrumentation:
(développement détecteurs + logiciel carte ETC + daq FPGA mesure de temps)
3) informatique: (acq+RHB)

V. Conclusions & prospective:

-**The CVD polycrystalline diamond based double sided strip detectors seems to be well suited to the requirements for a beam profiler for characterising low intensity radioactive heavy ion beams:**

- material: ELP (small bulk polarization; signal stable in time); P2 from Company 1, for example
- thickness: 200-300 µ adequate for R~50 µ
- electric field ~1V/µ; HV though Sh < Se
- strip: 1 mm pitch (0.9mm strip, inter-strip gap: 0.1mm), efficiency: 90-99% (localization with 1 mm resolution)
- small cross-talk effects
- signal shape study: ~1.5 ns rise time for 1 strip; PSA may bring interesting information ($\Delta Q < \Delta V_{extrem}$)

-**The further characterisation of such detectors and the engineering of the readout electronics and other associated elements of a fully fledged profiler are expected to be carried in the near future:**

- tests for radiation hardness
- more robust electric contacts between PCB and strips?
- line receiver multi-channel preamplifiers for low energies
- acquisition system: FASTER + SCATS or FPGA.

SCATS (Sixteen Channel Absolute Time Stamper)

To be used by a new 50 X 50 diamond BEAM PROFILER

- Note: The study of the diamond detector has already been subject for a few student stages

References

[1] E.-K. Souw, R.J. Meilunas, Nucl. Instr. And Meth. In Phys. Res. A 400 (1997) 69.
[2] S. Schwertel et al., „Diamond detectors for the R3B Experiment", GSI Scientific Report 2007 (GSI Report 2008-1), Instruments-Methods-10, (2007) 216.
[3] P. Moritz, E. Bedermann, K. Blasche, H. Rodl, H. Stelzer, F. Zeytouni, DIPAC III, Frascati (1997).
[4] J.-L. Lecouey at al., Abstract n°. 226, ANIMMA, Marseille (2009).
[5] P.Bergonzo, D. Tromson, H. Hamrita, C. Mer, N. Tranchant, M. Nesladek, Diamond and Related Materials 16 (2007) 1038.
[6]A. Brauning-Demian, E. Bedermann, P. Verma and P.H. Mokler, DIPAC III, Frascati (1997).

Data taken in collaboration with:

GSI (Darmstadt): Angela Bräuning-Demian, Elèni Berdermann, M. Traeger, M. Ciobanu & Detector Laboratory

LIST (CEA Saclay): Hassen Hamrita, Philippe Bergonzo

NIPNE Bucharest: Dana Dimitriu, Daniela Fluerasu

LPC Caen:

Jean-Marc Fontbone, Jérôme Perronnel, Hervé Plard, Jean-François Cam

Jean Hommet – acquisition; Yvan Merrer – mécanique + atelier mécanique

Lynda Achouri, Giacomo Randisi, Nigel Orr, Marian Pârlog

Actuellement: μ-électronique + Instru + FASTER TEAM

Remerciements:

Fac. Chimie: M. Ledauphin CRISMAT: Yohann Thimont, Séverine Mouchel

IPN Lyon: Michel Chevalier

CIMAP: Emmanuel Balanzat, Jean-Marc Ramillon, Stéphane Guillos
LPC: Joel Brégéault, Jean-Louis Gabriel, Albert Leconte, Christophe Vandamme, l'équipe informatique

Annexes

^{58}Ni: 10.9 AMeV

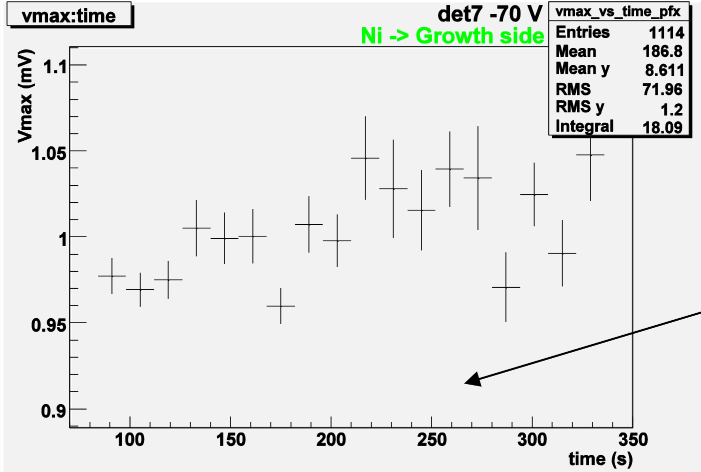

E=1V/μ

70 μ, Company 3

PSA: Different detectors, different behaviors

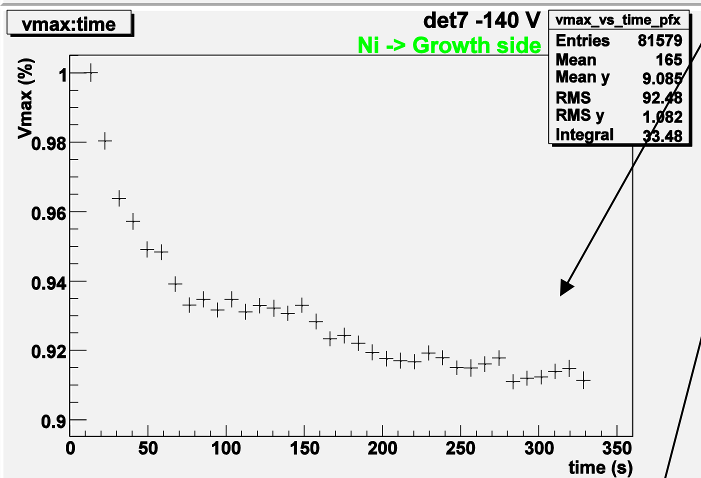

E=2V/μ

200 μ, Company 2

E=2.5V/μ

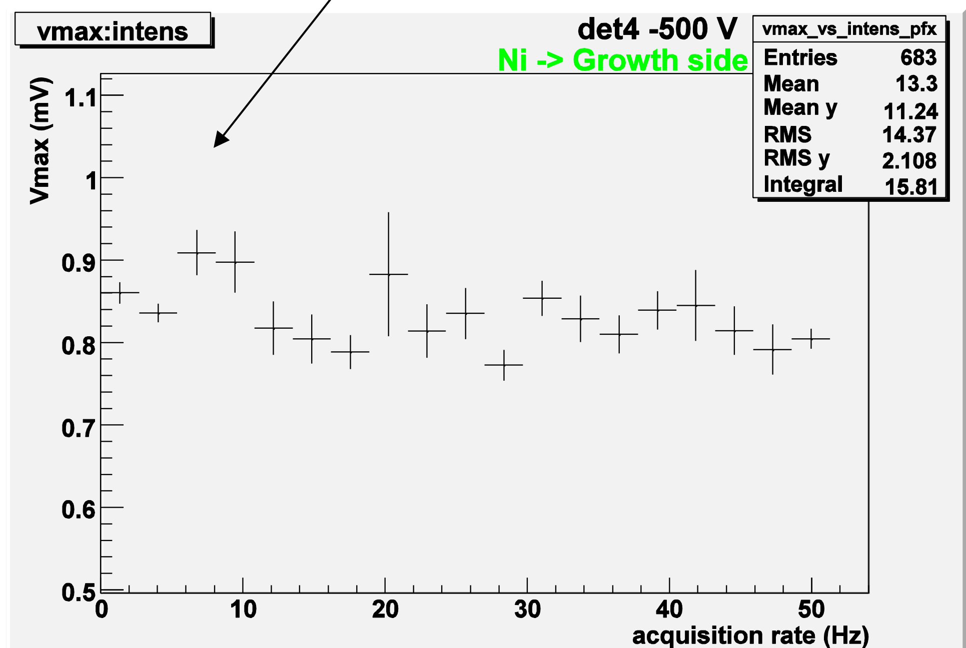

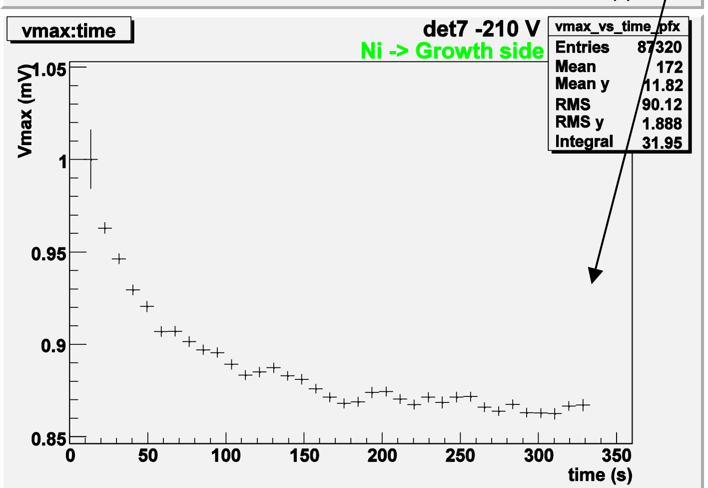

E=3V/μ

Single crystal DDL detector: 500 µ ^{132}Xe 7.6 AMeV

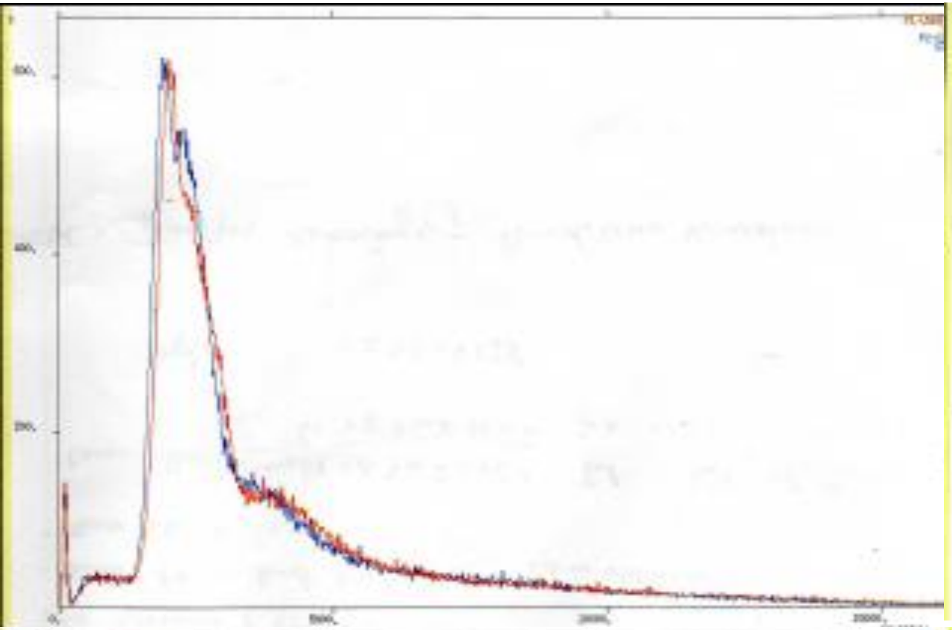

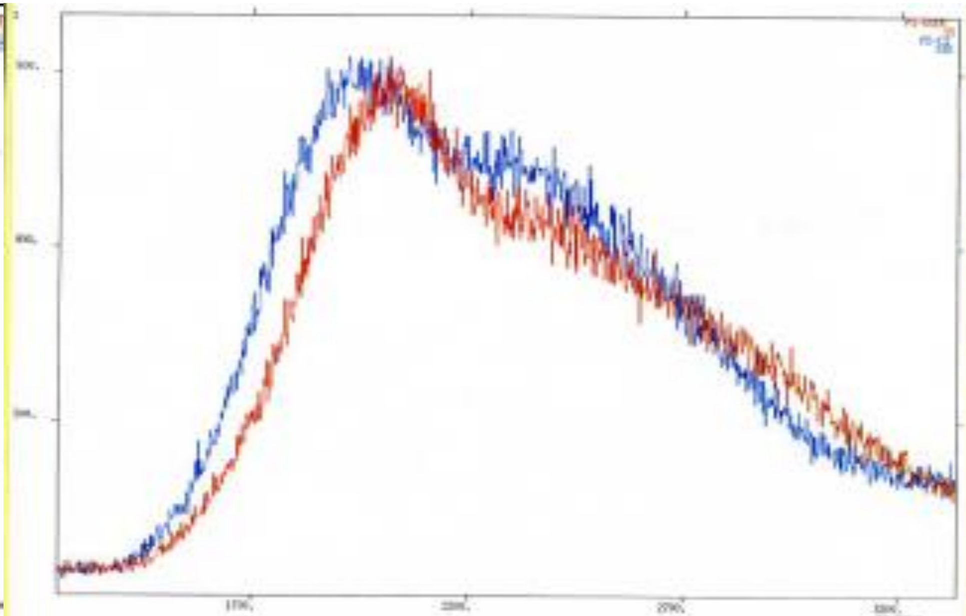

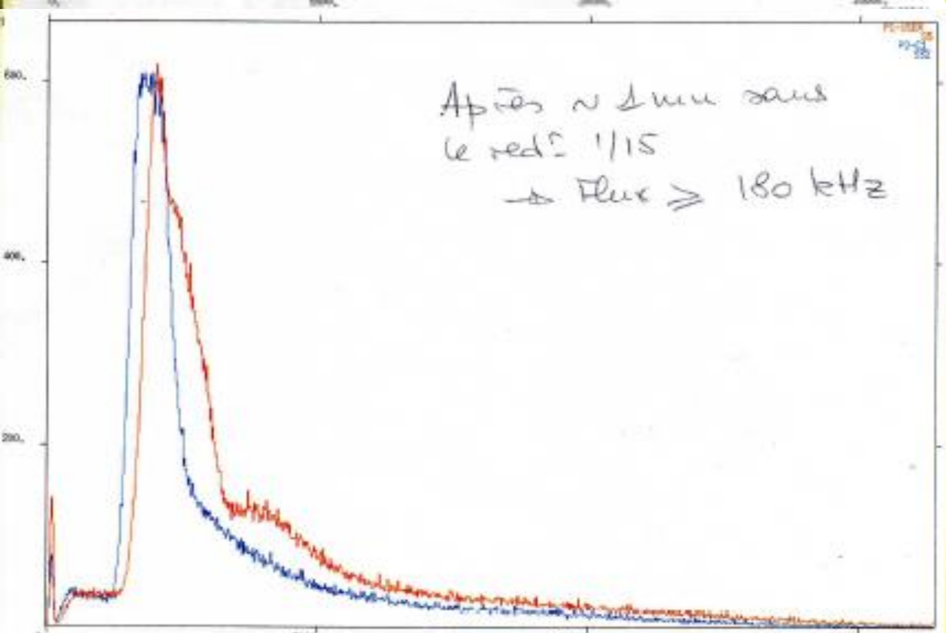

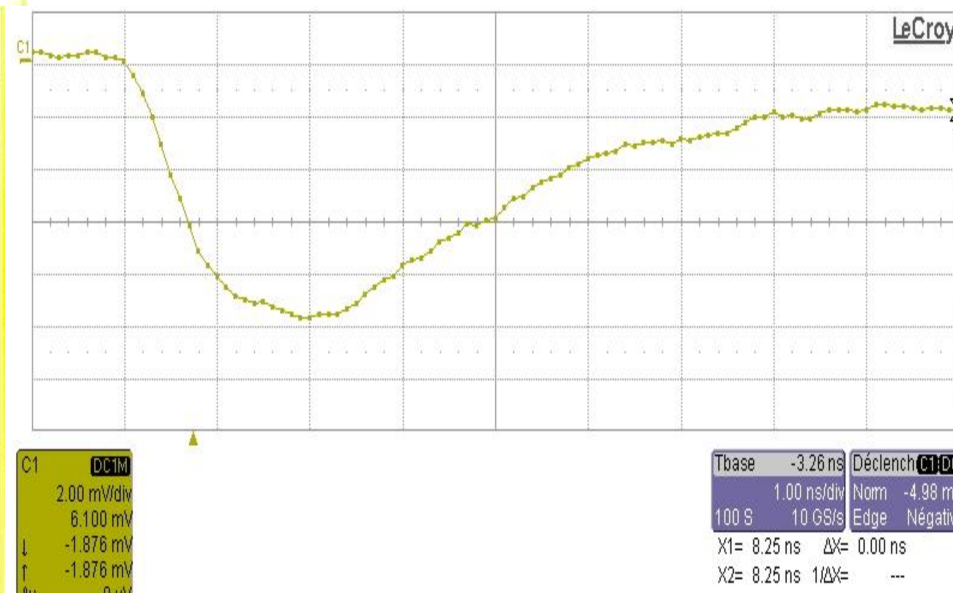

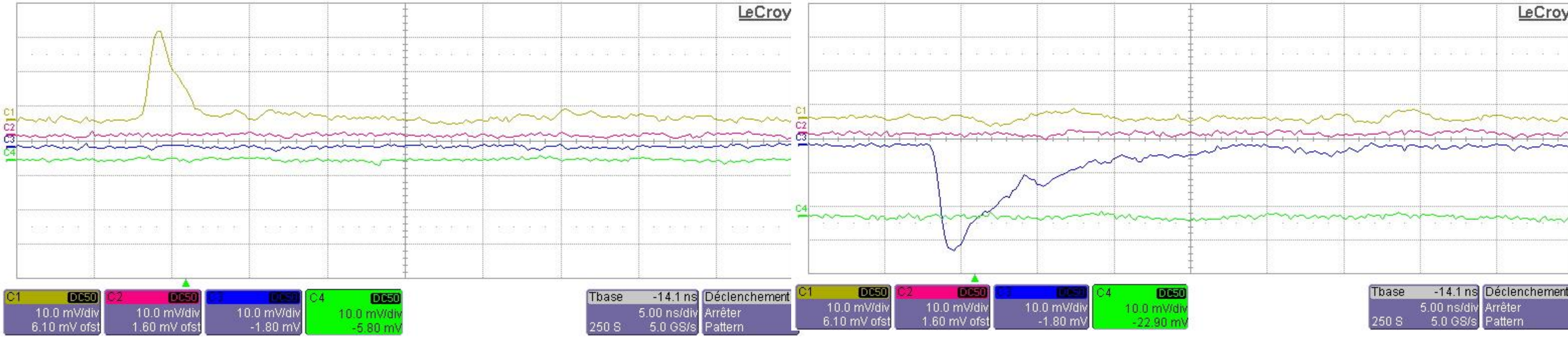

Signals from the strip no. 9 of the face a) - left (yellow curve) and from the strip 9 of the face b) - right (blue curve), amplified with the new preamplifier PRL developed at LPC; the signals were induced by the ^{70}Zn ions of 8.7 AMeV in the detector IV of ELP type for a voltage of -300 V applied on the face a) (growth), irradiated

Signaux coincidentes sur les deux faces du détecteur

HT sur la face a) irradiée (1V/µ)

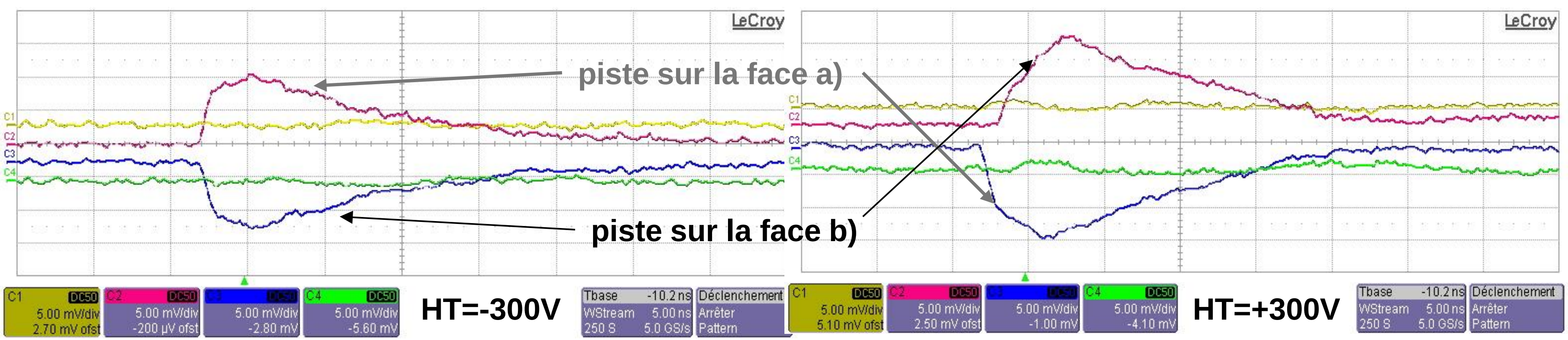

Signals induced by 70Zn of 8.7 AMeV in the detector IV of ELP type

Det iv ELP, 350μ, -200 V, E=0.6V/μ, board 3; O:13.7 AMeV

the 4 channels of Matacq board 3 give similar results

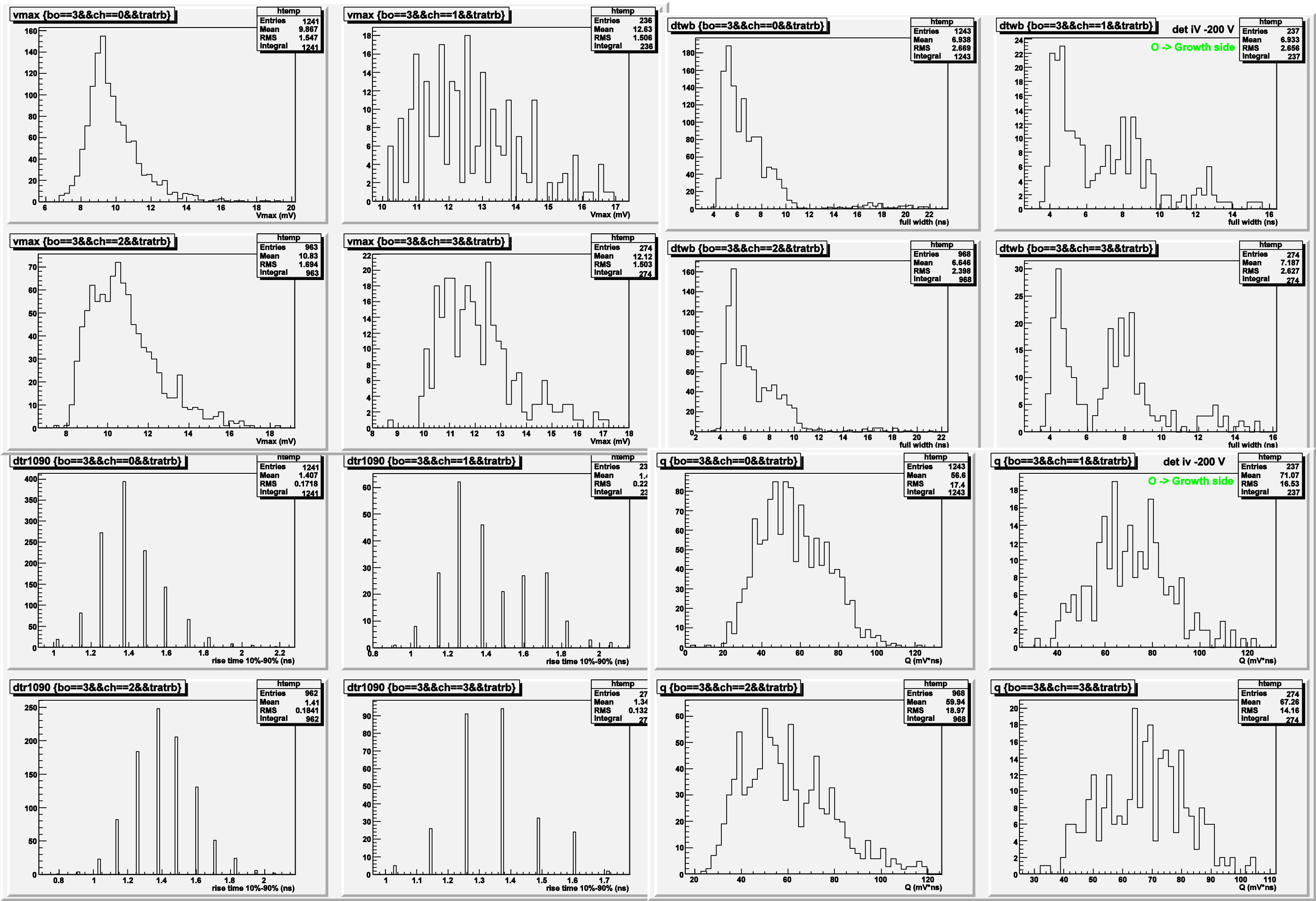

Det iv ELP, 350μ -200 V, E=0.6V/μ, board 3; O :13.7 AMeV

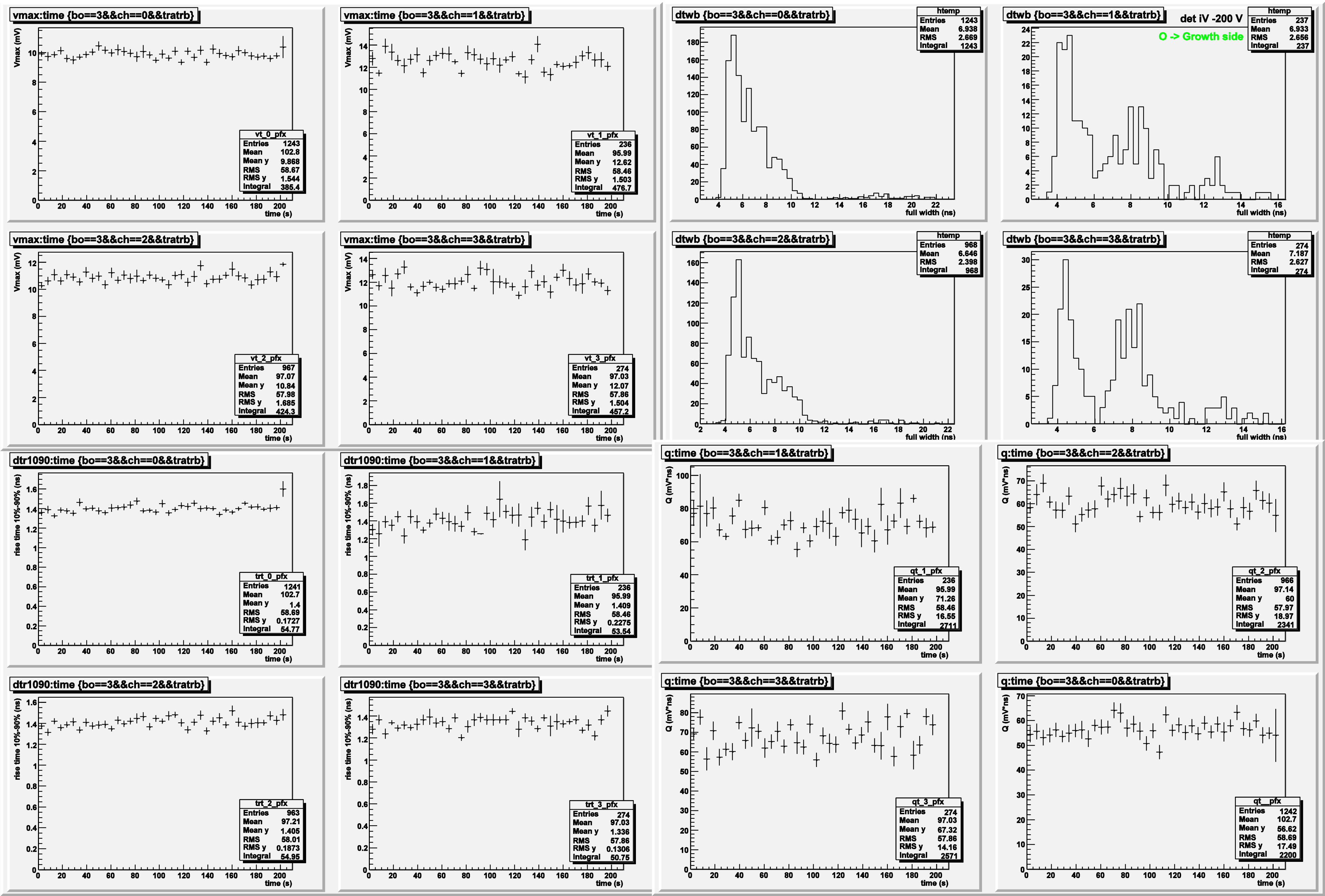

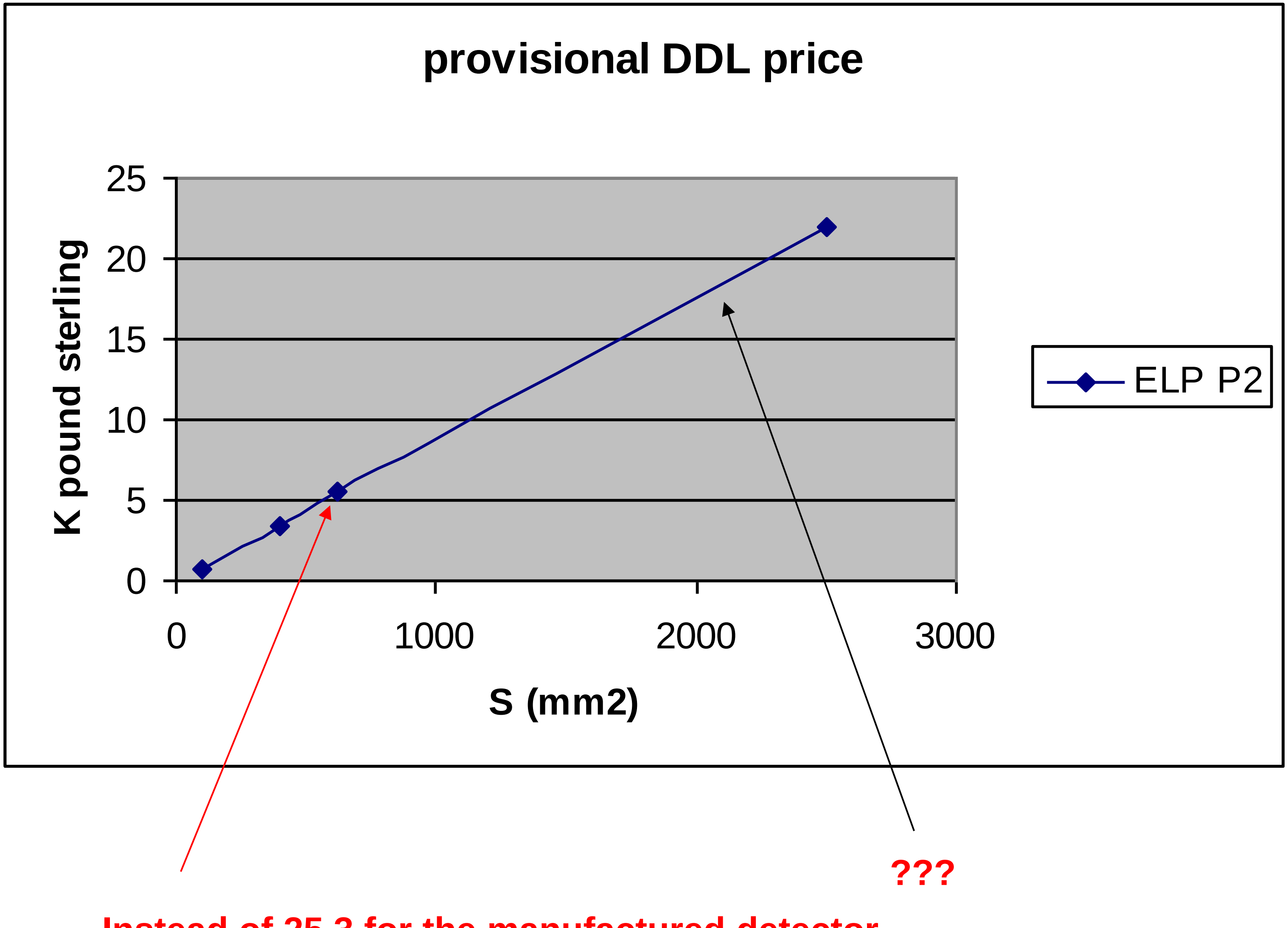

Instead of 25,3 for the manufactured detector

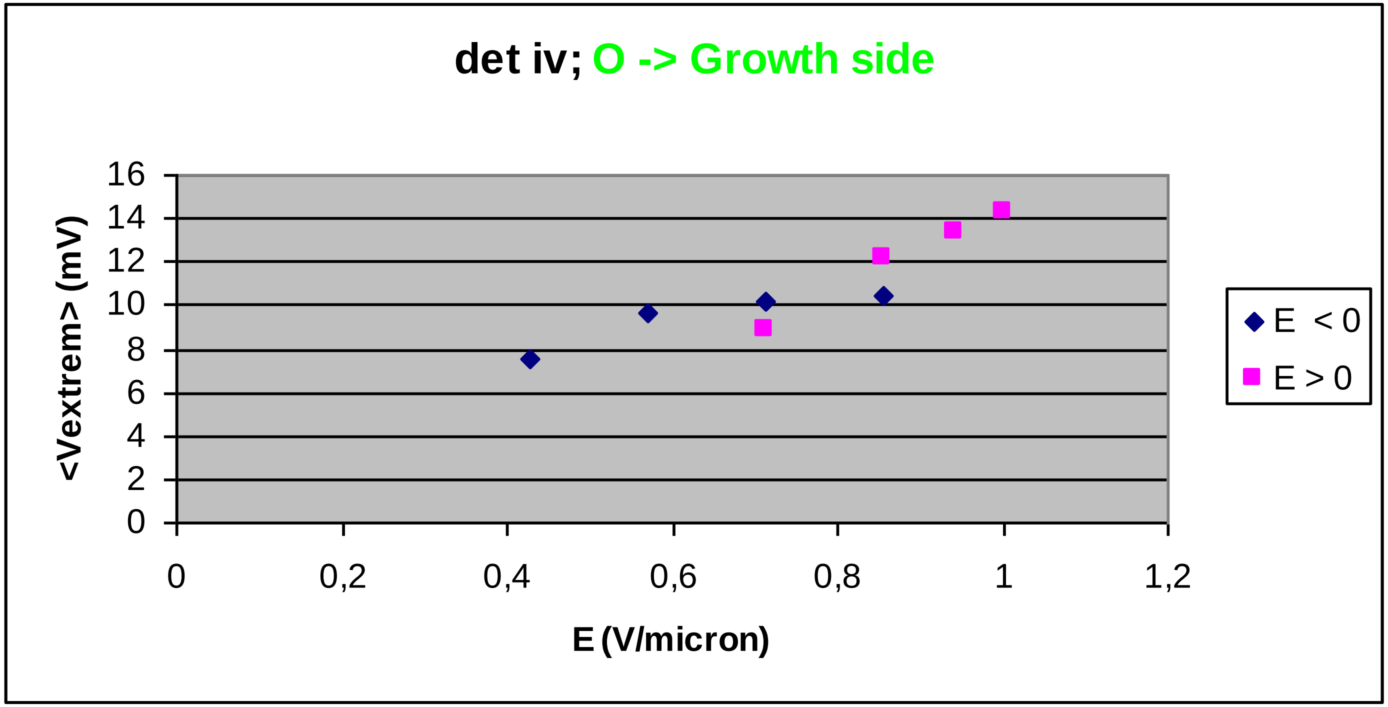
det iv; O -> Growth side
16
14
12
10
8
6
4
2
0
<Vextrem> (mV)
0
0,2
0,4
0,6
0,8
1
1,2
E (V/micron)
E < 0
E > 0

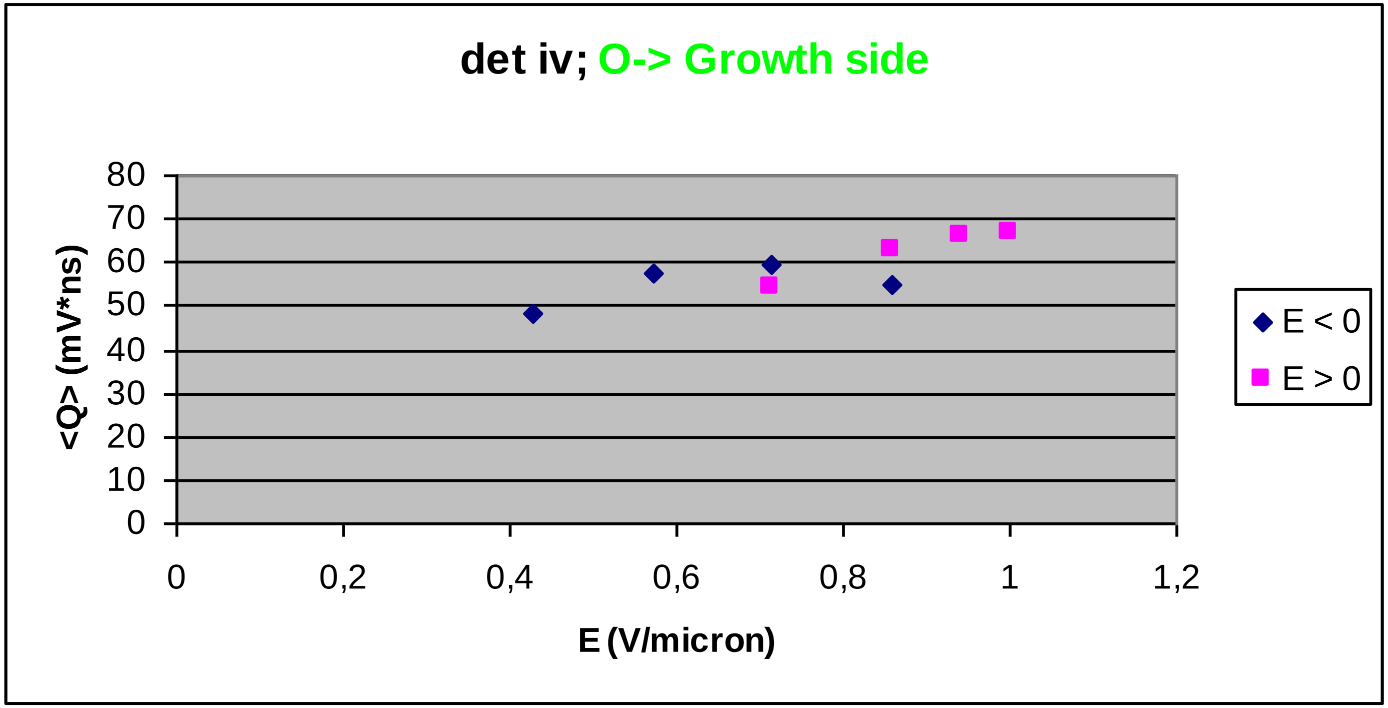
det iv; O-> Growth side
80
70
60
50
40
30
20
10
0
<Q> (mV*ns)
0
0,2
0,4
0,6
0,8
1
1,2
E (V/micron)
E < 0
E > 0

Start-Veto system readout electronics (W.Koenig - GSI)

Issues:

- ✓ High rate, up to 10^6/s per channel.
- ✓ Fast signals, analog signal from diamond – 200 ps rise time, base width < 1ns.

Our approach:

- ✓ Dedicated NINO based discriminator board with trigger functionality.
- ✓ Time measurement performed by HADES TRB board – based on HPTDC.

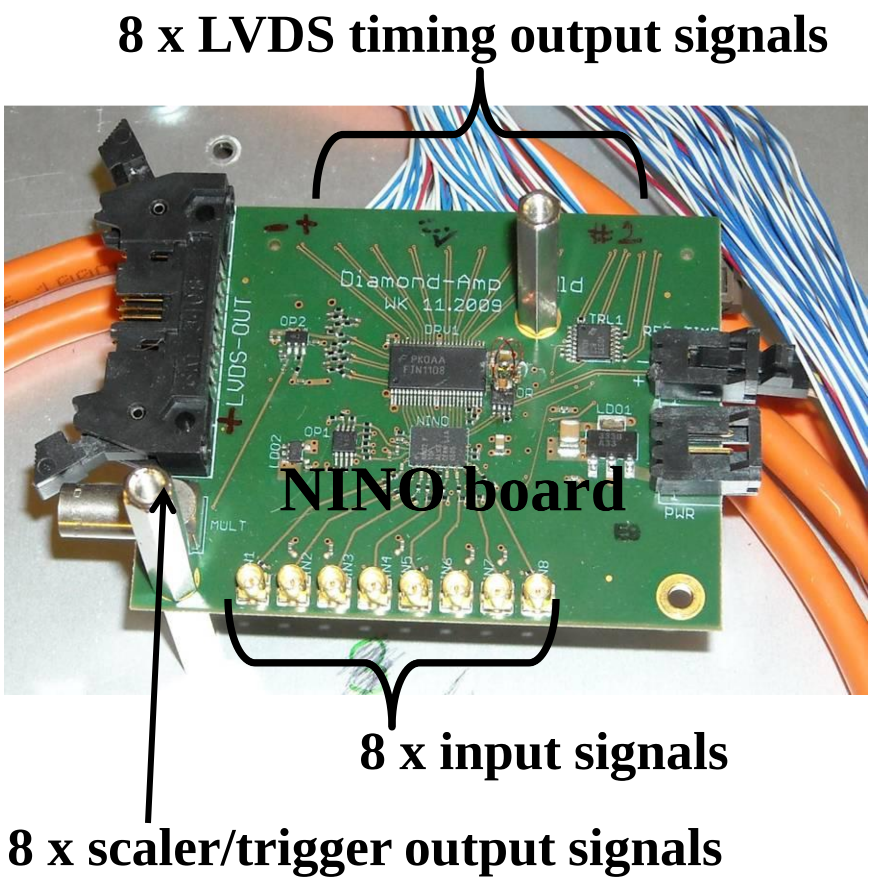

NINO chip: Developed for Time-of-flight measurements in the ALICE experiment

Key features:

- ✓ Adjustable discriminator thresholds.
- ✓ Front end time jitter <10ps.
- ✓ Sustains very high rate (>>10MHz)
- ✓ Peaking time: 1ns.
- ✓ Input signal range: 30fC - 2pC.
- ✓ Noise: <2500 e-.
- ✓ Discriminator threshold: 10fC - 100fC.
- ✓ Timing precision: <10ps jitter.
- ✓ Output: LVDS.

Det III ELS, 240 μ, -240 V, E=1V/μ; O: 13.7 AMeV

2 runs, threshold changed

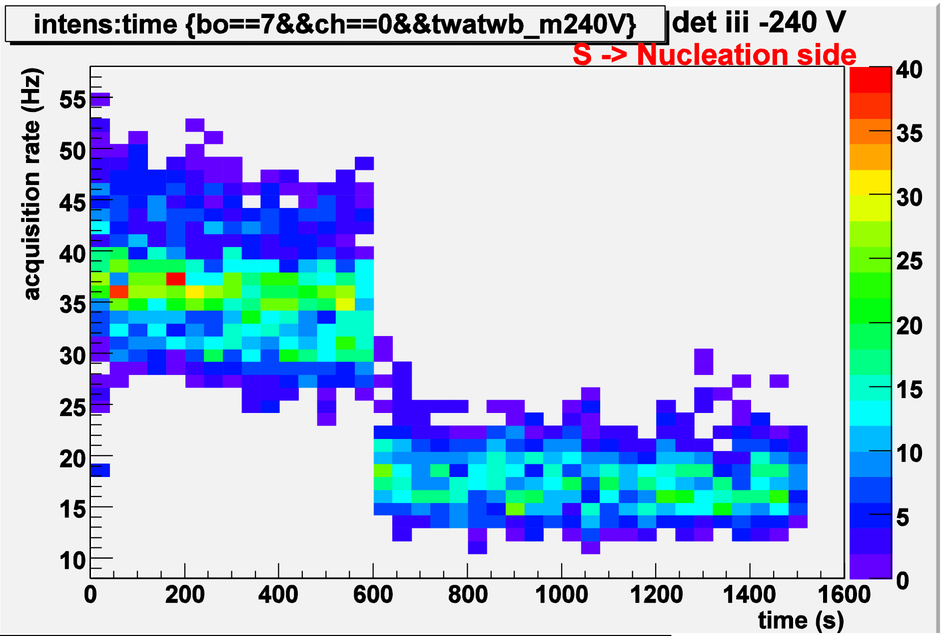

Acquisition:

-MATACQ – VME (400 MHz BW; 2GHz sampling) – 12 channels

-- oscillo LeCroy 64Xi (600 MHz BW; 10Gs/s) – 4 channels

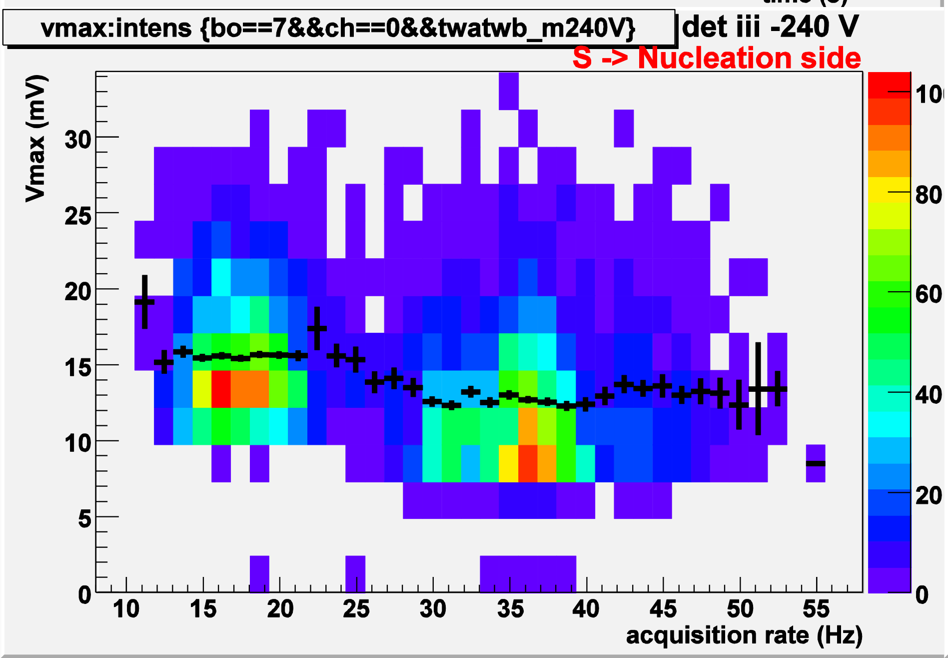

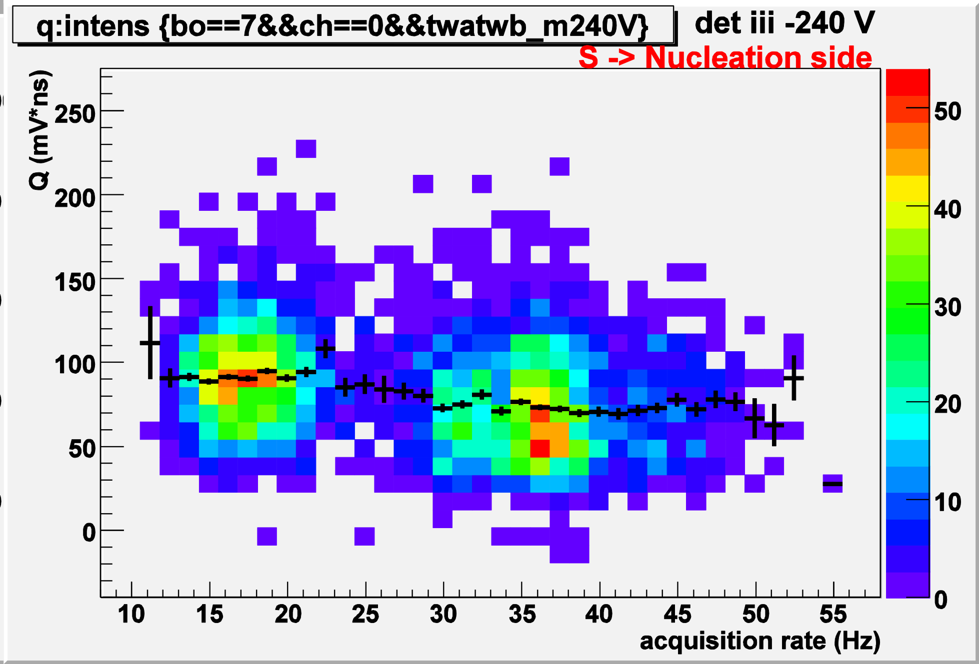

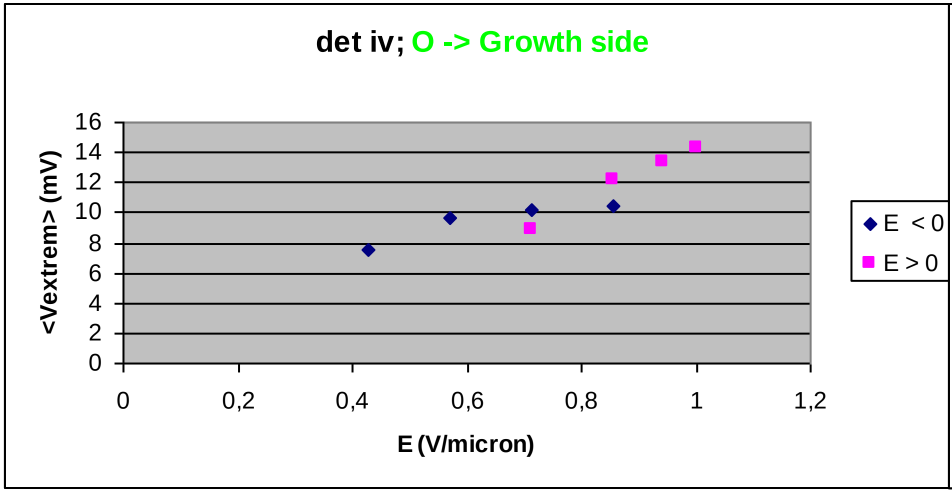
det iv; O -> Growth side
<Vextrem> (mV)
16
14
12
10
8
6
4
2
0
0
0,2
0,4
0,6
0,8
1
1,2
E (V/micron)
E < 0
E > 0

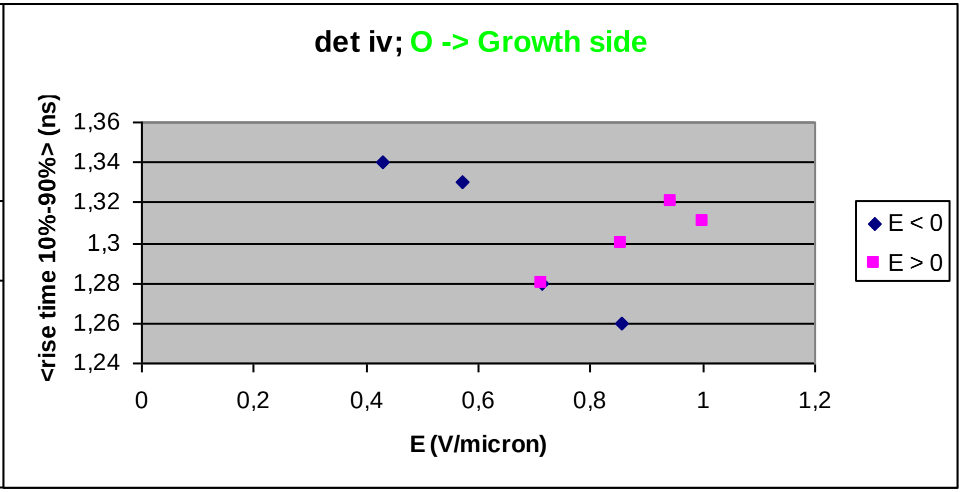
det iv; O -> Growth side
<rise time 10%-90%> (ns)
1,36
1,34
1,32
1,3
1,28
1,26
1,24
0
0,2
0,4
0,6
0,8
1
1,2
E (V/micron)
E < 0
E > 0

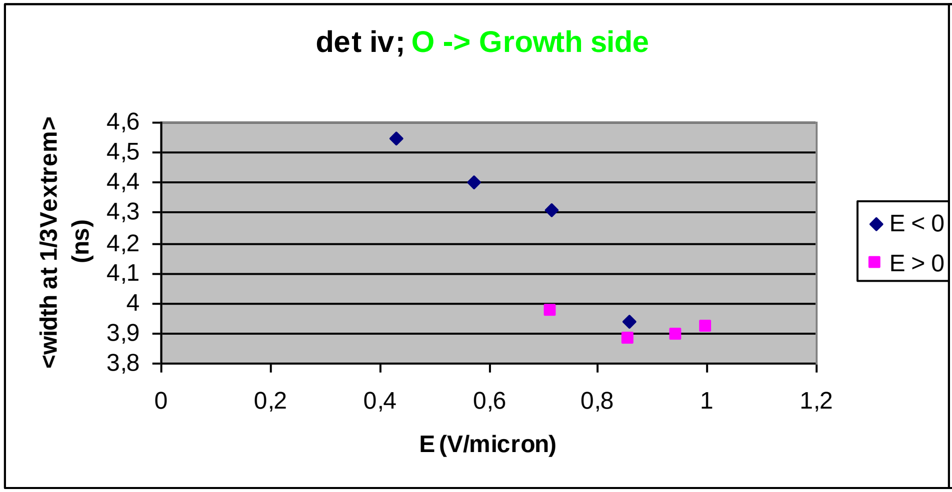
det iv; O -> Growth side
<width at 1/3Vextrem> (ns)
4,6
4,5
4,4
4,3
4,2
4,1
4
3,9
3,8
0
0,2
0,4
0,6
0,8
1
1,2
E (V/micron)
E < 0
E > 0

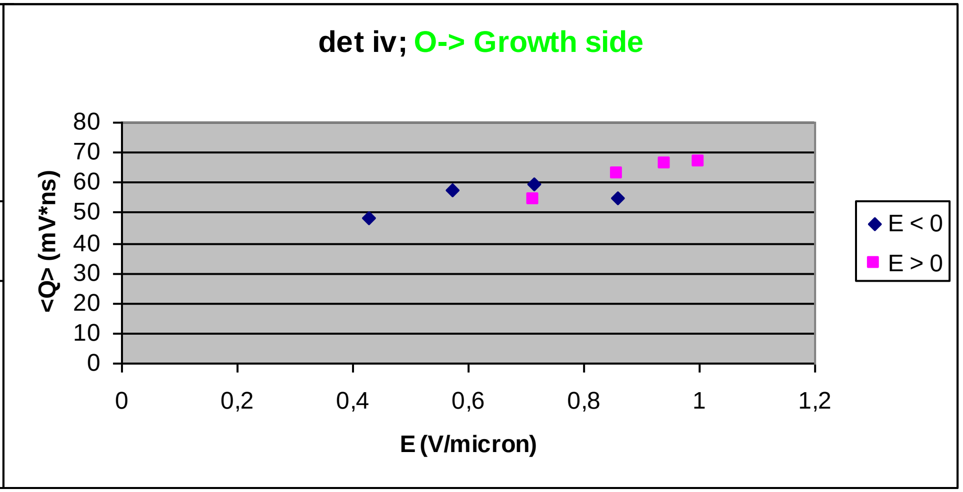
det iv; O-> Growth side
<Q> (mV*ns)
80
70
60
50
40
30
20
10
0
0
0,2
0,4
0,6
0,8
1
1,2
E (V/micron)
E < 0
E > 0

Discussions

Marian:

- présentation;
- explication: activité démarrée dans le cadre d'EURISOL, encouragée dans le cadre du NUPNET, mais dont le support a été arrêté depuis quelques années;
- pour montrer des résultats, on a besoin d'une lecture électronique qui nous manque actuellement;
- dans un 1-er temps, on la fera avec la carte ETC sur un détecteur de 8X8 voies
- dans un 2-e temps on va passer à 40X40 voies sur le diamant 46X46 mm2 (que nous ayons déjà);

Dominique:

- il faut chercher des applications - il ne faut pas que cette activité meure par faute d'applications;
- pour 2016 – la **solution II** est préférable, même la seule envisageable;

Rémi:

- y-a-t-il moyen d'utiliser les diamants pour faire l'identification d'ions dans le faisceau (à Catane, par exemple, ça est réalisée avec un silicium; à discuter avec eux quand j'irai pour la manip FAZIA - plutôt avec du monocristallin);

Nigel:

- Les diamants sont très intéressants sur LISE;
- D'après ses informations: à Riken, on pourrait les utiliser en tant que cible active de Carbone, avec la détermination du point d'impact du faisceau;